
Electronic Thesis and Dissertation Repository

6-14-2022 1:00 PM

Role of HXXXD-motif acyltransferases in suberin biosynthesis

Yudelkis Indira Queralta Castillo, *The University of Western Ontario*

Supervisor: Mark A. Bernards, *The University of Western Ontario*

Co-Supervisor: Isabel Molina, *Algoma University*

A thesis submitted in partial fulfillment of the requirements for the Master of Science degree in Biology

© Yudelkis Indira Queralta Castillo 2022

Follow this and additional works at: <https://ir.lib.uwo.ca/etd>



Part of the [Biology Commons](#), and the [Plant Biology Commons](#)

Recommended Citation

Queralta Castillo, Yudelkis Indira, "Role of HXXXD-motif acyltransferases in suberin biosynthesis" (2022). *Electronic Thesis and Dissertation Repository*. 8759.

<https://ir.lib.uwo.ca/etd/8759>

This Dissertation/Thesis is brought to you for free and open access by Scholarship@Western. It has been accepted for inclusion in Electronic Thesis and Dissertation Repository by an authorized administrator of Scholarship@Western. For more information, please contact wlsadmin@uwo.ca.

Abstract

Suberin is a complex polymer comprising an aliphatic polyester and an aromatic polymer, co-deposited with soluble waxes. The aliphatic polyester is composed of fatty acids, ω -hydroxy fatty acids, α,ω -dicarboxylic acids, fatty alcohols, glycerol, and ferulate. In potato, alkyl ferulates, are a major component of suberin-associated waxes. The lignin-like aromatic polymer is comprised of hydroxycinnamic acids and monolignols. Members of the HXXXD/BAHD acyltransferase family are required for the biosynthesis of the aliphatic suberin polyester and suberin-associated waxes, but their possible role in the biosynthesis of the phenolic domain of suberin remains unexplored. Here I studied the function of three BAHD candidate genes (*StFHT* and *StFACT* and *St430*) in the formation of the poly(phenolic) domain of suberin by characterization of wound-induced suberization in tubers from RNAi-knockdown lines. Overall, my results indicated that these genes may not function in the biosynthesis of the phenolic domain of suberin.

Keywords

Solanum tuberosum, potato, microtuber, periderm, wound-induced suberization, suberin, waxes, poly(phenolic) domain, poly(aliphatic) domain, BAHD acyltransferase, HXXXD-motif acyltransferases, hydroxycinnamic acid, gene silencing, plant transformation, gene expression, RT-qPCR, GC-MS, GC-FID

Summary for Lay Audience

Plants make suberin to control water and nutrient loss and to build a physical barrier against infectious agents such as viruses and bacteria. Suberin is an impermeable polymer that acts as a barrier between underground parts of plants and the environment. Wound healing also elicits the production of new suberized cell layers in plants. These suberized cells provide protection to the internal plant tissues exposed by wounding. This process is similar to the wound healing process in human skin where scabs develop to seal the wounded area and protect the internal tissues. Suberin is found in the cell wall of underground plant tissues such as the potato tuber skin, and in aboveground tissues like the bark of trees. One extreme example is that of the cork oak tree that has a very thick suberized bark layer that is sustainably harvested for the cork production. Understanding the function of suberin in different plants tissues, and the process by which the plant synthesizes suberin is important to improve plant growth and productivity under multiple environmental stresses and prevent spoilage of crops like potato in long-term storage. Chemically, suberin has two regions that differ in composition. One of the regions is composed of many aromatic compounds linked to each other by stable ether and carbon-carbon bonds. This region is referred to as the poly(aromatic) domain of suberin. The other region is composed of mostly aliphatic, and some aromatic compounds linked to each other by ester bonds. This region is referred to as the poly(aliphatic) domain of suberin. Studies to understand the function of suberin have been done mostly on the poly(aliphatic) domain of suberin. For example, the function of members of the BAHD family of enzymes, is well known to be involved in the formation of the poly(aliphatic) domain. Since these enzymes link aromatic and aliphatic components together, they may also function in the linking of poly(aromatic) and poly(aliphatic) domain of suberin. The objective of this research was to get a deeper understanding of the function of the BAHD family genes in the biosynthesis of the phenolic domain of suberin.

Acknowledgments

During the course of my Master study, I received help, guidance and support from various people, and I would like to take the time to acknowledge them here.

First, I would like to thank my supervisor Dr. Mark Bernards for the opportunity and privilege to work with him in his lab. I am grateful for all his support and encouragement throughout all this time and for his positive attitude, enthusiasm, motivation, and patience, especially when I was facing some problems during the first year of my Master program and during the writing process. I learned so much from him and whenever I needed his help, he supported me unconditionally. I also thank my co-supervisor Dr. Isabel Molina. She was the first person who believe that I could be a good scientist, and she gave me the opportunity to work in her lab during my undergraduate studies. The opportunity I had to work in her lab helped me realized my passion for research, and after I completed my undergraduate program, she encouraged me to continue to do research and motived me to do a Master's degree in Biology. I am forever grateful to her for all the doors of opportunity she opened in my life, for always believing in me and for her clear and precise orientations.

Furthermore, I would like to thank my advisory committee members, Dr. Sangeeta Dhaubhadel and Dr. Susanne Kohalmi for their advice, useful comments, and insightful questions. I thank Anica Bjelica for her cloning expertise as she helped me troubleshoot some cloning problems during my first year in the program, and I also thank Dr. Gurpreet Dhami for her help with the Bio-Rad CFX Connect Real-time PCR thermocycler and software.

Additionally, I would like to thank my fellow lab members for providing a good working environment. In particular, I want to thank Karina Kaberi for the moral support and friendship from day one, Jessica Sinka for her sincere friendship and great discussion about our projects, Dimitre Ivanov for his insightful comments and help in the lab, and Andrew Rabas for helping me with the R software.

Lastly, I would like to thank my mother, my brother, and my husband. To my mother, Ana Luz, for being a great example to me, for her understanding, for the confidence she has in me, and for always believing that I can achieve everything I set my mind to do. To my brother, Lester, for his collaboration whenever I needed him, and to my husband, Darien, for his understanding, love, and care at all times.

Table of Contents

Abstract	ii
Summary for Lay Audience	iii
Acknowledgments	iv
Table of Contents.....	vi
List of Figures	viii
List of Appendices	ix
List of Abbreviations	xi
1 Introduction	1
1.1 Plant-environment interactions.....	1
1.2 Land plants defensive mechanisms and adaptations.....	2
1.3 Suberin: deposition, physiological function, chemical composition, structure, and biosynthesis.....	2
1.3.1 Deposition and physiological function.....	2
1.3.2 Chemical composition and macromolecular structure.....	4
1.3.3 Biosynthesis.....	6
1.4 Role of BAHD/HXXXD acyltransferase family in suberin biosynthesis.....	8
1.5 Additional BAHD candidate genes.....	12
1.6 Rationale for using potato as a model for suberization.....	13
1.7 Thesis hypothesis and objectives.....	15
2 Materials and Methods	16
2.1 Plant material and growth conditions.....	16
2.2 Chemicals and Vectors.....	16
2.3 Identification of potato homologs of <i>A. thaliana</i> candidate genes.....	17
2.4 Sequence alignment and phylogenetic analysis.....	17
2.5 RNAi plasmid construction.....	17

2.6	Plant transformation for RNAi-mediated silencing	19
2.6.1	<i>Agrobacterium</i> transformation and culture preparation.....	19
2.6.2	Explant preparation, transformation, and regeneration.....	20
2.7	Genomic DNA extraction and genotype analysis.....	21
2.8	Suberization induction and isolation of potato microtuber wound periderm	21
2.9	RNA isolation, cDNA synthesis, and RT-qPCR analysis	22
2.10	Soluble waxes, soluble phenolic, and aliphatic suberin analyses	23
2.10.1	Wax analysis	24
2.10.2	Soluble phenolic compounds analysis	25
2.10.3	Aliphatic suberin analysis.....	26
2.11	Phenolic suberin analysis.....	26
2.11.1	Nitrobenzene oxidation.....	26
2.11.2	Derivatization followed by reductive cleavage.....	27
2.11.3	Statistical analysis.....	28
3	Results and Discussion.....	29
3.1	Identification of putative potato homologs.....	29
3.2	Generation and confirmation of StBAHD RNAi constructs.....	31
3.3	Generation, selection, and characterization of transgenic lines	33
3.4	Effects of <i>StBAHD</i> -RNAi knockdown lines on wax composition and soluble phenolic.....	36
3.5	Effects of StBAHD-RNAi knockdown lines on aliphatic suberin	43
3.6	Effects of <i>StBAHD</i> -RNAi knockdown line on cell wall phenolics.....	48
4	Conclusions and Future Directions	53
	References	56
	Appendices.....	65
	Curriculum Vitae	86

List of Figures

Figure 1.1 Proposed structure of suberin.....	6
Figure 1.2 Formation of alkyl hydroxycinnamates (AHC) catalyzed by BAHD/HXXXD-motif family acyltransferases.....	12
Figure 1.3 Schematic illustration Arabidopsis root showing how the organ undergo secondary growth.....	14
Figure 1.4 Potato diagram illustrating the main parts of a cut tuber (A), and the suberized layer post-wounding (B).	14
Figure 3.1 Phylogenetic analysis of select <i>A. thaliana</i> and potato candidate BADH acyltransferases.....	31
Figure 3.2 PCR screen of <i>StBAHD</i> candidate genes double insertion in the destination vector.....	33
Figure 3.3. Target gene expression in empty vector control and RNAi knockdown lines post-wounding.....	35
Figure 3.4. Soluble wax composition of potato knockdown lines.....	39
Figure 3.5. Total soluble ferulic acid esters composition of primary alcohols.....	42
Figure 3.6. Total aliphatic suberin monomers composition in wounded potato microtuber. .	47
Figure 3.7. Total monolignols composition in wound induced suberized tissues	49
Figure 3.8. Total poly(phenolics) composition.....	52

List of Appendices

Appendix A. Potato homologs of <i>A. thaliana</i> candidate genes with possible roles in suberin biosynthesis.....	65
Appendix B. Expression data used to select potato homologs of <i>A. thaliana</i> candidates genes (Woolfson, 2018)	65
Appendix C. Nucleotide sequence alignment of the selected potato homologs (DNAMAN)..	68
.....	
Appendix D. Amino acid sequence alignment of the Arabidopsis genes and selected potato homologs (DNAMAN).....	70
Appendix E. List of primers used for PCR amplification and genotype analyses.....	71
Appendix F. Gateway silencing vector and screening strategy for BAHD1, 2, 3 inserts orientation.	72
Appendix G. Medium composition for <i>Agrobacterium</i> infection, callus induction, shoot induction, and root induction.....	73
Appendix H. Gene information and primer sequences used for gene expression analysis (RT-qPCR).....	73
Appendix I. Transgenic plants identification by genotype analysis	74
Appendix J. Agarose gel picture of the genotype analysis for the <i>St430</i> transgenic lines.. ...	74
Appendix K. Agarose gel picture of the genotype analysis for the <i>StFACT</i> transgenic lines..	75
.....	
Appendix L. Agarose gel picture of the genotype analysis for the <i>StFHT</i> transgenic lines...	76
Appendix M. Gene knockdown verification by gene expression analysis	76
Appendix N. Soluble wax composition of potato knockdown lines.....	78

Appendix O. Soluble alkyl ferulates of potato knockdown lines..	80
Appendix P. Total aliphatic suberin monomers composition in <i>St430</i> transgenic line..	82
Appendix Q. Total aliphatic suberin monomers composition in <i>StFACT</i> transgenic line.....	83
Appendix R. Total aliphatic suberin monomers composition in <i>StFHT</i> transgenic line..	85

List of Abbreviations

4CL	4-coumaroyl-CoA ligase
ω -OH FAs	omega-hydroxy fatty acids
AHC	Alkyl hydroxycinnamates
AHCT	Anthocyanin <i>O</i> -hydroxycinnamoyltransferase
AIM	<i>Agrobacterium</i> infection medium
AMP	Adenosine monophosphate
ANOVA	Analysis of variance
ASFT	Aliphatic suberin feruloyl transferase
APCI	Atmospheric pressure chemical ionization
ATP	Adenosine triphosphate
BAHD	<u>B</u> enzylalcohol acetyltransferase, <u>A</u> nthranilate N- <u>H</u> ydroxycinnamoyl/benzoyltransferase, <u>D</u> eacetylvindoline acetyltransferase
BEAT	Benzylalcohol <i>O</i> -acetyltransferase
BSTFA	N,O-bis(trimethylsilyl)-trifluoroacetamide
C3H	<i>p</i> -coumaric acid 3-hydroxylase
C4H	Cinnamate 4-hydroxylase
CAD	Cinnamyl alcohol dehydrogenase
CCR	Cinnamoyl-CoA-reductase
CHCl ₃	Chloroform
CH ₂ Cl ₂	Dichloromethane
CH ₃ OH	Methanol
cDNA	Complementary DNA
CIM	Callus induction medium

CoA	Coenzyme A
COMT	Caffeic acid 3- <i>O</i> -methyltransferase
Cmr	Chloramphenicol resistance
CmrF	Cmr forward
CmrR	Cmr reverse
CTAB	Hexadecyltrimethylammonium bromide
CW	Cell wall
DAT	Deacetylindoline 4- <i>O</i> -acetyltransferase
ddH ₂ O	Double distilled water
DCAs	Dicarboxylic acids
DEPC	Diethylpyrocarbonate
DFRC	Derivatization followed by reductive cleave
DNA	Deoxyribonucleic acid
gDNA	Genomic DNA
E-value	Expected value
ECR	Enoyl CoA reductase
EDTA	Ethylenediaminetetraacetic acid
EV	Empty vector
F5H	Ferulate-5-hydroxylase
FACT	Fatty: caffeoyl-CoA caffeoyl transferase
FHT	Fatty ω -hydroxyacid/fatty alcohol hydroxycinnamoyl transferase
G unit	Guaiacyl unit
GC-FID	Gas chromatography-flame ionization detector
GC-MS	Gas chromatography-mass spectrometry

H	Hydrogen
H unit	p-hydroxyphenyl
HCBT	Anthranilate <i>N</i> -Hydroxycinnamoyl/benzoyltransferase
HCl	Hydrochloric acid
HHT	O-hydroxycinnamoy transferase
IAA	Isoamyl alcohol
KCS	β - ketoacyl-CoA synthases
LACS	Long-chain acyl-CoA synthetase
LB	Luria-Bertani
LiCl	Lithium chloride
LC-UV-MS	Liquid chromatography-ultraviolet-mass spectrometry
LRGC	London Regional Genomics Center
MgSO ₄	Magnesium sulfate
mRNA	Messenger RNA
MS	Murashige and Skoog
NaOH	Sodium hydroxide
Na ₂ SO ₄	Sodium sulfate
NBO	Nitrobenzene oxidation
NH ₄ Cl	Ammonium chloride
NTC	non-template control
N ₂	Nitrogen gas
NMR	Nuclear Magnetic Resonance
OCH ₃	Methoxy group
OH	Hydroxy group

OHFAs	ω -hydroxyfatty acids
OD	Optical density
PAL	Phenylalanine ammonia lyase
PCR	Polymerase chain reaction
PVP	Polyvinylpyrrolidinone
RT-qPCR	Reverse transcription-quantitative PCR
RIM	Root induction medium
RNA	Ribonucleic acid
RNAi	RNA interference
S unit	Syringyl unit
SDS	Sodium dodecyl sulfate
SIM	Shoot induction medium
SL	Suberin lamella
SPAD	Suberin poly(aliphatic) domain
SPPD	Suberin poly(phenolic) domain
TAIR	The Arabidopsis Information Resource
TCA	Tricarboxylic acid
TEM	Transmission electron microscope
TMS	Trimethylsilylated
UV	Ultraviolet
VLCFA	Very long chain fatty acids
WT	Wild type
YEP	Yeast extract peptone

1 Introduction

1.1 Plant-environment interactions

Biotic and abiotic stresses, such as pathogen infection, increased soil salinity, high and low temperature, and drought, threaten the growth and productivity of many of the plants that are the sources of medicines, food, and the ultimate source of metabolic energy on Earth (Akerle *et al.* 1991; Sitch *et al.* 2007). Unlike animals, plants are immobile. They cannot move from one place to another to avoid threatening conditions such as being eaten by herbivores, and they depend on pollinators for fertilization and reproduction (Smith and Chitwood, 2020). Plants need basic abiotic resources, including sunlight, water, and nutrients, to survive. These basic resources are not always available, leading to competition between individual plants for limited environmental resources. This can render plants more susceptible to biotic stress such pathogen and insect infection (Coakley *et al.*, 1999; Seherm and Coakley, 2003; Ziska *et al.*, 2010; Smith and Chitwood, 2020). Through the course of evolution, plants have developed adaptation strategies to deal with different stress factors. From this perspective, to improve stress tolerance in plants, crop productivity and yield, it is important to understand plant-environment interactions under unfavorable conditions, and the mechanisms that plants have developed to cope with environmental stressors. Plants growth and productivity can be affected by three types of stress: (1) a single stress, which occurs when a plant is affected by one stress factor only, (2) multiple stress, when the plant is affected by more than one stress but not at the same time, and (3) combined stress, representing the overlap between two or more stress factors (review in Pandey *et al.* 2017 and Ramegowda and Senthil-Kumar,2015). Although many studies focus on understanding how plants react under a specific stress situation (Mengiste *et al.*, 2003; Suzuki *et al.*, 2005; Senthil-Kumar *et al.*; 2013), in nature, plants are exposed to multiple stressors that can cause more damage to the plant than individual stresses alone. Multiple stresses can either occur simultaneously, or in sequence, wherein one stress condition can make the plants more susceptible to another stress (Coakley *et al.*, 1999; Rizhsky *et al.*, 2002; Scherm and Coakley, 2003; Bartels and Sunkar, 2005; Mittler, 2006; Mittler and Blumwald, 2010; Atkinson and Urwin, 2012; Pandey *et al.*, 2015).

Environmental stress interaction could be abiotic to abiotic and abiotic to biotic interactions which can affect plants differently depending on the type of stress, how much damage is caused to the plant and the length of the stress condition (review in Pandey et al., 2017). Among the abiotic factors, interactions between extreme temperature, drought, and salinity, are considered amongst the major problems affecting plant growth and reproduction (Bartels and Sunkar, 2005; Sahi et al., 2006; Bao et al., 2009; Tamirisa et al., 2014). Wang et al. (2003) suggested that by the year 2050, these abiotic factors could affect the average yield of crop plants by more than 50%. Salinization in the soil reduces water availability to the plant due to osmotic pressure, which in turn can affect the cellular activity of the plant. Sustained exposure to high salinity and drought can affect plant survival and can result in the death of plants (Chen and Jiang, 2010).

1.2 Land plants defensive mechanisms and adaptations

To minimize the impact of stress, it is important to understand the defense mechanisms and adaptations that land plants have evolved to succeed in their terrestrial habitats. These adaptations include specialized surface tissues or cells (vascular system, roots, and stomata), and cell wall modifications to protect the plants against ultraviolet (UV) radiation, pathogen infection, and to control the loss of water, nutrients, and gas exchange (Pollard et al., 2008; Cheynier et al., 2013). Cell wall modifications include two lipophilic barriers: cutin and suberin. Cutin is the polyester matrix of the plant cuticle that is deposited on the epidermis of green tissues in aerial plant surfaces and covers the outer surface of the primary cell wall. Suberin, which is the focus of this thesis, is a phenolic-lipid polymer deposited between the primary cell wall and the plasma membrane in cells of the periderms of underground organs and bark, seed coats and wounded tissues (Kolattukudy, 1980; Molina et al. 2008; Serra et al. 2010).

1.3 Suberin: deposition, physiological function, chemical composition, structure, and biosynthesis.

1.3.1 Deposition and physiological function

During plant development, suberin is synthesized and deposited in different external and internal plant tissues to form a barrier between the plant and the environment and to form

an interface that separates internal plants tissues (Franke and Schreiber, 2007; Pollard et al., 2008). External suberized cells are found in the secondary growth periderm of underground plants tissues and the surface layers of above-ground stems that undergo secondary thickening (review in Bernards, 2002; Franke and Schreiber, 2007; Pollard et al., 2008). The bark of the cork oak tree (*Quercus suber*) is a common example of a suberized periderm that protects the tree against water loss by making the cork layer (phellogen) more impermeable (Graça, and Pereira, 2000a; Silva et al., 2005; Soler et al., 2007). In underground tissues, such as mature roots and storage organs (i.e., tubers), suberin provides protection against biotic and abiotic stresses such as high salinity, dehydration, osmotic shock, extreme temperature changes, soil acidity, microbial attack, and wounding (Lulai and Corsini, 1998; Kolattukudy, 2001; Enstone et al., 2002). The suberized layer of potato (*Solanum tuberosum*) skin or periderm is a typical example of a storage tuber that has been used to study and understand suberization (Graça, and Pereira, 2000b; Kolattukudy, 2001; review in Bernards, 2002; Schreiber et al., 2005). After harvest, the suberization process in potato tuber periderm continues, allowing the potato tuber periderm to reach a mature state and control the loss of water (Lulai and Orr, 1994; Schreiber et al., 2005). Wounding also initiates suberization. For example, when a potato tuber is cut, a wound-induced suberized layer forms and seals the tissue (Lulai and Corsini, 1998; Kolattukudy, 2001). Other plants tissues, such as the leaves and fruit that are normally protected by cutin, can also produce suberin after wounding (Kolattukudy, 2001). For example, Dean and Kolattukudy (1976) found that wounded jade leaves, tomato fruit, and bean pods synthesized suberin. After chemical depolymerization and gas chromatography mass spectrometry (GCMS) analyses, they found aliphatic monomers that were typical for suberin, indicating that all plants organs can synthesis suberin, especially in response to wounding (Dean and Kolattukudy, 1976). Also, suberin is synthesized during the late stages of seed maturation. During disconnection of the seed from the vascular tissue, suberin seals off the chalaza micropyle region of the seed coat to prevents the loss of water, and in Brassicaceae species suberin is also found on the outer integument of the seed coat (Kolattukudy, 2001; Molina et al. 2006, 2008; Beisson et al., 2012). Internal suberized tissues include the endodermis of roots, the outer integument of the seed

coat in some species, and the bundle sheaths of monocots (Molina et al. 2008; Pollard et al., 2008).

1.3.2 Chemical composition and macromolecular structure

Structurally, suberin is a complex heteropolymer composed of both poly(aliphatic) and poly(aromatic) (also called phenolic) domains, co-deposited with soluble waxes (non-polymerized aliphatic and associated phenolics) (Kolattukudy, 2001; Graça, 2015; reviewed in Woolfson et al., 2022). As a reference, to differentiate the two domains, the poly(aliphatic) region was denoted as the suberin poly(aliphatic) domain or SPAD, whereas the poly(phenolic) region was referred to as the suberin poly(phenolic) domain or SPPD (reviewed in Bernards, 2002 and Woolfson et al., 2022). In the literature, while it is recognized that suberized cell walls contain both poly(aliphatic) and poly(phenolic) polymers, the molecular structure of suberin remains unclear (reviewed in Woolfson et al., 2022). Two models for the macromolecular assembly of suberin have been proposed, one being the integrated model illustrated as a heteropolymer with alternating aliphatic and phenolic layers (Kolattukudy, 1980; Graça, 2015), and the other one being the two-domain model (Figure 1.1) in which the macromolecular structure of suberin has two distinct domains that are covalently linked to each other (Stark and Garbow, 1992; reviewed in Bernards, 2002; Woolfson et al., 2018; Woolfson, 2018). While it is unresolved which macromolecular model represent the correct structure and assembly of suberin, both the aliphatic and phenolic metabolisms are involved in the synthesis of suberin, and chemical composition is very similar across species (reviewed in Woolfson et al., 2022). The poly(aliphatic) region is made from long-chain (C16-C18) and very-long-chain aliphatics (\geq C20) that include fatty acids, ω -hydroxy fatty acids (OHFAs), α,ω -dicarboxylic acids (DCAs), and fatty alcohols. Glycerol and variable proportions of hydroxycinnamic acid derivatives, mainly ferulate (Kolattukudy, 1981; Graça and Santos, 2006; Franke and Scheiber, 2007), are also part of the aliphatic polyester. The poly(phenolic) region is a lignin-like polymer presumed to be involved in the cross-link between the aliphatic domain and cell wall polysaccharides (reviewed in Bernards, 2002). It is mainly comprised of hydroxycinnamic acids (e.g., ferulic acid, *p*-coumaric acid, and caffeic acid) and monolignols (*p*-coumaryl alcohol – H unit, coniferyl alcohol – G unit, and sinapyl – S unit

alcohol) (Bernards et al., 1995; Bernards and Razem, 2001). Alkyl-hydroxycinnamate esters are major components of suberin-associated waxes and are comprised of hydroxycinnamic acids esterified to long chain saturated fatty alcohols and OHFAs (Graça and Pereira, 2000b; Graça and Santos, 2006; Kosma et al., 2015). Suberin-associated waxes also contain alkanes, fatty acids, fatty alcohols, and monoacylglycerols (Li et al., 2007b).

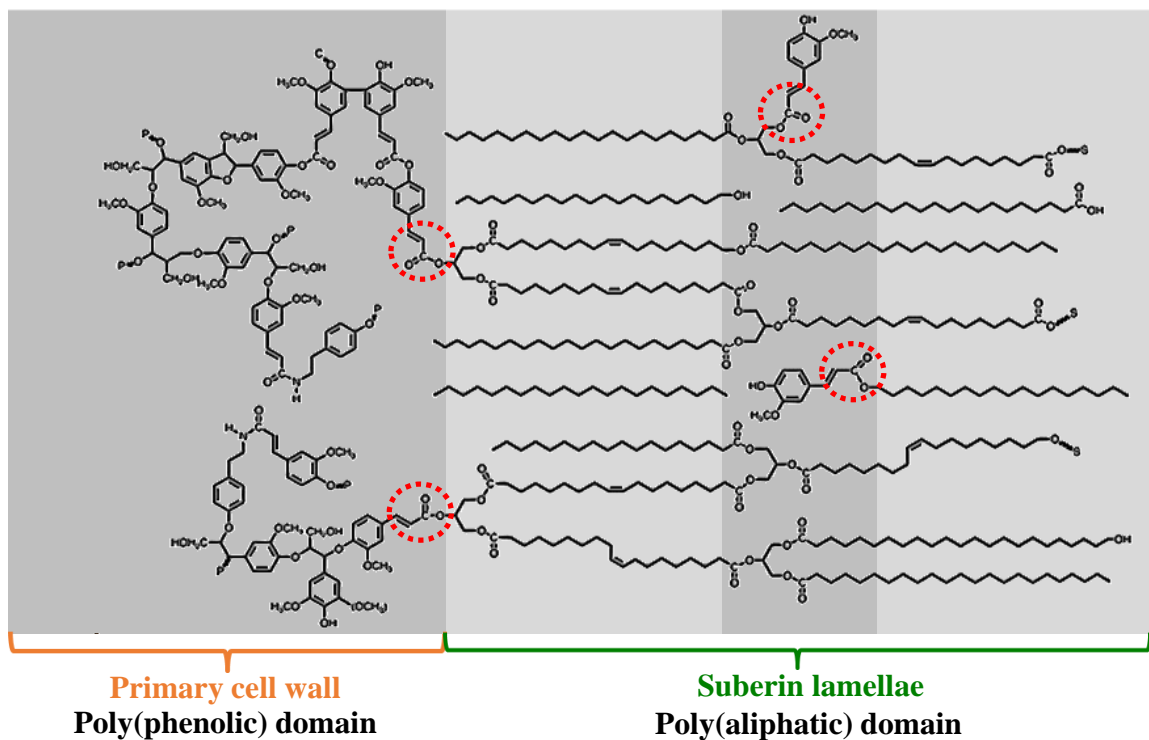


Figure 1.1 Proposed structure of suberin based on the two-domain model. Suberin is proposed to have two domains, the poly(phenolic) domain in the primary cell wall that is ester linked to a glycerol-based poly(aliphatic) domain, between the cell wall and the plasma membrane. Through transmission electron microscope (TEM), the suberin lamellae appears as alternate dark and light bands. According to this model, the dark bands correspond to the electron-dense aromatic and glycerol ester regions of the aliphatic domain, whereas the aliphatic hydrocarbon chains represent the electron-translucent bands. A partial structure is shown. The polymer extends beyond what is depicted through connections to additional aliphatic suberin (S), phenolics (P) and carbohydrate (C). The ester links between the aliphatics, glycerol and the aromatics compounds are highlighted in red. This figure is based on the suberin model proposed by Bernards (2002).

1.3.3 Biosynthesis

Over the past few years, details about the biosynthetic steps involved in the production of the SPAD and SPPD of suberin have been expanded. This has mostly been through the biochemical analysis conducted in potato tubers, after wound-induced suberization and other model plants such as *Arabidopsis thaliana* (reviewed in Woolfson

et al., 2022). The precursor aliphatic and phenolic monomers required for the assembly of the two domains of suberin are ultimately derived from pyruvate, phosphoenolpyruvate, and erythrose-4-phosphate, which are products of the carbohydrate metabolism (reviewed in Bernards, 2002). A key point of divergence during the biochemical process is at the beginning of the fatty acid synthesis that gives rise to the C16:0 and C18:0 fatty acids (the precursor for the aliphatic monomer of suberin) and the shikimate pathway that gives rise to phenylalanine, the precursor for almost all the phenylpropanoids (reviewed in Bernards, 2002).

The biosynthesis of the phenolic monomers of the SPPD start with the conversion of phenylalanine (derived from the shikimate pathway) into cinnamate, a reaction catalyzed by the enzyme phenylalanine ammonia lyase (PAL) (Havir and Hanson, 1970; reviewed in Woolfson et al., 2022). The next step is the production of four cinnamic acid derivatives, commonly known as hydroxycinnamic acids (*p*-coumaric, caffeic, ferulic, and sinapic acids), through the hydroxylation and the *O*-methylation reactions of cinnamate catalyze by cinnamate 4-hydroxylase (C4H), *p*-coumaric acid 3-hydroxylase (C3H), caffeic acid 3-*O*-methyltransferase (COMT), and ferulate-5-hydroxylase(F5H), respectively. These hydroxycinnamic acids are converted into their subsequent coenzyme A (CoA) esters derivative by 4-coumaroyl-CoA ligase (4CL) and are all part the of the phenolic domain of suberin (Meyer et al., 1998; Humphreys et al., 1999; Schneider et al., 2003, Do et al., 2007; Knollenberg et al., 2018; reviewed in Woolfson et al., 2022). After, the CoA thioester derivatives of the hydroxycinnamic acids are converted into monolignols by cinnamoyl-CoA-reductase (CCR) (to form the aldehyde intermediates), and cinnamyl alcohol dehydrogenase (CAD) (Larsen, 2004; reviewed in Woolfson et al., 2022) to form the monolignols.

Regarding the biosynthesis of the poly(aliphatic) domain of suberin, the metabolic routes of the major monomeric components (glycerol, fatty acids, and fatty alcohol) begin with the synthesis of palmitic acid (C16:0) and steric acid (C18:0) in the plastid using acetyl-CoA derived from lysis of citric acid from the tricarboxylic acid (TCA) cycle (Schreiber et al., 1999; reviewed in Vishwanath et al., 2015 and Woolfson et al., 2022).The acyl-CoA activation necessary for the downstream fatty acid metabolism is

likely catalyzed by the long-chain acyl-CoA synthetase (LACS) enzymes involved in cutin biosynthesis (Schnurr et al., 2004; reviewed in Woolfson et al., 2022). The main biosynthetic steps for SPAD monomer formation include the elongation of steric acid to generate very long chain fatty acids (VLCFA) that range between C20:0-C32:0 carbon atoms (reviewed in Woolfson et al., 2022). This metabolic process takes place at the endoplasmic reticulum and is catalyzed by four enzymes: β -ketoacyl-CoA synthases (KCS), β -ketoacyl-CoA reductase, 3-hydroxyacyl-CoA dehydrogenase, and enoyl CoA reductase (ECR) (Blacklock and Jaworski, 2006; Zheng et al., 2005; Bach et al., 2008; Beaudoin et al., 2009; reviewed in Woolfson et al., 2022). Additional biosynthetic steps include the oxidation of fatty acids (predominantly C18:1 unsaturated fatty acids) to generate ω -hydroxy fatty acids that are further oxidized to their corresponding dicarboxylic acids (reviewed in Woolfson et al., 2022). The oxidation step is catalyzed by three types of enzymes: ω -hydroxylase, (Benveniste et al., 1998; Compagnon et al., 2009; Serra et al., 2009b), ω -hydroxy fatty acid dehydrogenase (Agrawal and Kolattukudy, 1978), and fatty acid hydroxylase (Le Bouquin et al., 2001; Kandel et al., 2007). Lastly, long and VLCFAs can be reduced to primary alcohols, a metabolic process that is catalyzed by fatty acyl-CoA reductases (FARs) (Domergue et al., 2010). Additionally, VLCFAs acyl-CoA thioester are further reduced to alkanes through decarbonylation (Bernard et al. 2012, reviewed in Woolfson et al., 2022).

1.4 Role of BAHD/HXXXD acyltransferase family in suberin biosynthesis

Studies to understand the composition of suberin have been conducted using different plant species such as the cork oak tree (*Quercus suber*) (Lopes et al., 2000), potato tuber (*Solanum tuberosum*) (Graça and Pereira, 2000b; Schreiber et al., 2005), and Arabidopsis (*Arabidopsis thaliana*) (Molina et al., 2006). Based on both forward and reverse genetic approaches, it has been shown that members of the plant-specific BAHD acyltransferase family enzymes are associated with secondary metabolism and have roles in extracellular lipid biosynthesis (St-Pierre and De Luca, 2000; reviewed in Molina and Kosma, 2015;). The BAHD acyltransferase superfamily was named based on the first letters of names of the first four biochemically characterized enzymes members:

Benzylalcohol *O*-acetyltransferase (BEAT, from the plant species *Clarkia breweri*; Dudareva et al., 1998), **A**nthocyanin *O*-hydroxycinnamoyltransferase (AHCT, from plants species such as *Gentiana trifloral* and *Perilla frutescens* ; Fujiwara et al., 1998a; Fujiwara et al., 1998b), Anthranilate *N*-**H**ydroxycinnamoyl/benzoyltransferase (HCBT, from *Dianthus caryophyllus*; Yang et al., 1997), and **D**eacetylvindoline 4-*O*-acetyltransferase (DAT, from *Catharanthus roseus*; St-Pierre et al., 1998) (St-Pierre and De Luca, 2000; D’Auria, 2006). This superfamily of enzymes can be identified by two consensus motifs, HXXXD, which is shared by all the BAHD acyltransferases, and DFGWG, which is mostly, but not completely, conserved by this family of enzymes (D’Auria, 2006; Luo et al., 2007; Yu et al., 2009; Tuominen et al., 2011). The HXXXD motif has a catalytic histidine and is located close to the center portion of the enzyme globular structure, and the DFGWG is located close to the carboxyl terminus (away from the active site) and seems to have a structural role rather than a catalytic role (St-Pierre and De Luca, 2000; D’Auria, 2006). Aside from these two motifs, proteins of the BAHD superfamily also share 10-30% sequence identity, and several studies used protein alignment and phylogenetic analysis to identify genes that encode for BAHD proteins (Beekwilder et al., 2004; Stewart et al., 2005; Yu et al., 2009; Tuominen et al., 2011). Based on these analyses, D’Auria (2006) suggested the existence of five clades to help identify the enzyme substrates for putative BAHD members that were not biochemically characterized. More recently, using different plant models (*Arabidopsis*, *Populus trichocarpa*, *Medicago truncatula*, *Vitis vinifera*, and *Oryza*), Touminen et al. (2001) suggested the presence of eight clades within the BADH phylogeny instead of five, as well as the existence of clade specific motifs that can be related to substrate and donor specificities.

Enzymes of the BAHD acyltransferase family catalyze the transfer of acyl moieties from a range of coenzyme A-thioester donors (e.g., hydroxycinnamoyl-CoAs, acetyl-CoA, malonyl-CoA, and benzoyl-CoA), to acceptor alcohols (Figure 1.2) (St-Pierre and De Luca, 2000; D’Auria, 2006). The roles of several BAHD enzymes in the biosynthesis of surface lipids have been reported in potato (Serra et al., 2010; Jin et al., 2018), poplar (Cheng et al., 2013), and *Arabidopsis* (Gou et al., 2009; Molina et al., 2009; Kosma et al., 2012; Rautengarten et al., 2012). Two enzymes of the BAHD family of HXXXD-type

acyltransferases of Arabidopsis, aliphatic suberin feruloyl transferase (ASFT; *At5g41040*; Gou et al., 2009; Molina et al., 2009) and fatty alcohol: caffeoyl-CoA caffeoyl transferase (FACT; *At5g63560*) (Kosma et al., 2012), are known to be involved in the aliphatic suberin polyester biosynthesis and to produce wax-associated hydroxycinnamoyl esters, respectively. ASFT loss-of-function T-DNA insertion mutants showed a significant reduction in esterified ferulate content in both root and seed coat suberin (Gou et al. 2009; Molina et al. 2009). Alkyl hydroxycinnamate esters in root-associated waxes, however, were not affected in the *asft* knockout mutants (Molina et al. 2009). Recombinant enzyme assays supported the results obtained from the aliphatic suberin domain analysis, in that the *At5g41040* protein (ASFT) functioned as a feruloyl transferase by catalyzing the conjugation between ferulic acid and ω -hydroxy fatty acids and fatty alcohols. The *in vitro* enzyme analysis also showed that ASFT (to a lesser extent) could catalyze the transfer of caffeoyl-CoA and *p*-coumaroyl-CoA to fatty alcohols and fatty acids groups (Gou et al., 2009; Molina et al., 2009; reviewed in Molina and Kosma, 2015). Homologs of the Arabidopsis ASFT gene have similar activities in poplar (Cheng et al., 2013) and potato (Serra et al., 2010). Opposite to the *asft* knockout mutants, *fact* knockout mutants, were affected in the alkyl hydroxycinnamate ester content. Root wax chemical analysis showed a significant decrease in alkyl caffeates, a small reduction in alkyl ferulates, and a significant increase in alkyl coumarates. No changes were observed in the root suberin polyester composition, but the caffeate content was reduced in the seed coat (Kosma et al. 2012). *In vitro* enzyme assays confirmed the *in-planta* analyses, showing that the recombinant enzymes catalyze the transfer of caffeic acid from caffeoyl-CoA (the donor) to fatty alcohol (the acceptor). The recombinant protein assay also showed that FACT enzyme can use feruloyl-CoA and coumaroyl-CoA as acyl donors *in vitro* (Kosma et al. 2012; reviewed in Molina and Kosma, 2015). While these studies demonstrate the function of the BAHD family in aliphatic suberin polyester and suberin associated waxes, the role of BAHD family enzymes in the synthesis of the poly(aromatic) domain of suberin remains unproven or inconclusive. The potato homolog of the Arabidopsis ASFT gene, fatty ω -hydroxyacid/fatty alcohol hydroxycinnamoyl transferase (FHT), was functionally characterized through an RNAi silencing approach (Serra et al. 2010). It was shown that *FHT* RNAi native periderm had a reduced content of ferulic acid, ω -hydroxyacid (C18:1),

and many of the primary alcohols (Serra et al. 2010). Additionally, in the soluble wax fraction, alkyl ferulate and alkane amounts were reduced (Serra et al. 2010). Furthermore, solid-state ^{13}C nuclear magnetic resonance (NMR) analysis showed that the molecular structure and mechanical properties of the FHT deficient periderm were affected. The analysis showed aliphatic chains that were more flexible, and a substantial amount of aromatic components that resisted transesterification (Serra et al. 2014). More recently, to complement previous analysis, Jin et al. (2018) investigated the impact of FHT deficiency, in the chemical composition of wound suberized tissue. In this study, the *FHT* RNAi native and wound periderms were compared using a bottom-up metabolic approach, looking at the soluble and insoluble metabolites components of the poly(aliphatic) domain through chemical analysis along with solid-state ^{13}C NMR (Jin et al., 2018). It was shown that the content of alkyl ferulates was reduced in the FHT RNAi wound periderm like in the native periderm. Additionally, in this study, Jin et al. (2018) analyzed the poly(phenolic) domain of suberin using thioacidolysis. There were no statistical differences in the amounts of guaiacyl (G) and syringyl (S) units between the WT and the FHT knockdown plants, and no p-hydroxyphenyl (H) units were found (Jin et al., 2018). In this thesis, to complement previous analysis of the aromatic domain in the FHT gene, I further investigated soluble phenolics attained from the derivatization followed by reductive cleave (DFRC) and the nitrobenzene oxidation (NBO) analyses. Also, I explored the function of FACT and of a previously uncharacterized member of the BAHD family (described in section 1.5) in the poly(phenolic) domain of suberin.

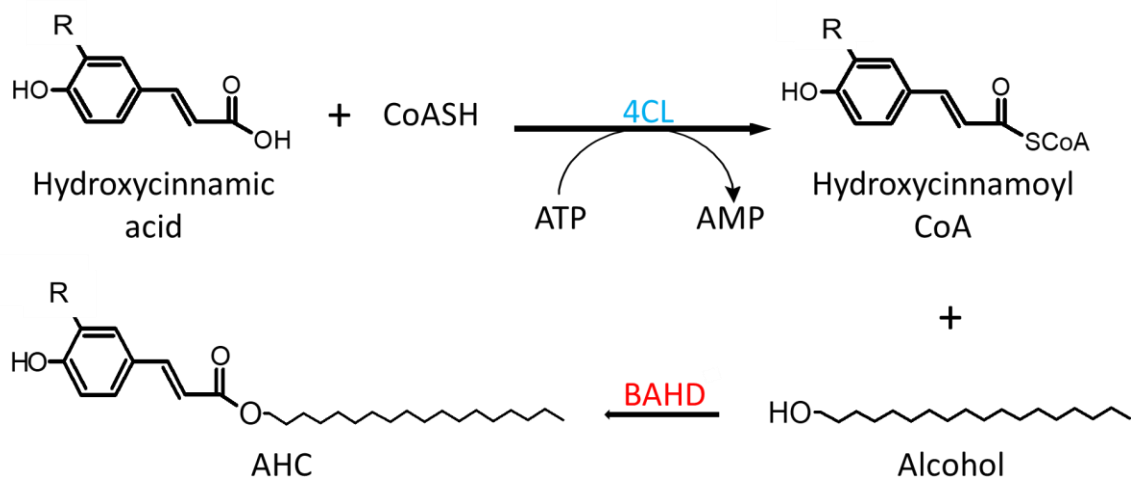


Figure 1.2 Formation of alkyl hydroxycinnamates (AHC) catalyzed by BAHD/HXXXD-motif family acyltransferases. To initiate the reaction, 4-coumarate: coenzyme A ligase (4CL; Lee and Douglas, 1996; Beuerle and Pichersky, 2002) is used to generate Acyl-CoA esters of specific hydroxycinnamic acid derivative (e.g., *p*-coumaric, ferulic and caffeic acids). Hydroxycinnamoyl-CoAs act as the acyl donor for the ester synthesis reaction, while an alcohol acts as the acceptor. This reaction is catalyzed by the BAHD acyltransferase family enzymes (e.g., ASFT or FACT) to obtain the alkyl hydroxycinnamate as the final product. R= H (hydrogen), OH (hydroxy group), or OCH₃ (methoxy group). ATP, Adenosine triphosphate, AMP, Adenosine monophosphate.

1.5 Additional BAHD candidate genes

Genetic approaches using transcriptome data and co-expression analysis have been useful tools to examine expression pattern similarities between genes with known and unknown function and to identify potential putative candidate genes (Stuart et al. 2003; Craigon et al., 2004; Wei et al., 2006; Zhong and Sternberg, 2006; Srinivasasainagendra et al. 2008). Arabidopsis genes such as GPAT5 (Beisson et al., 2007), CYP86A1 (Li et al., 2007a), ABCG20 (Yadav et al., 2014), and ASFT (Molina et al., 2009), with proven roles in suberin biosynthesis, have been used as baits for co-expression analyses to identify additional suberin associated genes (Wei et al. 2006; Molina et al. 2009; Boher, 2017). Using these four genes as baits, an additional putative BAHD acyltransferase gene, *At1g24430*, was identified (Boher, 2017). Additionally, *At1g24430*, was among the list of

genes that were differentially expressed in the cork phellem (Soler et al. 2007) and the list of genes with known and predicted roles in suberization that were highly expressed in the phellem cells of *Arabidopsis* roots (Leal et al., 2021). Preliminary chemical analysis of the knockout mutant for this gene in the *Arabidopsis* plant, suggested a possible function in the formation of suberin associated waxes through the synthesis of alkyl hydroxycinnamates (Fluke, 2015, Castillo, 2016). Unfortunately, chemical analyses of both suberin and wax composition were inconclusive. In one instance, both mutants had reduced alkyl esters (ferulate, caffeate and *p*-coumarate) in root wax (Fluke, 2015), but repeated experiments did not reproduce the same results (Castillo, 2016). Alkyl hydroxycinnamate esters were not affected, and there were no major changes in the aliphatic suberin polyester (Castillo, 2016). Given that the function of the *At1g24430* gene in aliphatic suberin biosynthesis and suberin associated waxes were inconclusive, and one of the chemicals results showed a reduction in the alkyl ferulate (Fluke, 2015), this putative gene could either have a redundant function with other BAHD acyltransferase genes or could have a role in suberin polyphenolic domain formation.

1.6 Rationale for using potato as a model for suberization

The aim of the present study was to gain a deeper understanding of the BAHD family protein function in extracellular lipid biosynthesis, particularly the phenolic domain of suberin. The phenolic domain of suberin has a high amount of hydroxycinnamic acids and some proportion of monolignols (reviewed in Bernards, 2002). However, it is very difficult to obtain vascular free suberin preparations from *Arabidopsis*, due to the interference of root vascular lignin (Figure 1.3); therefore, it is difficult to analyze the phenolic domain of suberin using this species. By contrast, wound healing potato tubers generate large quantities of suberized tissue that is free of interfering lignin (Figure 1.4). Consequently, potato homologs for the *Arabidopsis* candidate genes were identified and used to generate potato knockdown lines that were used to evaluate the function of HXXXD-motif/BAHD acyltransferases in phenolic suberin formation.

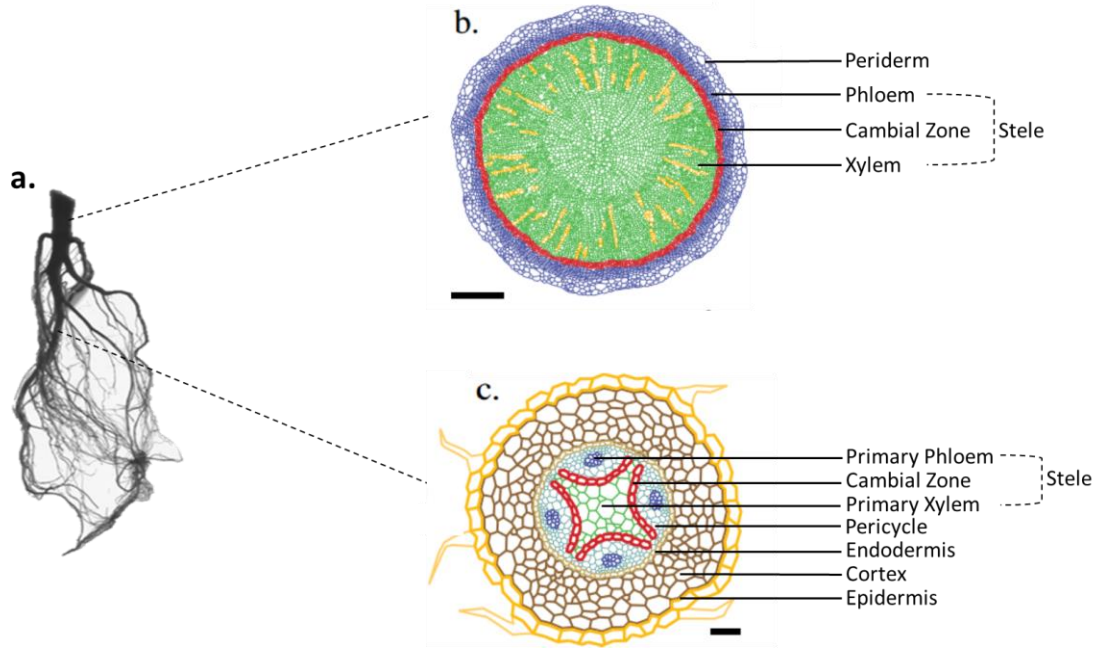


Figure 1.3 Schematic illustration of an Arabidopsis root showing how the organ undergoes primary and secondary growth. (a) Scanned image of Arabidopsis root.

Transverse sections of the hypocotyl (b) and the mid-section (c) of Arabidopsis root. Bar = 200 μ m. Adapted from Risopatron et al. (2010).

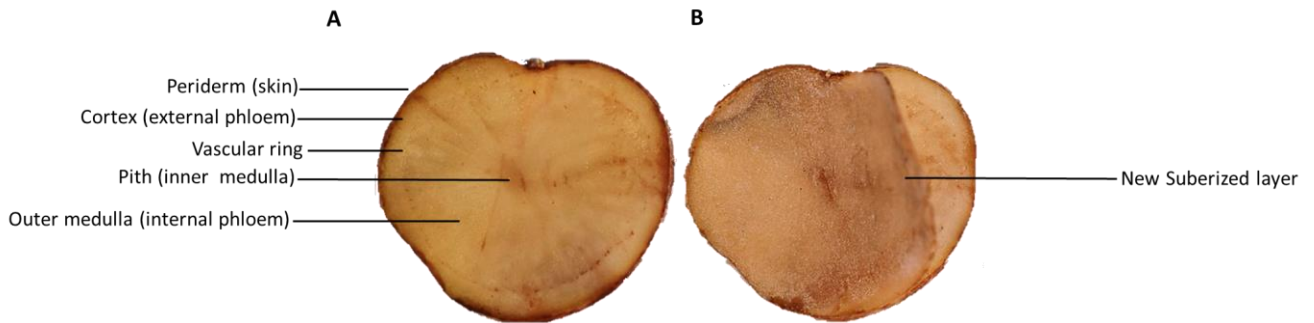


Figure 1.4 Potato diagram illustrating the main parts of a cut tuber (A), and the suberized layer post-wounding (B).

1.7 Thesis hypothesis and objectives

I hypothesize that HXXXD-motif/BAHD acyltransferase family genes are essential for normal phenolic suberin deposition. My specific objectives were to: (1) Identify potato homologs of *A. thaliana* HXXXD-motif/BAHD acyltransferases involved in suberin biosynthesis, (2) generate potato knockdown lines of HXXXD-motif/BAHD acyltransferases identified in objective 1, and (3) evaluate the impact of HXXXD-motif/BAHD acyltransferases knockdown on the poly(phenolic) and poly(aliphatic) domains of potato suberin.

2 Materials and Methods

2.1 Plant material and growth conditions

Commercial potato (*S. tuberosum*) cultivar Desiree was obtained as *in vitro* plantlets from the Canadian Potato Variety Repository at the Plant Propagation Center (New Brunswick) (<https://www2.snb.ca/content/snb/en/services>) and propagated *in vitro* for microtuber production. Plantlets were propagated and maintained in Murashige and Skoog (MS) basal salt medium (pH 5.8) supplemented with 3% (w/v) sucrose and solidified with 0.22% gelrite[®] (Sigma-Aldrich). Plantlets were grown in a growth cabinet under a light/dark photoperiod cycle of 16/8 h at 22°C and 67 $\mu\text{mol m}^{-2} \text{sec}^{-1}$ (Serra et al., 2009a; Serra et al., 2009b). Nodal sections containing at least one leaf were excised and sub-cultured in fresh medium every 4 weeks. For microtuber formation, nodal sections (0.5-1.0 cm long) containing at least one leaf were cut from axenic plantlets and sub-cultured in MS medium supplemented with 8% (w/v) sucrose. Tuber formation was initiated by incubating transferred nodes for 1 week under a short-day photoperiod (8/16 h light/dark) at 22°C and 67 $\mu\text{mol m}^{-2} \text{sec}^{-1}$. Potato cultures were then kept under dark conditions at 22°C to allow microtuber development (Dobránszki, 2001; Serra et al., 2010b). Wound-induced suberization of microtubers was initiated as described for regular tubers by Bernards and Lewis (1992) with some modification. Since the microtubers were already sterile, they were not surface sterilized. To initiate wound healing, microtubers were cut into quarters and put in magenta boxes lined with stainless-steel mesh atop wet filter papers. Several independent transgenic lines for each of the three gene were used for this research with empty vector and wild-type lines grown in parallel as controls for the analyses (see sections 2.9, 2.10 and 2.11 below).

2.2 Chemicals and Vectors

All solvents and chemicals were purchased from Thermo Fisher Scientific and Sigma-Aldrich unless otherwise specified. The Gateway[®] BP Clonase[™] enzyme mix, the LR Clonase[™] enzyme mix and the entry vector (pDONR[™]/Zeo), were purchased from Invitrogen. The silencing destination vector, pK7GWIWG2D(II),0, was obtained from VIB-UGent Center for Plant Systems Biology (<https://gatewayvectors.vib.be/>).

2.3 Identification of potato homologs of *A. thaliana* candidate genes

Full-length sequences of *Arabidopsis* genes *At1g24430*, ASFT (*At5g41040*), and FACT (*At5g63560*), were obtained from The Arabidopsis Information Resource (TAIR) database (<https://www.arabidopsis.org/index.jsp>). Potato homologs were identified through the search tools at the Spud DB Potato Genomics Resource (<http://solanaceae.plantbiology.msu.edu/index.shtml>). Potato wound response ribonucleic acid (RNA) transcriptome data (Woolfson, 2018) were used to narrow down potato candidates with potential acyltransferase function to those involved in wound suberin formation. The sequence ID search tool from the Spud DB Potato Genomics Resource was used to identify *A. thaliana* protein matches based on percent similarity (>50%), and a lower expected value (E-value) (closer to zero for significant match). The RNA transcriptome data were used again to narrow down the potato candidates lists (5-10, Appendix A and B), using their temporal expression patterns post-wounding. Inferred protein sequences of the Arabidopsis genes and the potato candidates were retrieved in FASTA format for multiple sequence alignment.

2.4 Sequence alignment and phylogenetic analysis

Amino acid sequence alignment was performed using the MUSCLE program in MEGA version 6 (Tamura et al., 2013). A phylogenetic tree was constructed using a neighbor-joining algorithm with 1000 bootstrap trials to show gene relationships and homology. Multiple sequence alignment using the nucleic acids of potato candidate genes were analyzed and edited in DNAMAN to identify conserved regions or areas with high similarity to avoid off-target genes for the RNA interference (RNAi) construct design (Appendix C).

2.5 RNAi plasmid construction

Gene specific silencing constructs were generated using Gateway® cloning technology. Polymerase chain reaction (PCR) was performed to amplify gene specific fragments (322-351 bps) from complementary deoxyribonucleic acid (cDNA) derived from messenger RNA (mRNA) isolated from wound healing potato tubers using gene

specific primers (Appendix E) including the *attB1* (for the forward primers) and *attB2* (for the reserve primers) recombinant sequences, respectively, at their 5' ends. The primer sets for the gene amplification were, ASFT-RNAi-F and ASFT-RNAi-R (for PGSC0003DMG400031731), FACT-RNAi-F and FACT-RNAi-R (for PGSC0003DMG400014152), At1g24430-RNAi-F and At1g24430-RNAi-R (for PGSC0003DMG400007171) (Appendix E). The PCR conditions were as follows: 94°C for 4 min, 30 cycles of 94°C for 30 s, 59°C for 1.30 min, 72°C for 1.30 min, and a final extension time at 72°C for 7 mins. After PCR amplification, the products were separated on 1.5% agarose gel, and a single band for each gene specific amplicons were cut and excised from the gel and purified using the QIAquick Gel Extraction Kit (Qiagen), following the manufacture protocol. The purified PCR products were cloned into the gateway entry vector pDONR/Zeo using the BP clonase II mix, and the reaction products were transformed into DH5 α competent *Escherichia coli* cells by the 90s heat shock method (Sambrook et al., 1989). The transformed competent cells were transferred into low salt agar Luria-Bertani (LB) medium plates containing 100 μ g/mL zeocin and incubated overnight at 37°C for bacteria growth. To confirm whether the bacteria colonies had successfully incorporated the recombinant plasmid (pDONR-StBAHD-1, 2 and 3), PCR was carried out using the gene specific primers designed for the genotype analysis, (ASFT-gDNA-F and ASFT-gDNA-R, FACT-gDNA-F, FACT-gDNA-R, At1g24430-gDNA-F and At1g24430-gDNA-R; Appendix E), and the products were separated on a 1.5% agarose gel to check the length of the different amplification products. Positive colonies that contained the recombinant plasmid were picked, transferred to LB liquid broth, and incubated overnight with shaking at 37°C. The overnight culture was then used to extract the plasmid deoxyribonucleic acid (DNA) using the QIAprep Spin Miniprep Kit (Qiagen), following the manufacture protocol. After PCR confirmation (as above), the pDONR-*StFHT*, *StFACT* and *StBAHD-At1g24430* plasmids were cloned into the RNAi destination vector pK7GWIWG2D(II) (Karimi et al. 2002) using the LR clonase II mix, according to manufacturer's instructions. The LR reaction products were transformed into DH5 α competent *E. coli* cells by the heat shock method and grown in LB plates containing 100 μ g/mL spectinomycin. To confirm that the final constructs had the gene-specific inserts in the correct orientation to create the hairpin RNA loops, bacteria colonies were

screened by PCR using the gene-specific forward primers designed for the genotype analysis, and the destination vector intron (the chloramphenicol resistance, Cmr, area) forward (CmrF: 5'-CGA TTC AGG TTC ATC ATG CCG TCT-3') and reverse (CmrR: 5'-TGA GCA ACT GAC TGA AAT GCC TCC-3') primers (Appendix E and F). Positive colonies were picked and grown in LB liquid medium to extract the plasmid DNA. The sequences of the final constructs were verified by Sanger sequencing at the London Regional Genomics Center (LRGC) with the above-mentioned primers.

2.6 Plant transformation for RNAi-mediated silencing

The RNAi recombinant plasmids (pK7GWIWG2D(II)RNAi) were transformed into *Agrobacterium tumefaciens* strain GV2260 (Höfgen and Willmitzer, 1988) and used to transform potato internodal explants (Banerjee et al., 2006; Chetty et al., 2015).

2.6.1 *Agrobacterium* transformation and culture preparation

The RNAi final constructs (pK7GWIWG2D(II)-*StFHT*, *StFACT*, and *StBAHD-At1g24430*) were transformed into the *Agrobacterium* strain GV2260 by electroporation using the MicroPulser Electroporator (Bio-Rad). For the electroporation steps, 0.5-1 µg of plasmid DNA (5 µL) was added into the *Agrobacterium* competent cells (50 µL/tube) and kept on ice for 15 minutes. Each individual competent cells and plasmid mixture was transferred to a prechilled cuvette (0.1 cm gap) and pulsed once for 5 milliseconds under the Agr mnemonic on the electroporator at an output voltage of 2.2 kV. The mixture was quickly removed from the cuvette, transferred to 1 mL of yeast extract peptone (YEP) liquid broth (without antibiotics) and incubated for 3 hours at 28°C with shaking at about 150 rpm. After incubation, the cells were harvested by centrifugation at 3000 rpm for 3 min, the pellets were resuspended in 200 µL of YEP medium and grown on YEP plates containing 50 µg/mL rifampicin and 100 µg/mL spectinomycin. The YEP plates were incubated at 28°C for two days. A single colony was used to inoculate each liquid culture (three constructs plus vector control) containing the above-mentioned antibiotics and incubated in a shaker (250 rpm) for two days at 28°C. After two days incubation, the cultures (100 µL) were then used to inoculate a 50 mL subculture of YEP medium containing the *Agrobacterium* strain and vector specific antibiotics. The cultures were

grown overnight at 28°C with shaking. The cells were harvested by centrifugation at 5000 rpm for 10 min and the pellets were resuspended in *Agrobacterium* infection medium (AIM, Appendix G) to yield an optical density (OD) reading (at 600 nm) of 0.6. To improve plant transformation efficiency, 20 µL of acetosyringone stock (74 mM) was added to 40 mL of the AIM diluted cultures and kept on ice until internodal explants were treated with *Agrobacterium* to initiate transformation.

2.6.2 Explant preparation, transformation, and regeneration

In preparation for *Agrobacterium* inoculation, internodal segments (about 5-10 mm in length) were excised from four-week-old *in vitro* plants. The internodal segments were then placed onto callus induction medium (CIM, Appendix G) in 100 x 15 mm petri-dishes (around 20 stem internodes per plates) and incubated in the dark for two days in a growth cabinet at 22°C, followed by a light/dark photoperiod cycle of 16/8 h and 67 µmol m⁻² sec⁻¹. For *Agrobacterium* infection, the internodal explants were transferred into previously prepared culture medium (AIM) and incubated for 20 min at room temperature with gentle agitation on a shaker at 50 rpm. Afterward, explants were transferred onto sterilized paper towels, blotted dry (to remove excess moisture), placed onto new CIM petri-plates, and incubated for two days at 22°C. After the two-day co-cultivation period, to avoid *Agrobacterium* overgrowth, the internodal segments were collected into sterile falcon tubes, rinsed with 40 mL autoclaved double distilled water (ddH₂O) containing 250 mg/L cefotaxime for 5 minutes (3 times) and blotted dry with sterilized paper towels. The internodal segments were then transferred to CIM plates containing 500 mg/L carbenicillin, 250 mg/L cefotaxime, and 100 mg/L kanamycin. Carbenicillin and cefotaxime were used to inhibit the growth of *Agrobacterium* in the inoculated plant tissues (Silva and Fukai, 2001), while kanamycin resistance was used as a selection marker for transgenic plants. The internode segments were transferred onto a fresh CIM every two weeks, and after the four weeks, to shoot induction medium (SIM, Appendix G) plates supplemented with the same antibiotics. Once shoot primordia appeared and developed into plantlets at least 2-cm-long, they were transferred to magenta boxes with root induction medium (RIM, Appendix G) supplemented with half concentrations of the same antibiotics and SIM and incubated as before. The transgenic plants were cut and re-propagated into fresh RIM as needed.

2.7 Genomic DNA extraction and genotype analysis

To confirm transformation and the correct construct insertion into transgenic plants (*StFHT*, *StFACT* and *StBAHD-At1g24430*), genomic deoxyribonucleic acid (gDNA) was extracted from young leaves (approximately 100-150 mg) using an extraction buffer (400 μ L/mg fresh tissue) composed of 200 mM Tris HCl pH 7.5, 250 mM NaCl, 25 mM ethylenediaminetetraacetic acid (EDTA), and 0.5% sodium dodecyl sulfate (SDS). The leaf tissue was ground directly in the extraction buffer inside a microtube, vortexed for 5 seconds, and centrifuged for 5 minutes at 13,000 rpm in a microcentrifuge. The supernatant (300 μ L) was collected, 300 μ L of isopropanol was added, mixed gently (by inverting the tube), precipitated for 2 minutes at room temperature, and harvested by centrifugation for 10 minutes at 13,000 rpm. The extracted DNA was then washed with 70% ethanol, dried at room temperature for 10 minutes, and dissolved in 50 μ L of sterile water. PCR was performed with the gene specific primers. The primer sets to check each gene insertions were, ASFT-gDNA-F and ASFT-gDNA-R (for PGSC0003DMG400031731), FACT-gDNA-F and FACT-gDNA-R (for PGSC0003DMG400014152), At1g24430-gDNA-F and At1g24430-gDNA-R (for PGSC0003DMG400007171) (Appendix E). To check for vector (pK7GWIWG2D(II)) insertion, in particular the chloramphenicol resistance area, the primer sets used were pK7GWIWG2-Fw and pK7GWIWG2-Rv, as well as the forward primer of the insert specific gene with the reverse primer of the empty vector (Appendix E). The PCR conditions for the gene specific primers were as follows: 94°C for 4 min, 30 cycles of 94°C for 30 s, 59°C for 1.30 min, 72°C for 1.30 min, and a final extension time at 72°C for 7 mins. The PCR conditions for the vector primer is the same as the insert primer with a different annealing temperature (55°C).

2.8 Suberization induction and isolation of potato microtuber wound periderm

In preparation for the gene expression analysis and chemical analysis, potato microtubers were wounded by cutting them into quarters under sterile conditions in a laminar flow hood. The cut microtubers were placed in sterile magenta boxes (see Section 2.1) and incubated in the dark at 25°C for three or seven days. After incubation, the

suberized layers were collected, frozen with liquid nitrogen, and ground to a fine power with a pestle and a mortar. Suberized tissues collected after three days wound healing were stored at -80°C for RNA isolation. The ground suberized layers collected after the seven days were stored at -20°C until used for the chemical analysis.

2.9 RNA isolation, cDNA synthesis, and RT-qPCR analysis

To confirm target gene knockdown in *StFHT*, *StFACT* and *StBAHD-At1g24430* plus empty vector control, pK7GWIWG2D(II) genotypes, total RNA was extracted from frozen, 3-day suberized tissues as described by Chang et al. (1993) with some modifications. First, autoclaved extraction buffer composed of 2% hexadecyltrimethylammonium bromide (CTAB), 2% polyvinylpyrrolidinone K30 (PVP), 100 mM Tris HCl (pH 8.0), 25 mM EDTA, 2.0 M NaCl, 0.5 g/L spermidine and 2% β -mercaptoethanol (added just before used), was warmed to 65°C in a water bath. Approximately 20-100 mg of suberized tissue was ground in liquid nitrogen and mixed quickly (by inverting the tube) with 0.75 mL extraction buffer. An equal volume of chloroform:isoamyl alcohol (CHCl₃:IAA) (24:1) was added to the samples, vortexed for 5 seconds, and centrifuged for 3 min at 10,000 rpm at room temperature in a microcentrifuge. The aqueous phase was collected and extracted twice more, with an equal volume of CHCl₃: IAA mix. Next, ¼ volume of 10 M lithium chloride (LiCl) was added to the collected aqueous phase, mixed, precipitated overnight at 4°C, and harvested by centrifugation at room temperature at 10,000 rpm for 30 min. After, the pellet was dissolved into 25 μ L of SSTE buffer (1.0 M NaCl, 0.5% SDS, 10 mM Tris HCl (pH 8.0), 1 mM EDTA), and precipitated again with 50 μ L of 100% ethanol at -80°C for 1 hour. Finally, the pellet was collected by centrifugation at 10,000 rpm for 20 min, dried, and resuspended in 20 μ L of diethylpyrocarbonate (DEPC) treated water. To assess the purity of the RNA, the samples were evaluated using a NanoDrop™ One Microvolume UV-Vis Spectrophotometers (Thermo Scientific) set for RNA determination. The purity of the RNA was evaluated following a spectrophotometer reading of A260/A280 >2.0 and A260/A30 ~2.0. RNA integrity was assessed using Agilent 2100 Bioanalyzer (RIN \geq 7). Next, RNA samples (0.1-0.2 μ g/50 μ L) were treated with Turbo DNase, to remove any contaminant DNA using the TurboDNA-free™ kit (Invitrogen), and cDNA was

synthesized using the Maxima Universal First Strand cDNA Synthesis Kit (Thermo Scientific) following manufacturer's protocols. Reverse transcription-quantitative PCR (RT-qPCR) analysis was performed to compare the gene expression between the wildtype, empty vector control, and the RNAi knockdown lines. The reaction was carried out using the synthesized cDNA, gene specific primers, (Appendix H), and PowerTrack™ SYBR Green Master Mix (Thermo Scientific) following manufacture's protocol. Primers for two endogenous controls EF1- α and APRT (Nicot et al., 2005) were used as a reference throughout the entire gene expression analyzes, for data normalization (Appendix H) The CFX Connect Real-time PCR Detection System (Bio-Rad) was used as the thermo cycler to run the samples. Primer efficiency was evaluated through a standard curve PCR reaction (in duplicate) using undiluted WT cDNA as the first point and performing a 1:10-dilution series (five points in total). To make sure there was no gDNA contamination, DNase treated RNA was used as the negative control, and to identify any other type of contamination, water was used as the non-template control (NTC).

The expression level between the WT and five biological replicates of the empty vector were measured in quadruplet using the target genes, specific primers (selected from the primer efficiency test). Once the expression level between the WT and the empty vector was determined, four biological replicates of the empty vector were used as the control to determine the knockdown level of the transgenic lines for each target genes. The reactions were measured in quadruplet, and after the amplification cycles were completed, melt curves were generated to assess whether the RT-qPCR reactions produced a single, specific product. Normalized expression ($\Delta\Delta Cq$) between the target genes transgenic lines and the empty vector were determined using the Cq value generated in the Bio-Rad CFX Manager software (version 3.1) and the relative to zero options, as there were four biological replicates of the empty vector as the control group.

2.10 Soluble waxes, soluble phenolic, and aliphatic suberin analyses

In order to establish whether target genes knockdown affected the poly(aliphatic) suberin domain, the aliphatic suberin and suberin-associated wax composition of wound-

induced microtuber periderm were analyzed by gas chromatography-mass spectrometry detector (GC-MS) and gas chromatography-flame ionization detector (GC-FID) as previously described by Meyer et al. (2011) with some modification. To determine whether the soluble phenolic compounds (i.e., alkyl ferulates) were affected, aliquots of the soluble extracts were analyzed by liquid chromatography-ultraviolet-mass spectrometry (LC-UV-MS) detector.

2.10.1 Wax analysis

Soluble lipids, including suberin-associated waxes, were extracted from frozen suberized periderm tissues (20-30 mg) using a micro-soxhlet extractor for 3.5 h (twice) with a mixture of chloroform and methanol ($\text{CHCl}_3/\text{CH}_3\text{OH}$, 2:1; v/v) followed by an overnight extraction with chloroform. The residual tissues were washed with acetone, air dried overnight in the fume hood, and stored at 4°C for the subsequent extraction of insoluble suberin compounds (Meyer et al., 2011). The chloroform and methanol extracts were pooled and dried on a rotary evaporator (Buchi, Switzerland) under vacuum at 40°C, quantitatively transferred to 4 mL glass vials and dried under a stream of nitrogen (N_2) gas. The dried soluble residues were redissolved with chloroform and methanol (2:1; v/v) in a fixed volume/mass ratio (1 mL/10 mg) to normalize the extracts, and 100 μL aliquots were transferred to a clean 4 mL glass vials and evaporated to dryness under nitrogen gas. The dried residues were then methylated (to yield methyl esters) by the addition of 3 M methanol/hydrochloric acid (500 μL) and heated at 80°C for 2 h in a water bath. The samples were cooled to room temperature, and 1 mL of saturated NaCl was added to stop the reaction. Triacontane (10 μL of 1 mg/mL stock) was added as the internal standard and the non-polar compounds extracted three times with 1 mL hexane each time. The hexane extracts were pooled into a clean vial and dried under a stream of N_2 gas. Finally, the samples were trimethylsilylated (TMS) by the addition of 50 μL each of pyridine and N,O-bis(trimethylsilyl)-trifluoroacetamide (BSTFA). After heating at 70°C for 40 min in a water bath, samples were cooled to room temperature and transferred to GC vials (Meyer et al., 2011). For calibration, a dilution series was prepared using ferulic acid standard as well as fatty acids, fatty alcohols, and omega-hydroxy fatty acids (ω -OH FAs) (100 $\mu\text{g}/\text{mL}$ - 0.024 $\mu\text{g}/\text{mL}$).

The samples were analyzed on a Varian CP-3800 Gas Chromatograph equipped with two detectors, the flame ionization detector (GC-FID) for quantification, and the Varian MS220 ion trap Mass spectrometer (GC-MS) for peak identification. In more detail, the GC was equipped with two CP-Sil 5 CB low bleed MS columns (WCOT silica 30 m x 0.25 mm ID). One of the columns was in line with the FID and the other one was in line with the MS. The injector temperature was programmed to 250°C, and FID oven was programmed to 300°C. The samples were injected to the columns (1 µL of samples for each column) in splitless mode and the compounds were eluted using the following oven program: 70°C for 2 min, increase to 200°C (40°C/min for 2 min), increase again to 300°C (3°C/min) and hold for 9.42 min, for a 50 min total run. The helium flow rate was set at 1 mL/min (Yang and Bernards, 2006; Meyer et al., 2011). Individual aliphatic compounds were quantified using calibration curves derived from authentic standards.

2.10.2 Soluble phenolic compounds analysis

Dried residues from 100 µL of the upper phase of the CHCl₃/CH₃OH (2:1; v/v) extracts (normalized to a fixed volume/mass ratio) were reconstituted in 40 µL CHCl₃. Then, 10 µL of 0.1 mg/mL ergosterol (in ethanol) were added as internal standard, and the samples diluted to 100 µL with methanol. For calibration, a dilution series (100 µg/mL down to 0.78 µg/mL) was prepared using a C22-alkyl ferulate standard. Standards were analyzed in triplicate. Alkyl ferulates were analyzed by LC-UV-MS in positive ion mode. Reconstituted samples (10 µL) were injected onto a C-8 column (Eclipse Plus RRHT, 2.1 x 50 mm, 1.8 mm; Agilent) and eluted with the following gradient: 70% A (0.1% formic acid in water), 30% B (0.1% formic acid in acetonitrile) for 2 min, followed by a linear gradient to 100% B over 10 min. After 15 minutes at 100% B, solvent conditions were brought back to 70% A/30% B and allowed to equilibrate for 12 minutes before the next sample was injected. The flow rate was set to 0.25 mL min⁻¹. Ferulates were quantified by UV absorbance at 324 nm, and identified by their exact mass ([M+1]⁺) using atmospheric pressure chemical ionization (APCI) in positive ion mode.

2.10.3 Aliphatic suberin analysis

The wax-free plant residues were used for the chemical depolymerization of insoluble aliphatic suberin. Dried periderm tissues (2-3 mg) were trans-esterified to hydrolyse the poly(aliphatic) domain by incubation at 80°C for 2 h with 500 μ L of 3 M MeOH/HCl (Meyer et al., 2011). This process allows for the release of esterified aliphatics as methyl esters and alcohols. The released aliphatics were recovered, TMS-derivatized and analyzed by GC-MS/FID using the same procedure as in Section 2.10.1.

2.11 Phenolic suberin analysis

Phenolic suberin monomer composition of wax-free, dried periderm tissues (Section 2.10) was analyzed using microscale nitrobenzene oxidation (NBO) according to Meyer et al. (1998) and as modified by Thomas et al. (2007) to quantify total phenolics, and derivatization followed by reductive cleave (DFRC) (Lu and Ralph, 1997) to quantify monolignols. The components released by these depolymerization methods were subsequently identified and quantified by GC-MS based on the retention time and quant ions.

2.11.1 Nitrobenzene oxidation

For the quantification of total poly(phenolics), extracted, dried periderm tissues (2-6 mg) were saponified with 1 M sodium hydroxide (5 mL) for 24 h at 37°C. The tissues were then washed with water (3 times), 80% methanol and 100% acetone (one time with each solvent) and air dried in the fume hood (Meyer et al., 1998; Thomas et al., 2007). Subsequently, 2 M sodium hydroxide (NaOH, 300 μ L) and nitrobenzene (15 μ L) were added to the saponified tissues (0.5-1 mg) in a 1 mL glass ampoule. The ampoules were flame-sealed and incubated at 160°C for 3 hours. When the samples cooled to room temperature, the ampoules were opened, and the internal standard was added: 20 mg/mL 3 ethoxy-4-hydroxybenzaldehyde (500 μ L to each sample) (Thomas et al., 2007). The samples were quantitatively transferred to 4 mL vials using water (about 2 mL) and the mixture was extracted twice with dichloromethane (1 mL). The aqueous phase was collected, acidified (pH 2) with 1 M hydrochloric acid (HCl), and extracted again with 900

μL of ethyl ether (twice). The organic ether phases were collected, dried over anhydrous sodium sulfate (Na_2SO_4), and evaporated to dryness under a stream of nitrogen gas (Meyer et al., 1998; Thomas et al., 2007). Finally, the samples were derivatized with 50 μL each of pyridine and BSTFA at 70°C for 40 min. Derivatized samples were transferred to GC vials and analyzed on an Agilent 7890A GC coupled with a Leco Pegasus BT mass spectrometer using the same column described in Section 2.10.1 and with the injector temperature programmed to 250°C. The samples (1 μL) were injected in splitless mode and eluted using the following oven program: initial temperature 140°C, hold for 4 min, increase to 300°C (12.5°C/min), and hold at 300°C for 3.6 min, for a 20 min total run. The helium flow rate was set at 1 mL/min (Meyer et al., 1998). The monomer composition of the poly(phenolic) domain of suberin was identified using the GC-MS by comparing the phenolic compounds with the trimethylsilyl (TMS) derivatives (*p*-hydroxybenzaldehyde, vanillin, vanillic acid, syringin, and syringic acid) obtained after the alkaline NBO degradation technique (Meyer et al., 1998; Thomas et al., 2007). Quantification of phenolic monomers was achieved using the quant ion integrated masses and normalized against the internal standard. Individual phenolic compounds were quantified using calibration curves derived from authentic standards.

2.11.2 Derivatization followed by reductive cleavage

For the quantification of monolignols, derivatization followed by reductive cleavage (DFRC) was used according to Lu and Ralph (1997). Briefly, extracted periderm tissue (5 mg) was transferred to a 4 mL glass vial to which 750 μL of acetylbromide (AcBr, 20:80 v/v stock) was added (as a derivatizing agent). The mixture was then incubated at 50°C for 3 hour and the solvent was evaporated under stream of N_2 gas. The residues were suspended in 750 μL acid solution (dioxane/acetic acid/water, 5:4:1, v/v/v), and 15 mg of zinc dust (the reductive agent) added. The mixture was agitated on a shaker (50 rpm) for 30 min. and then transferred quantitatively to a 30 mL separatory funnel using 3 mL of dichloromethane (CH_2Cl_2) and 4 mL of saturated ammonium chloride (NH_4Cl). Tetracosane (50 μL from a 1 mg/mL stock in methylene chloride) was added as the internal standard, and the pH of the solution was checked to make sure it was approximately 3 (Lu and Ralph, 1997). The mixture was thoroughly mixed, and after

separation, the water phase was re-extracted twice with 3 mL of CH₂Cl₂. The pooled organic phases were dried with magnesium sulfate (MgSO₄) and the solvent evaporated under nitrogen gas. Finally, acetyl derivatives were generated by the addition of 50 µL each of pyridine and acetic anhydride and incubated at room temperature for 40 min (Lu and Ralph, 1997). Derivatized samples were diluted in 400 µL CH₂Cl₂ and transferred to GC vial for GC-MS analysis. The GC-MS was the same used in Section 2.11.1; the parameters were as follow: the injector temperature was programmed to 250°C and the samples were injected into the column (1 µL, splitless mode). The compounds were eluted using the following oven program: 140°C for 4 min, increase to 240°C (3°C/min for 1 min), increase again to 310°C (30°C/min) and hold for 9.3 min, for a 50 min total run. The helium flow rate was set at 0.8 mL/min (Lu and Ralph, 1997). Individual monolignols were quantified using calibration curves derived from authentic standards.

2.11.3 Statistical analysis

All statistical analyses were performed using the GraphPad Prism software R (version 9.3.1) with a preset probability value of 0.05 ($p < 0.05$) to identify significant differences. For the gene expression data, one-way ANOVA followed by a post hoc Dunnett test were performed between four biological replicates of the WT and four independent empty vector lines. This was done to determine whether there were any differences in the expression levels between these two potential controls. Consequently, the empty vector independent lines were used as the control to check the gene expression of the target *StBAHD* gene knockdown lines. The RT-qPCR reaction was set up with four replicates for each transgenic line, and the data were analyzed using one-way ANOVA followed by the Dunnett test. The chemical analyses were done using three replicates of the identified RNAi knockdown lines for each *StBAHD* genes, and three independent empty vector transgenic lines. The data were normalized to the corresponding internal standard for each chemical analyses (refer to sections 2.10 and 2.11), and after, with the tissue surface area. Subsequently, to make sure the data were normally distributed, the values were log transformed, and a one-way ANOVA test follow by a post hoc Dunnett test were done to determine if there were differences in the suberin monomer compositions

for the poly(aliphatic) and poly(phenolic) domains among the empty vector control and the RNAi knockdown lines.

3 Results and Discussion

3.1 Identification of putative potato homologs

Potato homologs of Arabidopsis genes *At1g24430*, *AtASFT* (*At5g41040*), and *AtFACT* (*At5g63560*), with proposed and confirmed acyltransferase function (Woolfson, 2018), were identified through the search tools at the Spud DB Potato Genomics Resource along with RNA transcription data (Woolfson, 2018). A total of 11 potato candidate genes were selected based on sequence similarity (>50%), low E-value, and their expression level post-wounding (Appendix A and B). The inferred polypeptide sequence of the Arabidopsis and potato candidate genes were extracted to compile a multiple sequence alignment, and to construct a phylogenetic tree using a neighbor-joining algorithm (Figure 3.1). From the resulting tree, in combination with the RNA transcriptome data (Woolfson, 2018), three potato orthologs were selected for the subsequent analyses. In previous studies, the Arabidopsis genes *At5g41040* (ASFT) and *At5g63560* (FACT) were identified through co-expression analysis with suberin-associated genes (Wei et al., 2006; Molina et al., 2009). These genes were found together within the same clade in previous phylogenetic analyses (Molina et al., 2009; Yu et al., 2009), and the same clustering was observed in my analysis (Figure 3.1). In Arabidopsis, *AtASFT* was found to be involved in suberin biosynthesis and *AtFACT* was found to be involved in suberin-associated waxes (Molina et al., 2009; Kosma et al., 2012). Although these two genes have specific function, they are paralogs of one another, and they shared the same potato homolog genes with some variation in the percent sequence similarity (Appendix A and B). The potato gene with the protein sequence ID as PGSC0003DMP400054926 falls within the same clade as *AtASFT* (Figure 3.1). This gene was previously characterized by Serra et al., 2010, as a fatty ω -hydroxyacid/fatty alcohol hydroxycinnamoyl transferase (*StFHT*) and is the potato homolog for *AtASFT*. This potato ortholog shares 83% similarity with *AtASFT* according to the Spud DB Potato database. The phylogenetic relationship between

AtASFT and PGSC0003DMP400054926 (functionally identified as StFHT) was confirmed in my phylogenetic analysis (Figure 3.1), and this potato gene was selected as the candidate ortholog for the next steps. To select the potato homolog for the *AtFACT* gene, the next closely related clade included the PGSC0003DMP400024883 and PGSC0003DMP400019784 potato proteins. Out of these two genes, PGSC0003DMP400024883 was selected as the putative potato ortholog for the *AtFACT* gene (Figure 3.1), partly based on sequence similarity to AtFACT (56.2% according to the Spud DB Potato database), but also based on its expression level post-wounding (Woolfson, 2018) (Appendix B). For the *Atlg24430* gene two of the selected potato candidate genes clustered together with the *Arabidopsis* gene. Two genes (PGSC0003DMP400012715, PGSC0003DMP400028581) were more closely aligned with the protein encoded by the loci *Atlg24430* and from these two genes PGSC0003DMP400012715 (designated *St430*) was selected as the potato candidate gene for the analyses, based on the expression level post wounding (Woolfson, 2018) (Appendix B). Protein sequence alignments of the selected potato orthologous and the *Arabidopsis* genes (Appendix D) confirmed the presence of the two conserved motifs characteristic of the BAHD acyltransferase family, the HxxxD (with catalytic function) and DFGWG (located in the C-terminus) motifs (St-Pierre and De Luca, 2000; D'Auria, 2006).

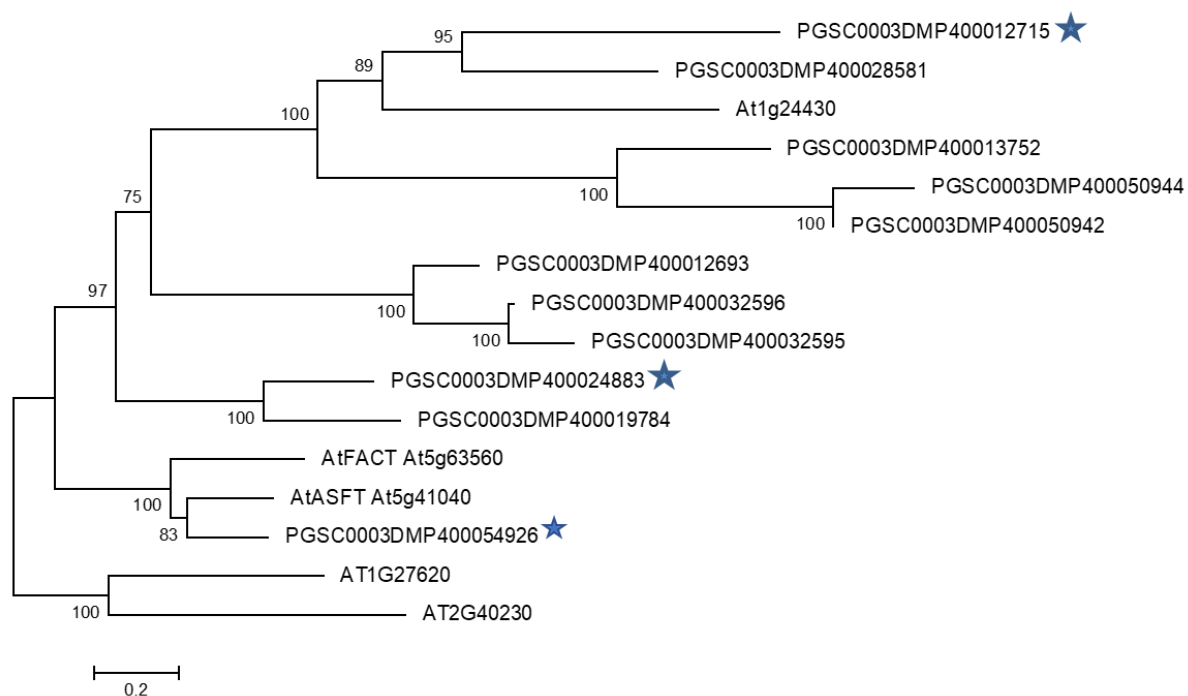


Figure 3.1 Phylogenetic analysis of select *A. thaliana* and potato candidate BADH acyltransferases. The phylogenetic tree was constructed using deduced protein sequences in FASTA format and multiple alignment was created using the MUSCLE program in MEGA version 6 (Tamura et al., 2013). The neighbour-joining option was used to generate the tree, with 1000 bootstrapped values to indicate the level of significance (%) of the branches. Two proteins encoded by the loci *At1g27620* and *At2g40230* were used as an outgroup. The stars indicate the selected potato candidates based on the wound-specific RNA expression data in Appendix B and this phylogenetic tree.

3.2 Generation and confirmation of StBAHD RNAi constructs

Once putative potato homologs were selected by sequence alignment, phylogenetic analysis, and expression pattern, RNAi constructs lines were generated following Gateway® cloning technology. To create the RNAi silencing constructs, gene specific target sequences of selected potato candidate genes (*StFHT*, *StFACT*, and *St430*) were cloned into the RNAi destination vector (pK7GWIWG2D(II), 0) in opposite orientation as described in section 2.5 and as illustrated in Appendix F. The final RNAi constructs were

screened by PCR using potato candidate gene specific forward primers, with either the vector chloramphenicol region forward primer (CmrF) or reversed primer (CmrR). This screening strategy allowed the visual identification and confirmation of the double insertion of the target specific sequences into the destination vector. The PCR reaction using the described primer combinations in section 2.5 generated two amplicons with different sizes to confirm the double insertion. Figure 3.2 illustrates the two amplicon sizes for each candidate genes. The primer combination between the gene specific forward primer with the CmrF generated a larger fragment compared to the primer combination between the gene specific forward primer and the CmrR. For *St430*, the expected amplicons sizes were 947 and 910 bps; for *StFHT* the expected products were 929 and 892 bps; and for *StFACT* the amplicons sizes were 976 and 939 bps (Figure 3.2). After PCR screening and sequencing confirmation, the final RNAi constructs were transformed into *Agrobacterium* and subsequently used for plant transformation. Plant internodes were co-cultured with individual *Agrobacterium* infection medium for 20 min and transferred to a callus induction media to allow the establishment of transgenic callus over four weeks. Next, explants with callus were transferred from the callus induction media to the shoot induction media, on which the first shoot primordia appeared from callus 63 days after the *Agrobacterium* infection, which was 25-30 days after the explants were transferred to the SIM media. Following the transfer of the elongated shoots into the root induction media, the leaves from mature *in-vitro* plants (from the gene specific transgenic plants) were used to extract the DNA for genotype analyses to confirm a successful plant transformation and the correct gene insertion into the transgenic plants. For *StFHT* transgenic plants a total of 17 transgenic lines were tested, 11 of which were confirmed to carry the gene insertion (64.7% transformation efficiency) (Appendix I and L). For *StFACT*, 13 transgenic lines were tested, with 12 out of the 13 lines being confirmed as successfully transformed with the gene insertion (92.3 % transformation efficiency) (Appendix I and K). For *St430*, the number of healthy transgenic plants was lower than the other two genes with only 4 out of 9 lines being confirmed as containing the target gene insertion (44.4 % transformation efficiency) (Appendix I and J). The empty vector was used to transform the potato plants as well, to be used as a control for the subsequent analyses, and in this case, the shoot primordia transformation rate was higher than the target genes specific transgenic lines. A

total of 26 lines were tested with 23 lines confirmed to have the vector insertion (88.5% transformation efficiency) (Appendix I, gel picture not shown).

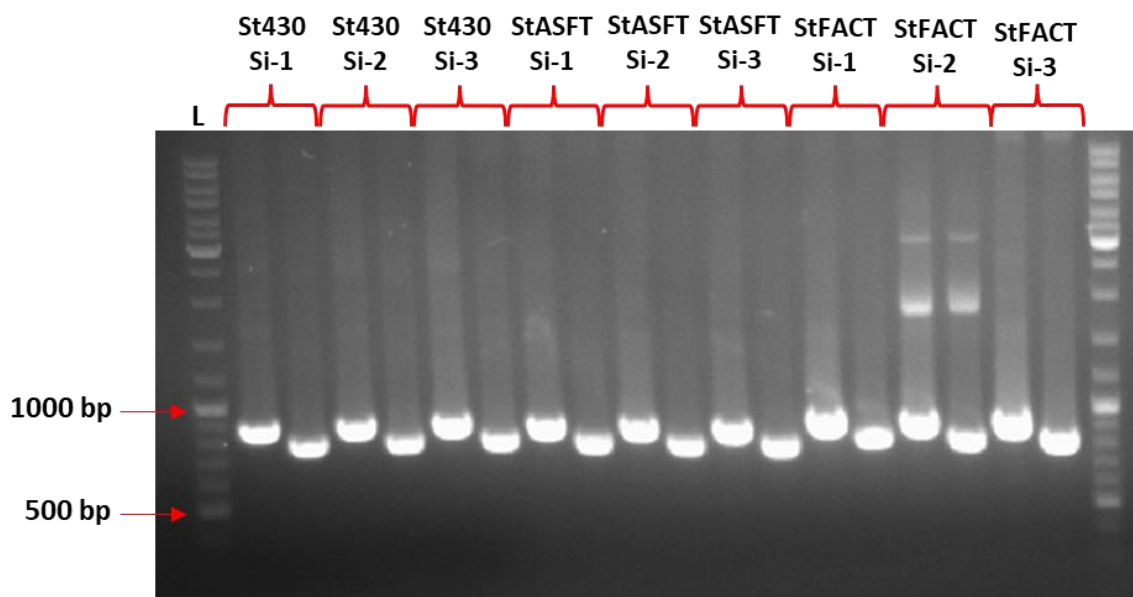


Figure 3.2 PCR screen of *StBAHD* candidate genes double insertion in the destination vector. Gene specific forward primers (*StBAHDsF*) and the vector chloramphenicol region forward and reverse primers (*CmrF* and *CmrR*) were used in the PCR reaction to produce two amplicons sizes for each specific genes. bp = base pair; L = ladder; Si = silencing; the numbers represent how many final constructs were tested for each gene.

3.3 Generation, selection, and characterization of transgenic lines

To determine target gene knockdown in *Stfht*, *Stfact* and *St430* transgenic lines plus gene expression levels in empty vector (EV) and wild type (WT) controls, microtubers were generated, and wounded. The RNA was extracted from the wound-induced suberized layer after 3 days of wound healing for the gene expression analysis by RT-qPCR. A comparison between microtubers from WT plants and the EV transgenic plants was done to evaluate the impact of the transformation on expression levels in the target genes and to select which one to be used as an appropriate control line for subsequent analyses (Figure 3.3. A). The RT-qPCR results showed that there was no significant difference in the expression levels in any of the three target genes between the WT and EV (Figure 3.3. A).

The empty vector transgenic lines were then chosen as the control to determine the knockdown level of the target gene transgenic lines. For the *St430* transgenic lines, out of the four confirmed lines (Appendix I), only three were tested by RT-qPCR since one of the transgenic plants did not grow fast enough to include in the analysis. It is important to note that in this regard the *St430* transgenic plants were phenotypically different compared to the WT and the EV plants as well as the transgenic plants for the other two gene knockdown lines (pictures not shown). The growth rate of the *St430* transgenic plants was slower than the other plants. Out of the three *St430* transgenic lines analyzed by RT-qPCR, line 1 appeared to be an overexpression line when compared to the empty vector, while there was no difference in expression level between line 2 and the EV control. However, in line 3, *St430* gene expression was knocked down by 57% compared to the EV control (Figure 3.3. B). Based on this result, for the *St430* gene, only one line was confirmed to have a greater than 50% knockdown level, by the gene expression analysis (Appendix M). For the *StFACT* transgenic plants, 9 out of 13 transgenic lines (confirmed by PCR) were screened by RT-qPCR (Appendix M). From these nine lines, four were confirmed knockdown lines when compared to the empty vector control (Figure 3.3. C). Here line 1 had a 62.8% knockdown level, line 2 had a 72.2% knockdown level, and lines 3 and 4 had 72.5% knockdown levels. Since four lines were sufficient for the chemical analysis, no further screening was done for the *StFACT* gene. Finally, for the *StFHT* transgenic plants, 7 out of the 11 confirmed (by the genotype analysis) transgenic plants were screened by RT-qPCR (Appendix M). From these seven plants, four were confirmed knockdown lines (greater than 50%) when compared to the EV control (Figure 3.3. D). Line 1 had a 57.2% knockdown level, line 2 had a 57.8% knockdown level, and lines 3 and 4 had 67.8% knockdown levels. Since four lines for the *StFHT* genes were knockdown, no further screening was done.

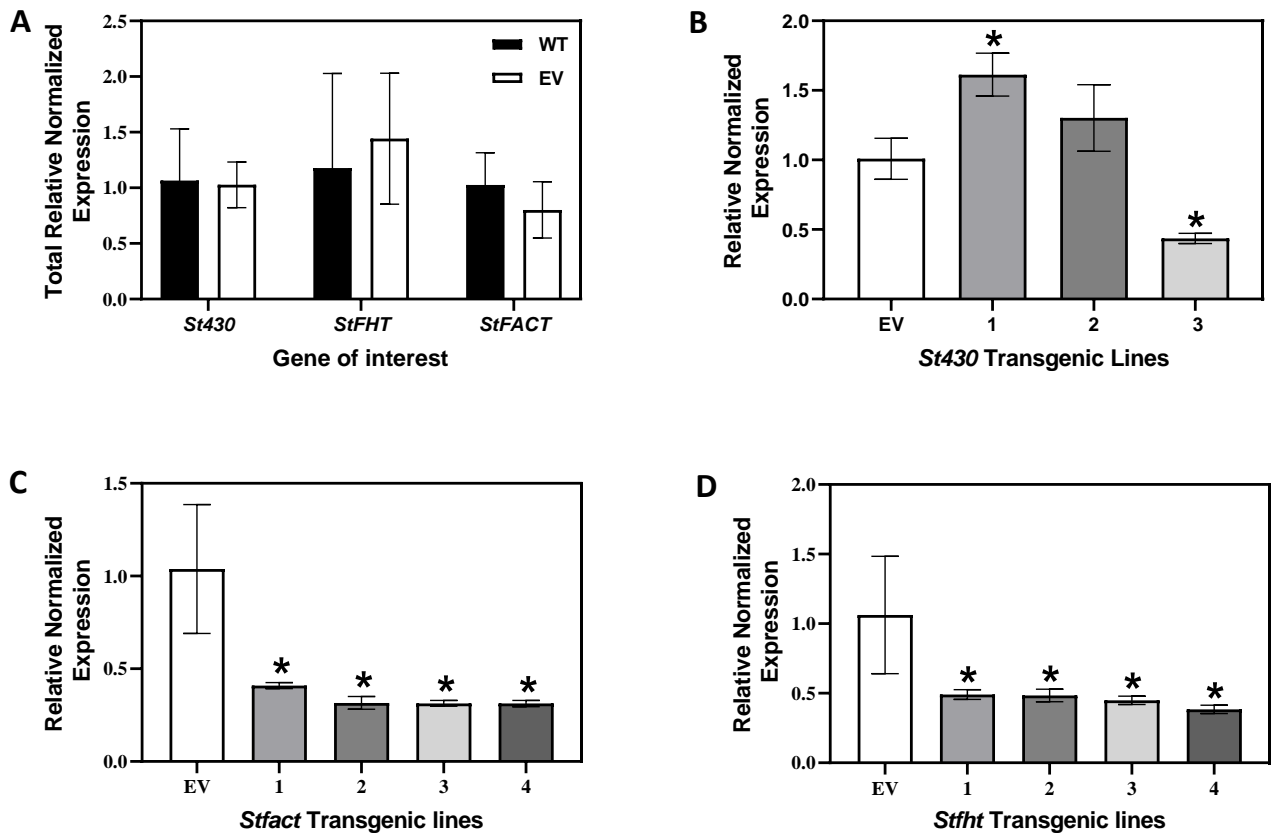
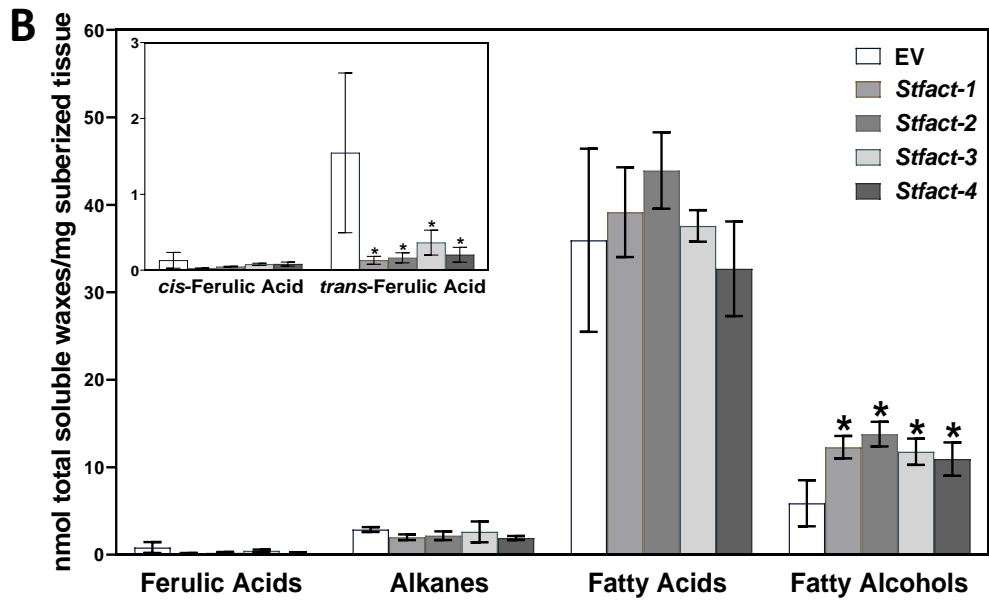
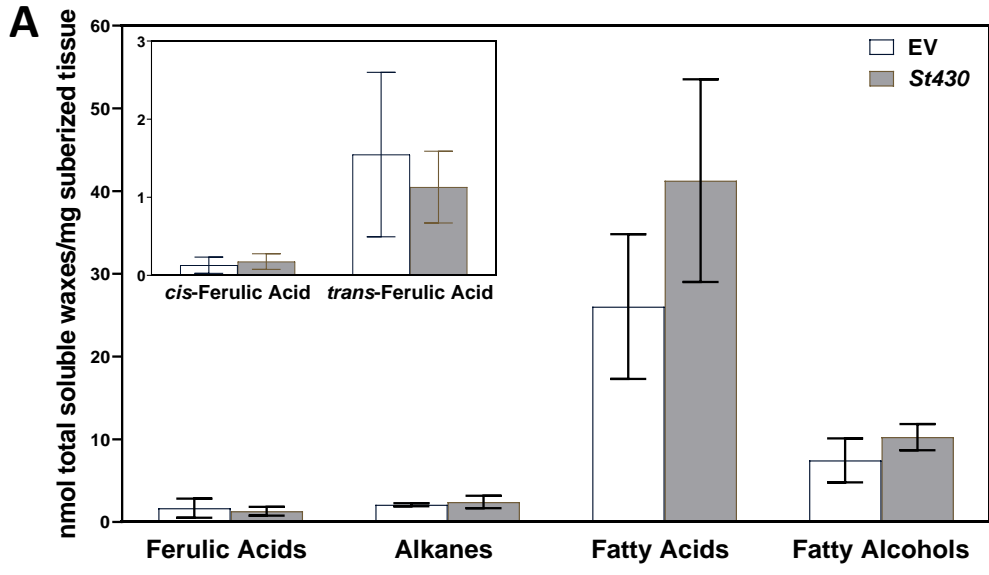


Figure 3.3. Target gene expression in empty vector control and RNAi knockdown lines post-wounding. Relative expression levels of *St430*, *StFHT*, *StFACT* in empty vector (EV), wild type (WT) and knockdown transgenic lines in wound suberizing tissue three days post-wounding was measured by RT-qPCR. Gene expression values were normalized with *StEF1- α* and *StAPRT* as the endogenous control genes. One-way ANOVA follow by Dunnett test (* $p < 0.005$) were performed to determine the significant differences in gene expression between the control and the target groups. (A) Comparison of the total normalized expression levels between the WT and EV using target genes specific primers. (B) Normalized expression level of *St430* in three *St430* transgenic lines compared to the EV control. (C) Normalized expression level of *StFACT* in four *Stfact* transgenic lines relative to the EV control. (D) Normalized expression level of *StFHT* in four *Stfht* transgenic lines in comparison with the EV control. Data are presented as the sample mean \pm SD (n = 4).

3.4 Effects of *StBAHD*-RNAi knockdown lines on wax composition and soluble phenolic

To establish the effects of the target *StBAHD* RNAi knockdown lines on the composition of suberin associated waxes, soluble waxes were extracted from wound induced suberized periderm tissues using a micro-soxhlet extraction apparatus with a mixture of chloroform: methanol (2:1 v/v) solvents, and the extracted components were analyzed by gas chromatography. Soluble ferulic acid-long chain alcohol esters (alkyl ferulates) were analyzed from the chloroform: methanol extracts by LC-UV-MS. For the *St430* transgenic line, after methanolic transesterification, the quantity of total soluble waxes, and the geometric isomers of ferulic acid were not significantly different relative to those in the EV control (Figure 3.4. A). Similarly, the overall individual wax compounds were not affected in the *St430* line when compared to the EV with only a significant increase in the C20:0 fatty acid and C22:0 fatty alcohol (Appendix N, A). In the *StFACT* knockdown lines (*Stfact-1*, *Stfact-2*, *Stfact-3*, and *Stfact-4*), the most significant impact of gene knockdown on waxes was seen in the reduction of *trans*-ferulic acid and increase on fatty alcohols compared to the EV control (Figure 3.4. B). Individual wax compounds in the *StFACT* transgenic lines were only affected in a few components (Appendix N, B). For example, *Stfact-1* showed a significant increase in the C22:0 and C26:0 fatty acids, in the very-long-chain fatty alcohols C22:0, C24:0, C26:0, C28:0, and C30:0, and a significant reduction in the C24:0 fatty acid. *Stfact-2* showed a significant reduction in the C24:0 fatty acid as well as a significant increase in the C26:0 and C22:0 ω -OH fatty acids and fatty alcohols (C22:0, C24:0, C28:0 and C30:0). Similarly, *Stfact-3* and *Stfact-4* had significantly increased C24:0 and C22:0 ω -OH fatty acids and C22:0, C24:0 and C30:0 fatty alcohols. Additionally, *Stfact-3* showed a significant increase in the C28:0 fatty alcohol (Appendix N, B). The amount and composition of suberin associated waxes in the *Stfht* transgenic lines showed a similar pattern to that seen in the *Stfact* lines. That is, the main significant difference was in the reduction of *trans*-ferulic acid in *Stfht-2* and *Stfht-3* transgenic lines. The *Stfht* transgenic lines were significantly reduced in the total alkane (Figure 3.4. C). A few individual components of the other soluble waxes were also reduced in some of the *StFHT* transgenic lines. For example, there was a significant increase in C18:0 (*Stfht-1* and *Stfht-2*), C24:0 (*Stfht-1*), C26:0 (*Stfht-1*, *Stfht-2*, and *Stfht-*

3), C28:0 (*Stfht-1*) and a significant reduction in C24:0 (*Stfht-2*) saturated fatty acids. Additionally, there was a significant reduction in the C16:0 (*Stfht-2*, and *Stfht-3*) and a significant increase in the C28:0 (*Stfht-1 and Stfht-3*) and C30:0 (*Stfht-3*) free fatty alcohols (Appendix N, C).



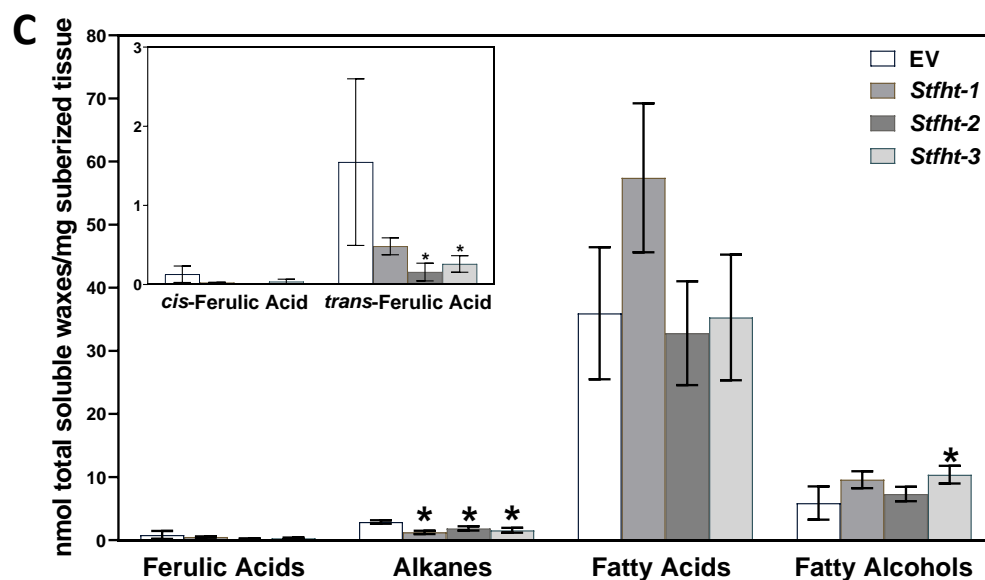
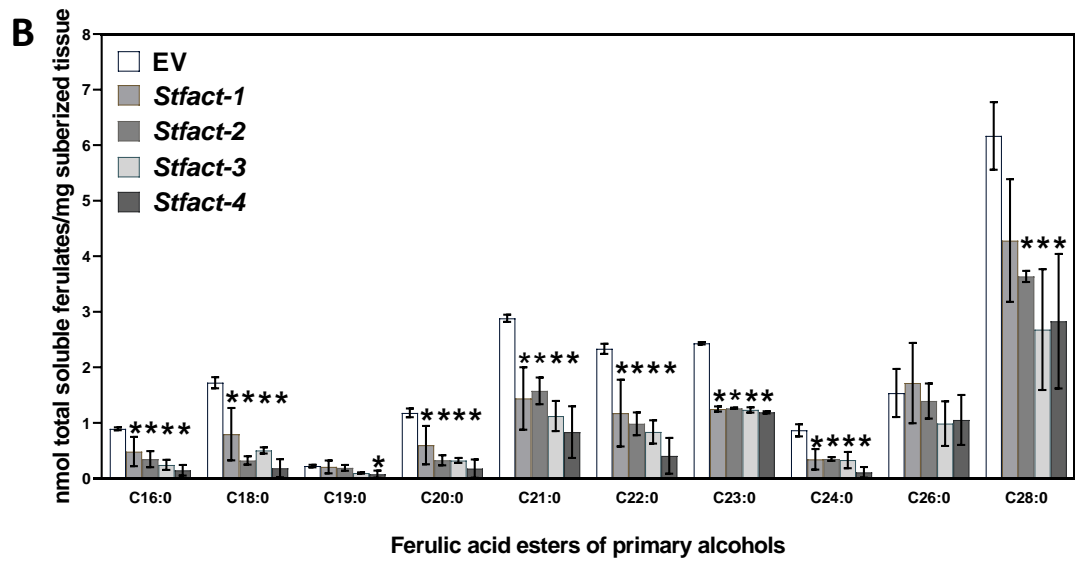
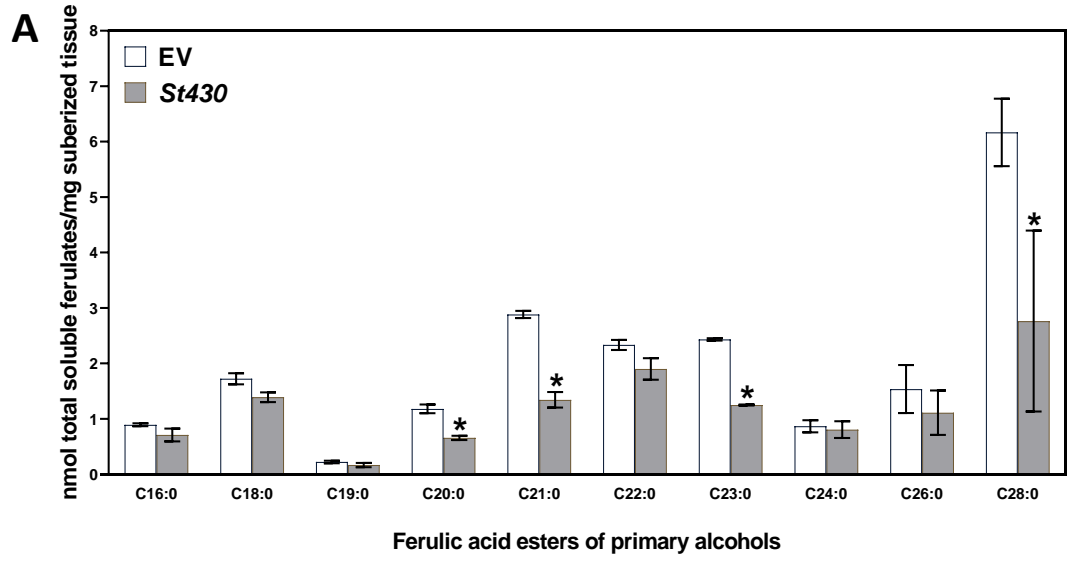


Figure 3.4. Soluble wax composition of potato knockdown lines. Total suberin-associated wax compounds of *StBAHD* RNAi knockdown lines and empty vector were released from wound induced suberized periderm tissues after chloroform: methanol (2:1 v/v) treatment and analyzed by GC-MS/GC-FID. Soluble waxes were extracted from (A) *St430*, (B) *Stfact* (*Stfact-1*, *Stfact-2*, *Stfact-3*, *Stfact-4*), and (C) *Stfht* (*Stfht-1*, *Stfht-2*, *Stfht-3*) transgenic lines, and empty vector (EV) control. Data are presented as the mean \pm SD of three biological replicates ($n = 3$, for each RNAi transgenic lines), and three independent empty vector ($n = 3$). Asterisks denote significant differences from empty vector control (one-way ANOVA followed by Dunnett test, $p < 0.05$).

Regarding soluble alkyl ferulates, in the *St430* transgenic line, the relative amounts of C20:0, C21:0, C23:0, and C28:0 alkyl ferulates (i.e., ferulic acid esterified to C20, C21, C23, and C28 fatty alcohols, respectively) were reduced compared to the EV control (Figure 3.5. A). Individual isomers of ferulic acid esters of primary alcohols in the *St430* transgenic line showed a significant reduction in the *cis* isomers (C16:0, C18:0, C20:0, C21:0, C22:0, C24:0 C26:0 and C28:0) and in a few of the *trans* isomers (C21:0, C23:0, and C28:0) (Appendix O, A). The level of total alkyl ferulates in *StFACT* RNAi knockdown lines were more significantly affected than the *St430* RNAi knockdown line. *StFACT* transgenic lines *Stfact-1* *Stfact-2*, *Stfact-3*, *Stfact-4* showed a significant decrease in the C16:0, C18:0, C19:0 (only in *Stfact-4*), C20:0, C21:0, C22:0, C23:0, C24:0, and C28:0 (except *Stfact-1*) ferulates when compared to the EV control (Figure 3.5. B). Unlike the *St430* transgenic line, individual geometric isomers of alkyl ferulates for *StFACT* transgenic lines, were affected in both *cis* and *trans* isomers (Appendix O, B). For instance, line *Stfact-1* showed a significant reduction in the C16:0, C22:0, and C24:0 *cis* and *trans* isomers, C18:0, C19:0, C21:0, and C23:0 *trans* isomers, C26 *cis* isomer, and a significant increase in *cis*-C19. Lines *Stfact-2*, *Stfact-3*, and *Stfact-4* showed a similar chemical phenotype with some variation. Together *Stfact-2*, *Stfact-3*, and *Stfact-4* showed significant reduction in the C16:0, C18:0, C20:0 (*cis* and *trans* isomers), C21:0 (*trans* isomer), C22:0 (*cis* and *trans* isomers), C23:0 (*trans* isomer), C24:0 (*cis* and *trans* isomers) and in C26:0 and C28:0 (*cis* isomers). Line *Stfact-3* and *Stfact-4* also showed a significant reduction in *trans*-C22 and *trans*-C28 (Appendix O, B). With regard to the *StFHT* RNAi knockdown lines, *Stfht-1*, *Stfht-2*, and *Stfht-3* were significantly affected in all alkyl ferulates as a whole (except the C26:0 chain length) when compared to the EV, while only the C26:0 alkyl ferulate was significantly decrease in *Stfht-2* (Figure 3.5. C). Individual ferulates isomers were significantly affected in the *trans* (C16:0, C18:0, C19:0, C21:0, C22:0, C23:0, C24:0, and C28:0) and *cis* isomers (C16:0, C18:0, C20:0, C22:0, C24:0, C26:0, and C28:0) in lines *Stfht-1*, *Stfht-2*, and *Stfht-3* with a few variations. *Trans*-C20 was only significantly reduced in line *Stfht-2*, and *cis*-C21 was decrease in lines *Stfht-1* and *Stfht-2* only (Appendix O, B).



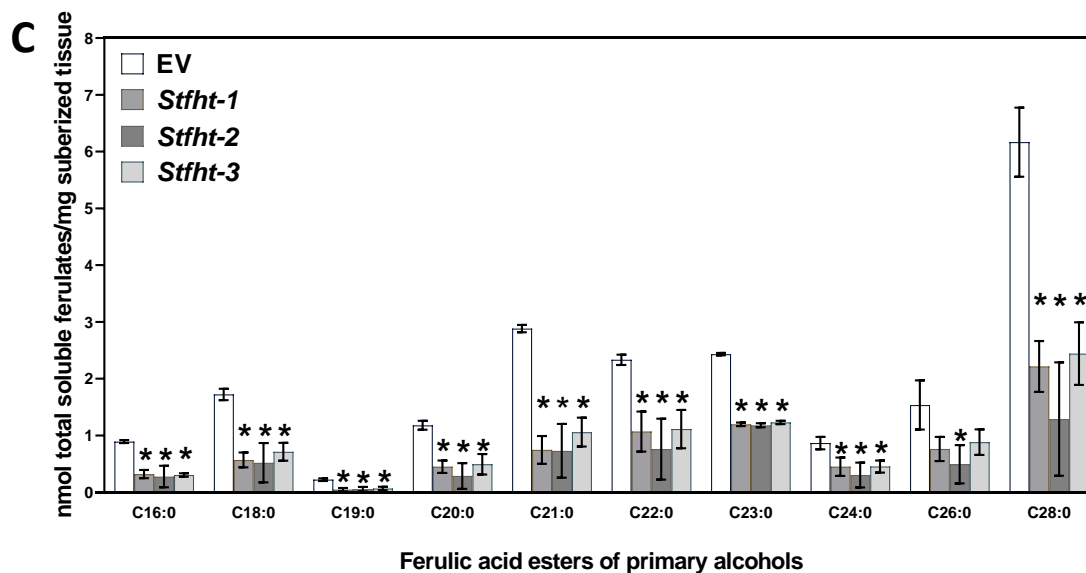


Figure 3.5. Total soluble ferulic acid esters composition of primary alcohols. Dried residues aliquot of the chloroform: methanol (2:1 v/v) treated samples were redissolved in methanol and analyzed by LC-UV-MS. Soluble phenolics were extracted from (A) *St430*, (B) *Stfact* (*Stfact-1*, *Stfact-2*, *Stfact-3*, *Stfact-4*), and (C) *Stfht* (*Stfht-1*, *Stfht-2*, *Stfht-3*) transgenic lines, and empty vector (EV) control. Data are presented as the mean \pm SD of three biological replicates ($n = 3$, for each RNAi transgenic lines), and three independent empty vector ($n = 3$). Asterisks denote significant differences from empty vector control (one-way ANOVA followed by Dunnett test, $p < 0.05$).

Overall, the soluble wax and alkyl ferulate phenotype of the *StFHT* transgenic lines was similar to that described by Serra et al. (2010) and Jin et al. (2018), providing some confidence in assessing the new aspects of the knockdown phenotype. A similar chemical phenotype of the soluble components (waxes and alkyl ferules) was showed in the *StFACT* transgenic lines. This result provides some confirmation that this gene is a BADH acyltransferase involved in alkyl ferulate biosynthesis. The impact of *Stfact* and *Stfht* knockdown on other wax components was less obvious, and inconsistent across different lines. By contrast, the wax phenotype of *St340* was not significantly different than that of the EV control. For the soluble phenolics, only a few alkyl ferules were affected, but there was not an impact overall. Based on this, *St430* does not appear to be involved in alkyl ferulate biosynthesis in potato.

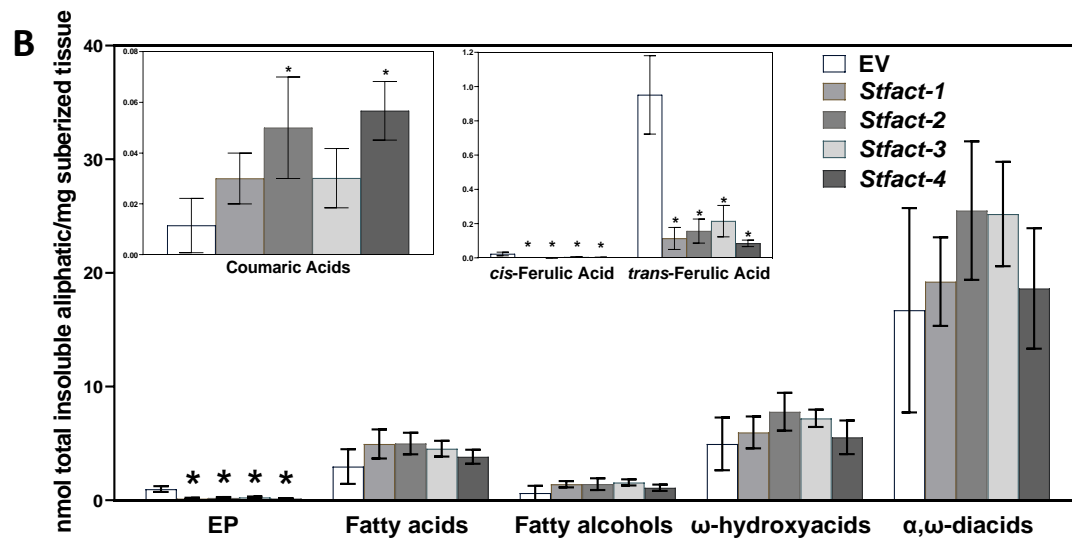
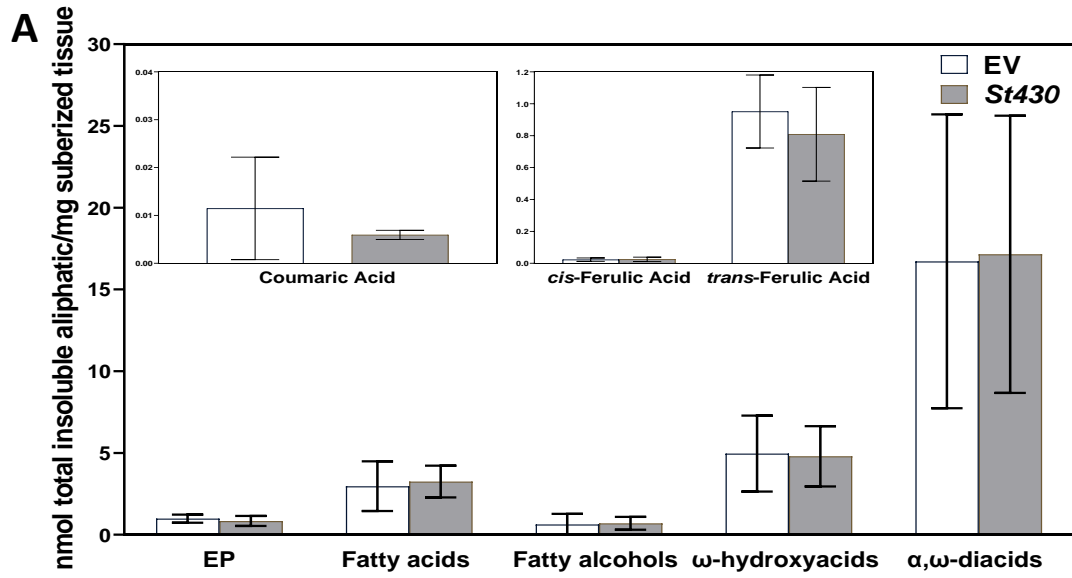
3.5 Effects of StBAHD-RNAi knockdown lines on aliphatic suberin

The effect of *StBAHD* gene knockdown in the RNAi lines on the aliphatic suberin composition was analyzed using methanolic-HCl transesterification and gas chromatography-mass spectrometry. For the *St430* transgenic lines, the total load of monomers released after transesterification of delipidated suberized periderm tissues showed no significant difference from the EV control (Figure 3.6. A). The individual concentrations of monomers in the insoluble aliphatic domain were also indistinguishable from the EV control in the *St430* transgenic line (Appendix P, A and B). The levels of esterified phenolic, ferulic acid, and coumaric, were not affected in the knockdown line of this gene (Figure 3.6. A). In the case of the *Stfact* transgenic lines, only the levels of hydroxycinnamates were significantly affected in the total load of monomers released by transesterification. For example, transgenic lines *Stfact-1*, *Stfact-2*, *Stfact-3*, and *Stfact-4* showed a significant reduction in the total concentration of hydroxycinnamates (Figure 3.6. B). Upon closer inspection, however, I found that the level of *p*-coumaric acid was significantly increased only in lines *Stfact-2* and *Stfact-3*, while transgenic lines *Stfact-1*, *Stfact-2*, *Stfact-3*, and *Stfact-4* all showed a significant reduction in both *cis*- and *trans*-ferulic acid isomers (Figure 3.6. B). Individual insoluble monomers compounds in the *Stfact* transgenic lines were not significantly different compared to the EV control overall

(Appendix O, A and B). The *Stfht* transgenic lines showed a similar phenotype to that described for the *Stfact* lines (Figure 3.6. C). Specifically, the total aliphatic suberin monomers composition was not affected by the knockdown expression of the gene, but the total hydroxycinnamates, in particular the ferulic acid isomers, were significantly reduced in lines *Stfht-1*, *Stfht-2*, and *Stfht-3*. There were no changes in *p*-coumaric acid levels, compared to the empty vector control (Figure 3.6. C). With regard to the individual insoluble monomers in the *Stfht* transgenic lines, there were no significant differences when compared to the EV control (Appendix R, A and B)

In general, the results obtained indicate that the *St430* gene does not play a role in the synthesis of the aliphatic domain of suberin. This result is consistent to the preliminary analysis with *Arabidopsis thaliana* mutants (Castillo, 2016); although there were no changes in the load of aliphatic suberin, gene redundancy with other BAHD genes cannot be ruled out. Regarding the *StFHT* transgenic lines, the major changes observed were in the hydroxycinnamic acids, in particular ferulic acid. The hydroxycinnamic acids released by transesterification represent “esterified” phenolics commonly associated with the aliphatic domain of suberin. These represent a distinct pool of compounds from the hydroxycinnamic acids (including alkyl ferulates) analyzed as part of the soluble waxes. However, like the alkyl ferulates, esterified phenolics are likely incorporated into the poly(aliphatic) domain of suberin via an acyltransferase. The significant change in ferulic acid for the *StFHT* transgenic lines was similar to the results described by Serra et al., (2010), proving once more the function of this gene as a feruloyl transferase. Serra et al. (2010) also found an overall increase in coumaric acid, and in most of the individual monomer compounds, as well as a significant decrease in longer chain of primary alcohols (C24:0, C26:0, C28:0, and C30:0) and the C18:1 ω -hydroxy fatty acid. However, contrasting with Serra et al., (2010) results, my analysis indicated that there were no major changes in the insoluble aliphatic compounds compared to the empty vector. Although my data show a similar trend for some of the monomer such as C18:1 ω -hydroxy fatty acid, and the shorter chain of fatty alcohols, only three replicates (for each transgenic lines and EV control) were used for the analysis. This means that there is not enough statistical power to claim significant differences between the knockdown lines and the empty vector

control. Also, Serra et al., (2010) presented their data as the relative amount of percent mass which makes it difficult to determine how different the lipid monomer compositions of the FHT knockdown lines described in their paper were compared to the WT control. Regarding the *StFACT* transgenic lines, a similar chemical phenotype in the ferulic acid content was showed in the knockdown lines. This result also supports the conclusion that this BAHD acyltransferase gene plays a role in the synthesis of suberin. Other insoluble aliphatic components were not affected in the *Stfact* knockdown lines while the trends in the chemical phenotype indicated that there could be an increase in some of the fatty acid contents (C24:0 and C26:0); however more replicates are needed to eliminate the variation in the data, and for a stronger statistical power.



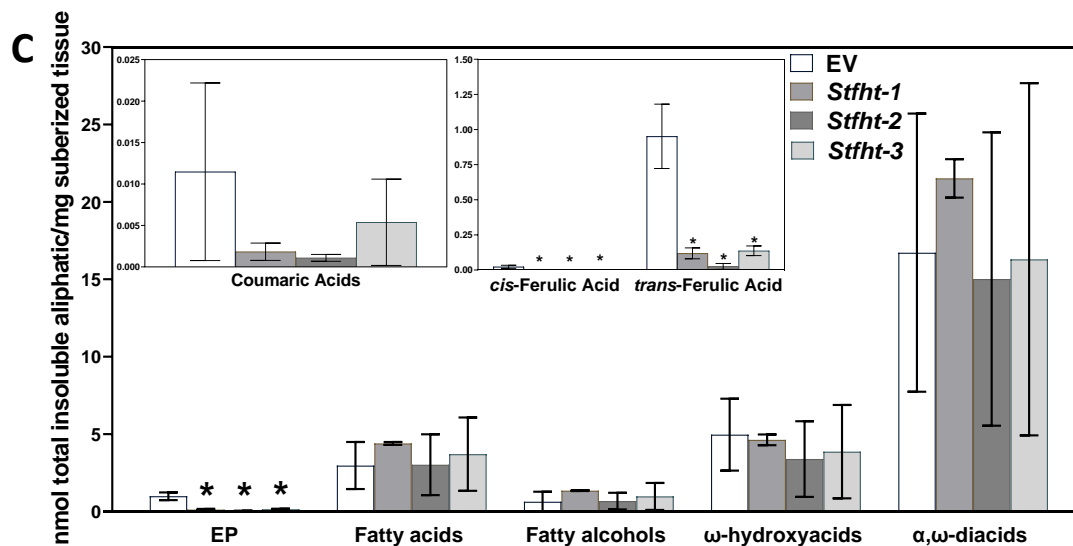


Figure 3.6. Total aliphatic suberin monomers composition in wounded potato microtuber. Total insoluble aliphatic suberin monomers were released after methanolic trans-esterification of wax-free suberized tissues from the from (A) *St430*, (B) *Stfact* (*Stfact-1*, *Stfact-2*, *Stfact-3*, *Stfact-4*), and (C) *Stfht* (*Stfht-1* *Stfht-2*, *Stfht-3*) transgenic lines, and empty vector (EV) control. Data are presented as the mean \pm SD of three biological replicates ($n = 3$, for each RNAi transgenic lines), and three independent empty vector ($n = 3$). Asterisks denote significant differences from empty vector control (one-way ANOVA followed by Dunnett test, $p < 0.05$). EP, esterified phenolics.

3.6 Effects of *StBAHD*-RNAi knockdown line on cell wall phenolics

One of the main objectives of this study, was to evaluate the impact of the target *StBAHD* acyltransferase knockdown lines on the formation of the poly(phenolic) domain of suberin. To quantify the monolignol composition in wax-free wound induced periderm tissues, the DFRC technique developed by Lu and Ralph in 1997, was used to cleave β -aryl ethers (β -O-4) in the phenolic polymers within the suberized tissues (reviewed in Bernards, 2002). In lignified tissues, the DFRC technique yields 20-40% of lignin monomers, which is equivalent to the results obtained from thioacidolysis. On the other hand, the thioacidolysis and DFRC analyses in suberized potato tissues only yields about 10% of monolignols when compared to lignified tissues (review in Bernards, 2002). Razem and Bernards (2002) found that in suberized potato tissues, the amount of syringyl alcohol diacetate (S unit) and coniferyl alcohol diacetate (G unit) released after the DFRC procedure, are significantly lower than the amount of monolignol released from lignified tissues. The results obtained in this study (Figure 3.7) are consistent with amount of monolignols that could be observed/recovered from wound-induced suberized potato tissues (Bernards et al., 1995; Negrel, et al., 1996). Only two monolignols were recovered as their diacetate derivatives: coniferyl alcohol and sinapyl alcohol, (Figure 3.7). This is consistent with earlier reports of monolignols in potato suberin (Negrel et al., 1996; Jin et al., 2018). In the *St430* transgenic line the total load of monolignols showed no significant differences compared to the EV control (Figure 3.7. A). On the contrary, all the transgenic lines for the *StFACT* gene showed a significant reduction in monolignol concentration when compared to the empty vector, indicating a possible function for this gene in the formation of the poly(phenolic) domain of suberin (Figure 3.7. B). In the *Stfht* knockdown lines, *Stfht-1* and *Stfht-2* showed a similar significant reduction in both coniferyl and sinapyl alcohols, while *Stfht-3* showed a significant reduction in sinapyl alcohol levels only (Figure 3.7. C).

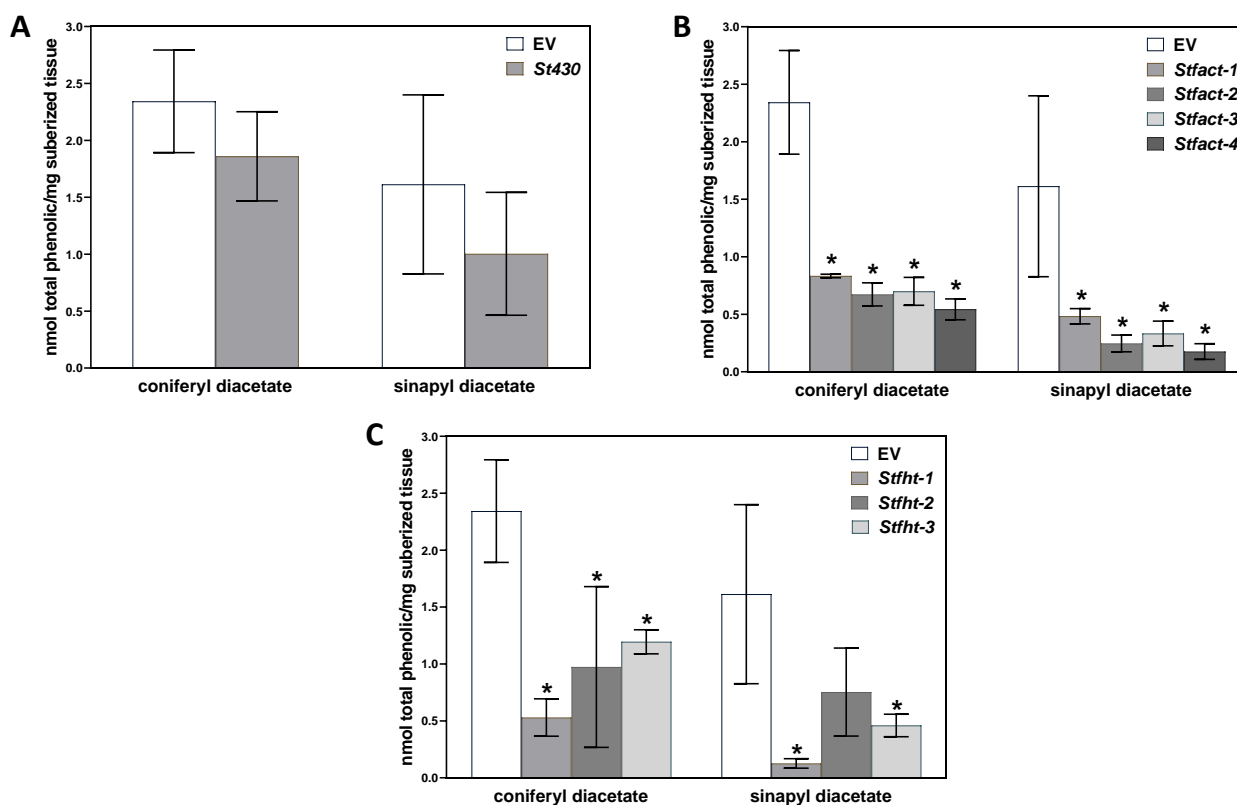


Figure 3.7. Total monolignols composition in wound induced suberized tissues.

Monolignols were extracted from (A) *St430*, (B) *Stfact* (*Stfact-1*, *Stfact-2*, *Stfact-3*, *Stfact-4*), and (C) *Stfht* (*Stfht-1*, *Stfht-2*, *Stfht-3*) transgenic lines, and empty vector (EV) control. The samples were quantified by the derivatization followed by reductive cleavage (DFRC) method and analyzed by GC-MS. Data are presented as the mean \pm SD of three biological replicates ($n = 3$, for each RNAi transgenic lines), and three independent empty vector ($n = 3$). Asterisks denote significant differences from empty vector control (one-way ANOVA followed by Dunnett test, $p < 0.05$)

As a complementary method to DFRC, and to observe the full composition of cell wall phenolics, as well as to potentially understand the function of the *StBAHD* genes in the formation of the poly(phenolic) domain of suberin, nitrobenzene oxidation (NBO) was used. This degradative technique was used to quantify total phenolics and results in the cleavage of phenylpropanoid side chains. The resulting yield includes a range of aromatic derivatives including benzaldehydes and benzoates (reviewed in Bernards, 2002). The problem with this technique is that the identity of the parent phenolic compounds is lost, and only the aromatic ring substitution patterns are preserved: e.g., *p*-hydroxyphenyl, guaiacyl (i.e., 3-methoxy-4-hydroxy) and syringyl (3,5-dimethoxy-4-hydroxy). Thus, the data cannot be used to differentiate between monolignols, hydroxycinnamic acids and other phenolics such as tyramine (Bland and Logan, 1965; Borg-Olivier and Monties, 1993; review in Bernards 2002). In this study, the total amount of phenolics in the *StBAHD* knockdown lines was not affected (Figure 3.8). That is, there were no differences in the amounts of phenolics in the cell walls of any of the lines analyzed. Unfortunately, there was substantial variation in the data, which could be due to the limited amount of tissues used in the analysis and/or the number of replicates, precluding a more rigorous statistical analysis.

The results from both the DFRC and the NBO analyses in combination, could indicate that *St430*, *StFACT*, and *StFHT* genes may not have any function in the phenolic domain of suberin, or any involvement in the ester link between the poly(aliphatic) and poly(phenolic) domains. Few papers include the poly(phenolic) analysis of BAHD acyltransferase knockdown lines, in *Arabidopsis* for example, Gou et al. (2009) performed thioacidolysis on acyltransferase *At5g41040* mutants lines, albeit with seeds, and little new information was gained. Gou et al. (2009) mentioned that due to the complex structural and chemical composition of the phenolic domain of suberin, as well as the possible degradation of the aromatics in the poly(phenolic) domain due to the harsh chemical analysis that is needed to break the ether and carbon-carbon bonds, it is difficult to identify and quantify all the phenolics. In potato, Jin et al. (2018) performed thioacidolysis analysis on the *FHT*-RNAi and WT native periderm tissues. The authors were able to detect the G and S units, but not the H unit, observing that the proportion of G units was higher than

that of the S units, which is consistent with a previous report on potato periderm (Lapierre et al., 1995). In addition, Jin et al. (2018) concluded that, although there were no statistical differences between the WT and the *FHT*-RNAi native periderm tissues, the G unit to S unit ratio was higher in the *FHT*-RNAi tissue compared to the WT. The result obtained from the thioacidolysis analysis is equivalent to the result obtained from the DFRC analysis, since the two techniques are based on the same chemistry (Lu and Ralph, 1997). In this thesis using the DFRC method, I analyzed the monolignol content in the wounded periderm. I was able to identify the G and the S units, but not the H unit, consistent with previous analyses (Lapierre et al., 1995; Jin et al., 2018). In opposite to the study done by Jin et al. (2018), I found a significant difference in the monolignol content of the wound periderm of *fht* transgenic lines. This discrepancy could be related to the tissue analyzed, since I performed the DFRC analysis on wounded periderm tissues while Jin et al. (2018) analyzed in the native periderm.

The total amount of monolignols recovered from the DFRC analysis, supports the statement that the SPPD is a lignin-like polymer, very little relative to other phenolics (likely hydroxycinnamic acids and their derivatives) released by NBO treatment. This confirms that the poly(phenolic) domain of potato suberin contains less monolignol than other phenolics and emphasize the differences between lignin and the SPPD of suberin. This means that the observed impact in the *StFACT* and *StFHT* transgenic lines on the monolignol levels is likely not that important to determine the involvement of these genes in the phenolic domain of suberin. Also, in the context of the overall macromolecular structure of potato suberin, the composition of the poly(phenolic) domain differs from that of the esterified phenolics in the poly(aliphatic) domain. The phenolic domain contains p-hydroxyphenyl (H), guaiacyl (G), and syringyl (S) units whereas the esterified phenolics are mostly G unit, supporting the proposed two domain model for suberin. To confirm these results, the experiment should be repeated with more tissues, and more replicates.

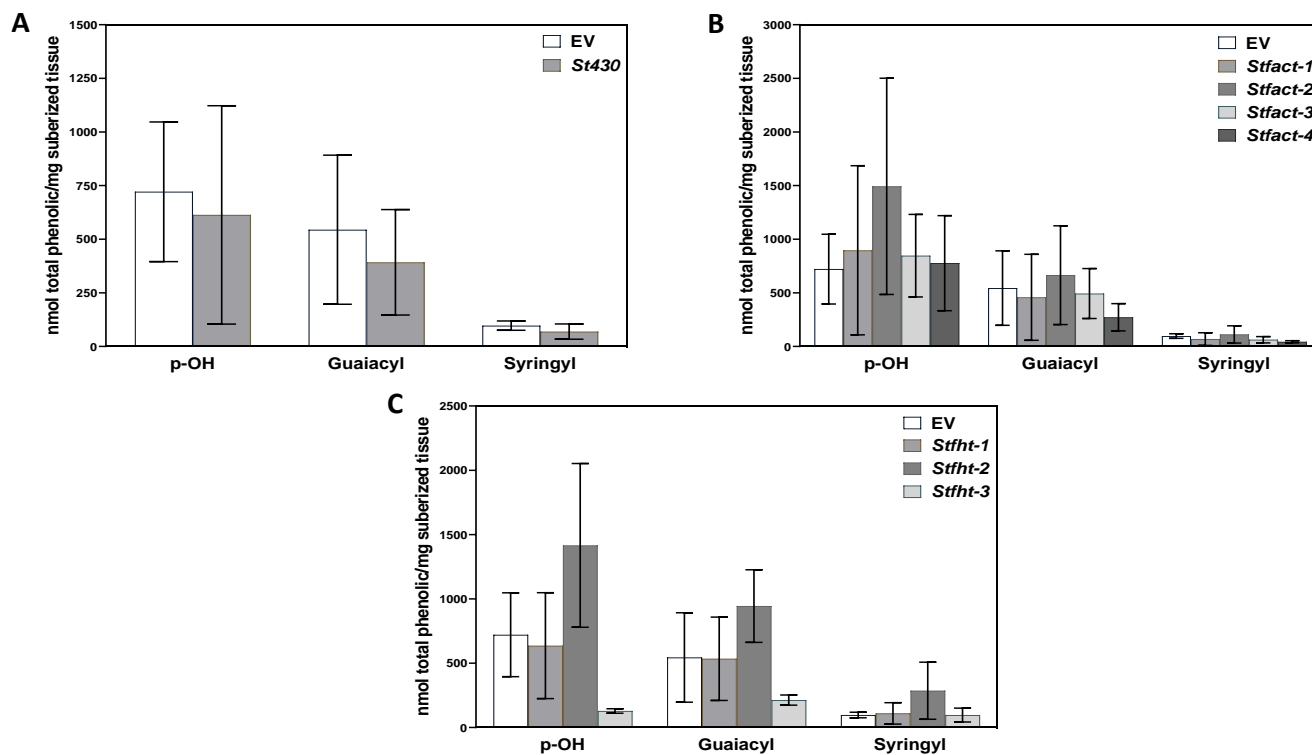


Figure 3.8. Total poly(phenolics) composition. Dried wound-induced periderm tissues were used to extract poly(phenolics) in (A) *St430*, (B) *Stfact* (*Stfact-1*, *Stfact-2*, *Stfact-3*, *Stfact-4*), and (C) *Stfht* (*Stfht-1*, *Stfht-2*, *Stfht-3*) transgenic lines, and empty vector (EV) control. The samples were quantified by the nitrobenzene oxidation (NBO) method and analyzed by GC-MS. Data are presented as the mean \pm SD of three biological replicates ($n = 3$, for each RNAi transgenic lines), and three independent empty vector ($n = 3$). Asterisks denote significant differences from empty vector control (one-way ANOVA followed by Dunnett test, $p < 0.05$).

4 Conclusions and Future Directions

The main goal of this study was to expand our understanding of the function of the BAHD acyltransferase family enzymes in extracellular lipid biosynthesis in *Solanum tuberosum* wound periderm, particularly the phenolic domain of suberin. It was hypothesized that specific members of this family are essential for a normal phenolic suberin deposition. To address this hypothesis, the role of three BAHD family genes, *StFHT*, *StFACT*, and *St430*, in wound-induced suberized tissues were analyzed. This was done using the loss of function approach by the generation of RNAi knockdown lines. The transgenic potato explants for this gene showed a reduction in the alkyl ferulate content, as well as the amount of ferulic acid esterified within the SPAD. Thus, the phenotypic chemical profile of the *StFHT* transgenic lines in the aliphatic domain and soluble waxes confirmed that *StFHT* catalyzes the synthesis of ferulic acid esters in the synthesis of suberin and suberin-associated waxes. Previously, a similar function was identified for the Arabidopsis gene *At5g41040* that encodes the ASFT/ HYDROXYCINNAMOYL-CoA:ω-HYDROXYACID *O*-HYDROXYCINNAMOYL TRANSFERASE (HHT) enzyme (Gou et al., 2009; Molina et al., 2009). Serra et al. (2010) identified the potato ortholog for this Arabidopsis gene, *FHT*. It was found that the protein encoded by both the *At5g41040* and *FHT* genes share a high degree of sequence similarity compared to the other analyzed BAHD enzymes (Serra et al., 2010). To follow up the *FHT* analysis described by Serra et al. (2010), Jin et al. (2018) compared native versus wounded periderm to get a deeper understanding on how the *FHT* down-regulation would impact potato native or wounded periderm tissues. In my study I targeted the same gene, and the result from phylogenetic analysis was consistent to what it was found by Serra et al. (2010). The results from the soluble and insoluble chemical analysis conducted in my study were also similar to the results reported by Serra et al. (2010) as well as Jin et al. (2018). The *StFACT* transgenic line showed a similar chemical phenotype as the *StFHT* transgenic lines, indicating the function of this gene in the synthesis of suberin-associated waxes as well as in the synthesis of the aliphatic domain of suberin. The *StFACT* candidate genes were identified through phylogenetic analysis and sequence similarity to the Arabidopsis gene *At5g63560*. This Arabidopsis gene was previously characterized and known to function in root suberin-associated wax biosynthesis as a caffeoyl-CoA transferases (Kosma et al., 2012).

The mutant *Arabidopsis* lines for this gene showed a complete reduction in the alkyl caffeates, and a small reduction in alkyl ferulates (Kosma et al., 2012). Aside from having a strong enzyme activity as a caffeoyl transferase, FACT was also capable of utilizing *p*-coumaroyl-CoA and feruloyl-CoA as the acyl donors during the enzyme assay (Kosma et al., 2012, reviewed in in Molina and Kosma, 2015). In the suberin of potato periderm tissues, the main phenolic component in the aliphatic domain is ferulic acid that is esterified to primary alcohols and ω -hydroxy fatty, and to primary alcohols in the soluble waxes (Graça, and Pereira, 2000b; Schreiber et al., 2005, Graça, and Santos, 2007). This is important because even though the *Arabidopsis* gene *At5g63560* encodes a caffeoyl-CoA transferase, the individual mutant lines also showed a reduction in ferulic acid ester content, which is the predominant phenolic in the aliphatic domain of suberin and associated waxes. In this study, both, the esterified ferulic acid, and the alkyl ferulates of the *SFACT* transgenic lines were reduced, indicating a function not only in the suberin-associated waxes, but also in the aliphatic domain of suberin. In the case of the *St430* gene, the results obtained from the knockdown transgenic line indicated that this gene does not play a role in wax alkylhydroxycinnamate synthesis or in the synthesis of the poly(aliphatic) domain of suberin in potato. This is consistent with one of the preliminary results in *Arabidopsis* (Castillo, 2016). Although there was a small reduction in the alkyl ferulate content, the overall soluble phenolic composition was not impacted. With regard to the analysis of the poly(phenolic) domain of suberin, the results from this study indicated that these three genes do not have a role in the synthesis of the phenolic domain of suberin. The amount and type of phenolic monomers released from empty vector tuber suberin, after the harsh chemical analyses, were consistent with previous studies (Bland and Logan, 1965; Borg-Olivier and Monties, 1993; Negrel et al., 1996; Lu and Ralph, 1997; Razem and Bernards, 2002; Jin et al., (2018)). However, none of the transgenic lines for the candidates BAHD genes had altered phenolic content in the poly(phenolic) domain of suberin.

Overall, although the chemicals analyses conducted in this study provided some insight into the function of the BAHD acyltransferase family genes in the phenolic domain of suberin, my analyses did not uncover any roles for acyltransferases in the formation of

the SPPD. One area not explored by the techniques used was the cross-linking between the phenolic and aliphatic domains. Also, there was a substantial variation in the data due to the limited amount of tissue, and the number of replicates used for the analyses. For these reasons, the experiment should be repeated, and future analyses need to focus on how the loss of function of a gene can affect both the macromolecular structure of suberin and the cross-linking between the phenolic and aliphatic domains. For example, the knockdown effect of the *StFHT*, *StFACT* and *St430* genes on the ultrastructure of suberin can be examined by transmission electron microscopy (TEM). Under TEM, the suberin lamellae shows a dark and light bands alternation. Based on the proposed two domain structure, the dark bands correspond to the electron-dense aromatic and glycerol ester regions of the aliphatic domain, whereas the light bands correspond to the electron-translucent aliphatic hydrocarbon chains. If there is an effect in the lamellation structure of suberin in TEM images, it could be an indication that these genes could be important in the crosslink between the phenolic and aliphatic domain of suberin. Serra et al., 2010 also examined the impact of the *FHT* down regulation by TEM, and although they did not find any major changes in the lamella structure of suberin when compared to the WT control, the lamella seems to be more wavy, suggesting that the SPPD and SPAD were not as well connected as in WT suberin. Additionally, the other main conclusion from this thesis is that is that *StFACT* is likely involved in suberin formation along with *StFHT*; however, I cannot rule out off-target effects because I did not measure the expression of *StFHT* in *StFACT* knockdowns, and vice versa.

My thesis research contributes to the overall understanding of extracellular, cell wall-specific polymer biosynthesis. Specifically, it helps to further understand the function of the BAHD acyltransferase candidate genes in the biosynthesis of the poly(phenolic) and poly(aliphatic) domains of suberin. While there is a substantial amount of work that focuses on the poly(aliphatic) domain of suberin, the BAHD genes involved in the phenolic synthesis of suberin remain unknown. More work needs to be done to identify and characterize potential BAHD/HXXXD acyltransferase genes involved in the synthesis of the phenolic domain of suberin or in the cross-linkage between the two domains.

References

- Agrawal, V. P., and Kolattukudy, P. E. (1978). Purification and characterization of a wound-induced ω -hydroxyfatty acid: NADP oxidoreductase from potato tuber disks (*Solanum tuberosum* L.). *Archives of Biochemistry and Biophysics*, 191(2), 452-465.
- Akerlele, O., Heywood, V., and Synge, H. (Eds.). (1991). Conservation of medicinal plants. Cambridge University Press.
- Banerjee, A. K., Prat, S., and Hannapel, D. J. (2006). Efficient production of transgenic potato (*S. tuberosum* L. ssp. *andigena*) plants via *Agrobacterium tumefaciens*-mediated transformation. *Plant Science*, 170(4), 732-738.
- Bach, L., Michaelson, L. V., Haslam, R., Bellec, Y., Gissot, L., Marion, J., ... and Faure, J. D. (2008). The very-long-chain hydroxy fatty acyl-CoA dehydratase PASTICCINO2 is essential and limiting for plant development. *Proceedings of the National Academy of Sciences*, 105(38), 14727-14731.
- Beaudoin, F., Wu, X., Li, F., Haslam, R. P., Markham, J. E., Zheng, H., ... and Kunst, L. (2009). Functional characterization of the Arabidopsis β -ketoacyl-coenzyme A reductase candidates of the fatty acid elongase. *Plant Physiology*, 150(3), 1174-1191.
- Beisson, F., Li, Y., Bonaventure, G., Pollard, M., and Ohlrogge, J. B. (2007). The acyltransferase GPAT5 is required for the synthesis of suberin in seed coat and root of Arabidopsis. *The Plant Cell*, 19(1), 351-368.
- Beisson, F., Li-Beisson, Y., and Pollard, M. (2012). Solving the puzzles of cutin and suberin polymer biosynthesis. *Current Opinion in Plant Biology*, 15(3), 329-337.
- Beekwilder, J., Alvarez-Huerta, M., Neef, E., Verstappen, F. W., Bouwmeester, H. J., and Aharoni, A. (2004). Functional characterization of enzymes forming volatile esters from strawberry and banana. *Plant Physiology*, 135(4), 1865-1878.
- Benveniste, I., Tijet, N., Adas, F., Philipps, G., Salaün, J. P., and Durst, F. (1998). Cyp86a1 from Arabidopsis thaliana encodes a cytochrome p450-dependent fatty acid omega-hydroxylase. *Biochemical and Biophysical Research Communications*, 243(3), 688-693.
- Bernard, A., Domergue, F., Pascal, S., Jetter, R., Renne, C., Faure, J. D., ... and Joubès, J. (2012). Reconstitution of plant alkane biosynthesis in yeast demonstrates that Arabidopsis ECERIFERUM1 and ECERIFERUM3 are core components of a very-long-chain alkane synthesis complex. *The Plant Cell*, 24(7), 3106-3118.
- Bernards, M. A., and Lewis, N. G. (1992). Alkyl ferulates in wound healing potato tubers. *Phytochemistry*, 31(10), 3409-3412.
- Bernards, M. A., Lopez, M. L., Zajicek, J., and Lewis, N. G. (1995). Hydroxycinnamic acid-derived polymers constitute the polyaromatic domain of suberin. *Journal of Biological Chemistry*, 270(13), 7382-7386.

- Bernards, M. A., and Razem, F. A. (2001). The poly (phenolic) domain of potato suberin: a non-lignin cell wall bio-polymer. *Phytochemistry*, 57(7), 1115-1122.
- Bernards, M. A. (2002). Demystifying suberin. *Canadian Journal of Botany*, 80(3), 227-240.
- Beuerle, T., and Pichersky, E. (2002). Enzymatic synthesis and purification of aromatic coenzyme A esters. *Analytical biochemistry*, 302(2), 305-312.
- Bland, D. E., and Logan, A. F. (1965). The properties of syringyl, guaiacyl and p-hydroxyphenyl artificial lignins. *Biochemical Journal*, 95(2), 515.
- Boher Genís, P. (2017). Functional genomics of the periderm: the biosynthetic gene FHT, the transcriptional regulator StRiK and the transcriptome deciphering. PhD Thesis, University of Girona, Girona, Catalonia, Spain.
- Borg-Olivier, O., and Monties, B. (1993). Lignin, suberin, phenolic acids and tyramine in the suberized, wound-induced potato periderm. *Phytochemistry*, 32(3), 601-606.
- Blacklock, B. J., and Jaworski, J. G. (2006). Substrate specificity of Arabidopsis 3-ketoacyl-CoA synthases. *Biochemical and Biophysical Research Communications*, 346(2), 583-590.
- Castillo, I. Q. (2016). Functional Characterization of HXXXD-motif Acyltransferases in Arabidopsis thaliana [honours thesis]. Sault Ste. Marie (ON): Algoma University.
- Chen, H., and Jiang, J. G. (2010). Osmotic adjustment and plant adaptation to environmental changes related to drought and salinity. *Environmental Reviews*, 18(NA), 309-319.
- Cheng, A. X., Gou, J. Y., Yu, X. H., Yang, H., Fang, X., Chen, X. Y., and Liu, C. J. (2013). Characterization and ectopic expression of a populus hydroxyacid hydroxycinnamoyltransferase. *Molecular Plant*, 6(6), 1889-1903.
- Chetty, V. J., Narváez-Vásquez, J., and Orozco-Cárdenas, M. L. (2015). Potato (*Solanum tuberosum* L.). In *Agrobacterium Protocols* (pp. 85-96). Springer, New York, NY.
- Cheynier, V., Comte, G., Davies, K. M., Lattanzio, V., and Martens, S. (2013). Plant phenolics: recent advances on their biosynthesis, genetics, and ecophysiology. *Plant Physiology and Biochemistry*, 72, 1-20.
- Compagnon, V., Diehl, P., Benveniste, I., Meyer, D., Schaller, H., Schreiber, L., ... and Pinot, F. (2009). CYP86B1 is required for very long chain ω -hydroxyacid and α , ω -dicarboxylic acid synthesis in root and seed suberin polyester. *Plant physiology*, 150(4), 1831-1843.
- Craigon, D. J., James, N., Okyere, J., Higgins, J., Jotham, J., and May, S. (2004). NASCArrays: a repository for microarray data generated by NASC's transcriptomics service. *Nucleic Acids Research*, 32(suppl_1), D575-D577.
- D'Auria, J. C. (2006). Acyltransferases in plants: a good time to be BAHD. *Current Opinion in Plant Biology*, 9(3), 331 -340.
- Dean, B. B., and Kolattukudy, P. E. (1976). Synthesis of suberin during wound-healing in jade leaves, tomato fruit, and bean pods. *Plant Physiology*, 58(3), 411-416.

- Dobránszki, J. (2001). Effects of light on in vitro tuberization of the potato cultivar Desirée and its relatives. *Acta Biologica Hungarica*, 52(1), 137-147.
- Do, C. T., Pollet, B., Thévenin, J., Sibout, R., Denoue, D., Barrière, Y., ... and Jouanin, L. (2007). Both caffeoyl Coenzyme A 3-O-methyltransferase 1 and caffeic acid O-methyltransferase 1 are involved in redundant functions for lignin, flavonoids and sinapoyl malate biosynthesis in Arabidopsis. *Planta*, 226(5), 1117-1129.
- Domergue, F., Vishwanath, S. J., Joubès, J., Ono, J., Lee, J. A., Bourdon, M., ... and Rowland, O. (2010). Three Arabidopsis fatty acyl-coenzyme A reductases, FAR1, FAR4, and FAR5, generate primary fatty alcohols associated with suberin deposition. *Plant physiology*, 153(4), 1539-1554.
- Dudareva, N., D'auria, J. C., Nam, K. H., Raguso, R. A., and Pichersky, E. (1998). Acetyl-CoA: benzylalcohol acetyltransferase—an enzyme involved in floral scent production in *Clarkia breweri*. *The Plant Journal*, 14(3), 297-304.
- Enstone, D. E., Peterson, C. A., and Ma, F. (2002). Root endodermis and exodermis: structure, function, and responses to the environment. *Journal of Plant Growth Regulation*, 21(4), 335-351.
- Fluke A. (2015). Functional characterization of candidate acyltransferase genes for Plant Lipid Polyester Biosynthesis by Mutant Analysis [honours thesis]. Sault Ste. Marie (ON): Algoma University.
- Franke, R., and Schreiber, L. (2007). Suberin—a biopolyester forming apoplastic plant interfaces. *Current Opinion in Plant Biology*, 10(3), 252-259.
- Fujiwara, H., Tanaka, Y., Yonekura-Sakakibara, K., Fukuchi-Mizutani, M., Nakao, M., Fukui, Y., ... and Kusumi, T. (1998a). cDNA cloning, gene expression and subcellular localization of anthocyanin 5-aromatic acyltransferase from *Gentiana triflora*. *The Plant Journal*, 16(4), 421-431.
- Fujiwara, H., Tanaka, Y., Fukui, Y., Ashikari, T., Yamaguchi, M., and Kusumi, T. (1998b). Purification and characterization of anthocyanin 3-aromatic acyltransferase from *Perilla frutescens*. *Plant science*, 137(1), 87-94.
- Gou, J. Y., Yu, X. H., and Liu, C. J. (2009). A hydroxycinnamoyltransferase responsible for synthesizing suberin aromatics in Arabidopsis. *Proceedings of the National Academy of Sciences*, 106(44), 18855-18860.
- Graça, J., and Pereira, H. (2000a). Methanolysis of bark suberins: analysis of glycerol and acid monomers. *Phytochemical Analysis: An International Journal of Plant Chemical and Biochemical Techniques*, 11(1), 45-51.
- Graça, J., and Pereira, H. (2000b). Suberin structure in potato periderm: glycerol, long-chain monomers, and glyceryl and feruloyl dimers. *Journal of Agricultural and Food Chemistry*, 48(11), 5476-5483.
- Graça, J., and Santos, S. (2006). Glycerol-derived ester oligomers from cork suberin. *Chemistry and Physics of Lipids*, 144(1), 96-107.
- Graça, J., and Santos, S. (2007). Suberin: a biopolyester of plants' skin. *Macromolecular Bioscience*, 7(2), 128-135.

- Graça, J. (2015). Suberin: the biopolyester at the frontier of plants. *Frontiers in Chemistry*, 3, 62.
- Gou, J. Y., Yu, X. H., and Liu, C. J. (2009). A hydroxycinnamoyltransferase responsible for synthesizing suberin aromatics in Arabidopsis. *Proceedings of the National Academy of Sciences*, 106(44), 18855-18860.
- Havir, E. A., and Hanson, K. R. (1970). [72a] l-phenylalanine ammonia-lyase (potato tubers). In *Methods in Enzymology* (Vol. 17, pp. 575-581). Academic Press.
- Höfgen, R., and Willmitzer, L. (1988). Storage of competent cells for Agrobacterium transformation. *Nucleic acids Research*, 16(20), 9877.
- Humphreys, J. M., Hemm, M. R., and Chapple, C. (1999). New routes for lignin biosynthesis defined by biochemical characterization of recombinant ferulate 5-hydroxylase, a multifunctional cytochrome P450-dependent monooxygenase. *Proceedings of the National Academy of Sciences*, 96(18), 10045-10050.
- Jin, L., Cai, Q., Huang, W., Dastmalchi, K., Rigau, J., Molinas, M., ... and Stark, R. E. (2018). Potato native and wound periderms are differently affected by down-regulation of FHT, a suberin feruloyl transferase. *Phytochemistry*, 147, 30-48.
- Kandel, S., Sauveplane, V., Compagnon, V., Franke, R., Millet, Y., Schreiber, L., ... and Pinot, F. (2007). Characterization of a methyl jasmonate and wounding-responsive cytochrome P450 of Arabidopsis thaliana catalyzing dicarboxylic fatty acid formation in vitro. *The FEBS journal*, 274(19), 5116-5127.
- Karimi, M., Inzé, D., and Depicker, A. (2002). Gateway vectors for Agrobacterium-mediated plant transformation. *Trends Plant Science*, 7(5), 193-195.
- Kolattukudy, P. E. (1980). Biopolyester membranes of plants: cutin and suberin. *Science*, 208(4447), 990-1000.
- Kolattukudy, P. T. (1981). Structure, biosynthesis, and biodegradation of cutin and suberin. *Annual Review of Plant Physiology*, 32(1), 539-567.
- Kolattukudy, P. E. (2001). Polyesters in higher plants. In *Biopolyesters* (pp. 1 -49). Springer, Berlin, Heidelberg.
- Kosma, D. K., Molina, I., Ohlrogge, J. B., and Pollard, M. (2012). Identification of an Arabidopsis Fatty Alcohol: Caffeoyle-Coenzyme A Acyltransferase Required for the Synthesis of Alkyl Hydroxycinnamates in Root Waxes¹. *Plant Physiology*, pp-112.
- Kosma, D. K., Rice, A., & Pollard, M. (2015). Analysis of aliphatic waxes associated with root periderm or exodermis from eleven plant species. *Phytochemistry*, 117, 351-362.
- Knollenberg, B. J., Liu, J., Yu, S., Lin, H., and Tian, L. (2018). Cloning and functional characterization of a p-coumaroyl quinate/shikimate 3'-hydroxylase from potato (*Solanum tuberosum*). *Biochemical and Biophysical Research Communications*, 496(2), 462-467.

- Lapierre, C., Pollet, B., and Rolando, C. (1995). New insights into the molecular architecture of hardwood lignins by chemical degradative methods. *Research on Chemical Intermediates*, 21(3), 397-412.
- Larsen, K. (2004). Molecular cloning and characterization of cDNAs encoding cinnamoyl CoA reductase (CCR) from barley (*Hordeum vulgare*) and potato (*Solanum tuberosum*). *Journal of Plant Physiology*, 161(1), 105-112.
- Le Bouquin, R., Skrabs, M., Kahn, R., Benveniste, I., Salaün, J. P., Schreiber, L., ... and Pinot, F. (2001). CYP94A5, a new cytochrome P450 from *Nicotiana tabacum* is able to catalyze the oxidation of fatty acids to the ω -alcohol and to the corresponding diacid. *European Journal of Biochemistry*, 268(10), 3083-3090.
- Lee, D., and Douglas, C. J. (1996). Two divergent members of a tobacco 4-coumarate: coenzyme A ligase (4CL) gene family (cDNA structure, gene inheritance and expression, and properties of recombinant proteins). *Plant Physiology*, 112(1), 193-205.
- Leal, A. R., Barros, P. M., Parizot, B., Sapeta, H., Vangheluwe, N., Andersen, T. G., ... and Oliveira, M. M. (2021). Phellem translational landscape throughout secondary development in *Arabidopsis* roots. *bioRxiv*.
- Li, Y., Beisson, F., Koo, A. J., Molina, I., Pollard, M., and Ohlrogge, J. (2007a). Identification of acyltransferases required for cutin biosynthesis and production of cutin with suberin-like monomers. *Proceedings of the National Academy of Sciences*, 104(46), 18339-18344.
- Li, Y., Beisson, F., Ohlrogge, J., and Pollard, M. (2007b). Monoacylglycerols are components of root waxes and can be produced in the aerial cuticle by ectopic expression of a suberin associated acyltransferase. *Plant Physiology*, 144(3), 1267-1277.
- Lopes, M. H., Neto, C. P., Barros, A. S., Rutledge, D., Delgadillo, I., and Gil, A. M. (2000). Quantitation of aliphatic suberin in *Quercus suber* L. cork by FTIR spectroscopy and solid-state ^{13}C -NMR spectroscopy. *Biopolymers: Original Research on Biomolecules*, 57(6), 344-351.
- Lu, F., and Ralph, J. (1997). Derivatization followed by reductive cleavage (DFRC method), a new method for lignin analysis: protocol for analysis of DFRC monomers. *Journal of Agricultural and Food Chemistry*, 45(7), 2590-2592.
- Lulai, E. C., and Orr, P. H. (1994). Techniques for detecting and measuring developmental and maturational changes in tuber native periderm. *American Potato Journal*, 71(8), 489-505.
- Lulai, E. C., and Corsini, D. L. (1998). Differential deposition of suberin phenolic and aliphatic domains and their roles in resistance to infection during potato tuber (*Solanum tuberosum*L.) wound-healing. *Physiological and Molecular Plant Pathology*, 53(4), 209-222.
- Luo, J., Nishiyama, Y., Fuell, C., Taguchi, G., Elliott, K., Hill, L., ... and Parr, A. (2007). Convergent evolution in the BAHD family of acyl transferases: identification and

- characterization of anthocyanin acyl transferases from *Arabidopsis thaliana*. *The Plant Journal*, 50(4), 678-695.
- Meyer, K., Shirley, A. M., Cusumano, J. C., Bell-Lelong, D. A., and Chapple, C. (1998). Lignin monomer composition is determined by the expression of a cytochrome P450-dependent monooxygenase in *Arabidopsis*. *Proceedings of the National Academy of Sciences*, 95(12), 6619-6623.
- Meyer, C.J., Peterson, C.A. and Bernards, M.A. (2011) A comparison of suberin monomers from the multiseriate exodermis of *Iris germanica* during maturation under differing growth conditions. *Planta*, 233(4), 773-786.
- Molina, I., Bonaventure, G., Ohlrogge, J., and Pollard, M. (2006). The lipid polyester composition of *Arabidopsis thaliana* and *Brassica napus* seeds. *Phytochemistry*, 67(23), 2597-2610.
- Molina, I., Ohlrogge, J. B., and Pollard, M. (2008). Deposition and localization of lipid polyester in developing seeds of *Brassica napus* and *Arabidopsis thaliana*. *The Plant Journal*, 53(3), 437-449.
- Molina, I., Li-Beisson, Y., Beisson, F., Ohlrogge, J. B., and Pollard, M. (2009). Identification of an *Arabidopsis* feruloyl-coenzyme A transferase required for suberin synthesis. *Plant Physiology*, 151(3), 1317-1328.
- Molina I. [Internet]. (2010). Biosynthesis of Plant Lipid Polyesters. Urbana (IL): LipidLibrary.aocs.org; [updated 2010 Jun 28; cited 2015 Nov 12]. Available from: <http://lipidlibrary.aocs.org/Biochemistry/content.cfm?ItemNumber=40311>
- Molina, I., and Kosma, D. (2015). Role of HXXXD-motif/BAHD acyltransferases in the biosynthesis of extracellular lipids. *Plant Cell Reports*, 34(4), 587-601.
- Negrel, J., Pollet, B., and Lapiere, C. (1996). Ether-linked ferulic acid amides in natural and wound periderms of potato tuber. *Phytochemistry*, 43(6), 1195-1199.
- Pollard, M., Beisson, F., Li, Y., and Ohlrogge, J. B. (2008). Building lipid barriers: biosynthesis of cutin and suberin. *Trends in Plant Science*, 13(5), 236-246.
- Razem, F. A., and Bernards, M. A. (2002). Hydrogen peroxide is required for poly (phenolic) domain formation during wound-induced suberization. *Journal of Agricultural and Food Chemistry*, 50(5), 1009-1015.
- Ranathunge, K., Schreiber, L., and Franke, R. (2011). Suberin research in the genomics era—new interest for an old polymer. *Plant Science*, 180(3), 399-413.
- Rautengarten, C., Ebert, B., Ouellet, M., Nafisi, M., Baidoo, E. E., Benke, P., Stranne, M., Mukhopadhyay, A., Keasling, J. D., Sakuragi, Y., and Scheller, H. V. (2012). *Arabidopsis* deficient in cutin ferulate encodes a transferase required for feruloylation of ω -hydroxy fatty acids in cutin polyester. *Plant Physiology*, 158(2), 654-665.
- Risopatron, J. P. M., Sun, Y., and Jones, B. J. (2010). The vascular cambium: molecular control of cellular structure. *Protoplasma*, 247(3-4), 145-161.

- Sambrook, J., Fritsch, E. F., and Maniatis, T. (1989). *Molecular cloning: a laboratory manual* (No. Ed. 2). Cold Spring Harbor Laboratory Press.
- Schreiber, L., Hartmann, K., Skrabs, M., and Zeier, J. (1999). Apoplastic barriers in roots: chemical composition of endodermal and hypodermal cell walls. *Journal of Experimental Botany*, 50(337), 1267-1280.
- Schneider, K., Hövel, K., Witzel, K., Hamberger, B., Schomburg, D., Kombrink, E., and Stuible, H. P. (2003). The substrate specificity-determining amino acid code of 4-coumarate: CoA ligase. *Proceedings of the National Academy of Sciences*, 100(14), 8601-8606.
- Schnurr, J., Shockey, J., and Browse, J. (2004). The acyl-CoA synthetase encoded by LACS2 is essential for normal cuticle development in Arabidopsis. *The Plant Cell*, 16(3), 629-642
- Schreiber, L., Franke, R., and Hartmann, K. (2005). Wax and suberin development of native and wound periderm of potato (*Solanum tuberosum* L.) and its relation to peridermal transpiration. *Planta*, 220(4), 520-530.
- Schreiber, L. (2010). Transport barriers made of cutin, suberin and associated waxes. *Trends in Plant Science*, 15(10), 546-553.
- Serra, O., Soler, M., Hohn, C., Franke, R., Schreiber, L., Prat, S., Molinas, M., and Figueras, M. (2009a) Silencing of StKCS6 in potato periderm leads to reduced chain lengths of suberin and wax compounds and increased peridermal transpiration. *Journal of Experimental Botany*, 60(2), 697-707.
- Serra, O., Soler, M., Hohn, C., Sauveplane, V., Pinot, F., Franke, R., Schreiber, L., Prat, S., Molinas, M., and Figueras, M. (2009b). CYP86A33-targeted gene silencing in potato tuber alters suberin composition, distorts suberin lamellae, and impairs the periderm's water barrier function. *Plant Physiology*, 149(2), 1050-1060.
- Serra, O., Hohn, C., Franke, R., Prat, S., Molinas, M., and Figueras, M. (2010). A feruloyl transferase involved in the biosynthesis of suberin and suberin-associated wax is required for maturation and sealing properties of potato periderm. *The Plant Journal*, 62(2), 277-290.
- Serra, O., Chatterjee, S., Figueras, M., Molinas, M., and Stark, R. E. (2014). Deconstructing a plant macromolecular assembly: chemical architecture, molecular flexibility, and mechanical performance of natural and engineered potato suberins. *Biomacromolecules*, 15(3), 799-811.
- Silva, J. D., and Fukai, S. (2001). The impact of carbenicillin, cefotaxime and vancomycin on chrysanthemum and tobacco TCL morphogenesis and Agrobacterium growth. *J. Appl. Hort*, 3(1), 3-12.
- Silva, S. P., Sabino, M. A., Fernandes, E. M., Correlo, V. M., Boesel, L. F., and Reis, R. L. (2005). Cork: properties, capabilities and applications. *International Materials Reviews*, 50(6), 345-365.

- Sitch, S., Cox, P. M., Collins, W. J., and Huntingford, C. (2007). Indirect radiative forcing of climate change through ozone effects on the land-carbon sink. *Nature*, 448(7155), 791.
- Soler, M., Serra, O., Molinas, M., Huguet, G., Fluch, S., and Figueras, M. (2007). A genomic approach to suberin biosynthesis and cork differentiation. *Plant Physiology*, 144(1), 419-431.
- Srinivasasainagendra, V., Page, G. P., Mehta, T., Coulibaly, I., and Loraine, A. E. (2008). CressExpress: a tool for large-scale mining of expression data from Arabidopsis. *Plant physiology*, 147(3), 1004-1016.
- Stark, R. E., and Garbow, J. R. (1992). Nuclear magnetic resonance relaxation studies of plant polyester dynamics. 2. Suberized potato cell wall. *Macromolecules*, 25(1), 149-154.
- Stewart Jr, C., Kang, B. C., Liu, K., Mazourek, M., Moore, S. L., Yoo, E. Y., ... and Jahn, M. M. (2005). The Pun1 gene for pungency in pepper encodes a putative acyltransferase. *The Plant Journal*, 42(5), 675-688.
- Stuart, J. M., Segal, E., Koller, D., and Kim, S. K. (2003). A gene-coexpression network for global discovery of conserved genetic modules. *Science*, 302(5643), 249-255.
- St-Pierre, B., and De Luca, V. (2000). Origin and diversification of the BAHD superfamily of acyltransferases involved in secondary metabolism. *Recent Adv. Phytochem*, 34, 285-315.
- St-Pierre, B., Laflamme, P., Alarco, A. M., and Luca, E. (1998). The terminal O-acetyltransferase involved in vindoline biosynthesis defines a new class of proteins responsible for coenzyme A-dependent acyl transfer. *The Plant Journal*, 14(6), 703-713.
- Tamura, K., Stecher, G., Peterson, D., Filipowski, A., and Kumar, S. (2013). MEGA6: molecular evolutionary genetics analysis version 6.0. *Molecular Biology and Evolution*, 30(12), 2725-2729.
- Thomas, R., Fang, X., Ranathunge, K., Peterson, C.A. and Bernards, M.A. (2007) Soybean Root Suberin: Anatomical Distribution, Chemical Composition and Relationship to Partial Resistance to *Phytophthora sojae*. *Plant Physiology*, 144, 299-311.
- Tuominen, L. K., Johnson, V. E., and Tsai, C. J. (2011). Differential phylogenetic expansions in BAHD acyltransferases across five angiosperm taxa and evidence of divergent expression among *Populus* paralogues. *BMC Genomics*, 12(1), 236.
- Vishwanath, S. J., Delude, C., Domergue, F., and Rowland, O. (2015). Suberin: biosynthesis, regulation, and polymer assembly of a protective extracellular barrier. *Plant Cell Reports*, 34(4), 573-586.
- Wei, H., Persson, S., Mehta, T., Srinivasasainagendra, V., Chen, L., Page, G. P., ... & Loraine, A. (2006). Transcriptional coordination of the metabolic network in Arabidopsis. *Plant Physiology*, 142(2), 762-774.
- Woolfson, K. N., Haggitt, M. L., Zhang, Y., Kachura, A., Bjelica, A., Rey Rincon, M. A., ... and Bernards, M. A. (2018). Differential induction of polar and non-polar

- metabolism during wound-induced suberization in potato (*Solanum tuberosum* L.) tubers. *The Plant Journal*, 93(5), 931-942.
- Woolfson, K.N. (2018) Suberin biosynthesis and deposition in the wound-healing potato (*Solanum tuberosum* L.) Tuber model. PhD Thesis, University of Western Ontario, London, On. Canada.
- Woolfson, K. N., Esfandiari, M., and Bernards, M. A. (2022). Suberin Biosynthesis, Assembly, and Regulation. *Plants*, 11(4), 555.
- Yadav, V., Molina, I., Ranathunge, K., Castillo, I. Q., Rothstein, S. J., and Reed, J. W. (2014). ABCG transporters are required for suberin and pollen wall extracellular barriers in *Arabidopsis*. *The Plant Cell*, 26(9), 3569-3588.
- Yang, Q., Reinhard, K., Schiltz, E., and Matern, U. (1997). Characterization and heterologous expression of hydroxycinnamoyl/benzoyl-CoA: anthranilate N-hydroxycinnamoyl/benzoyltransferase from elicited cell cultures of carnation, *Dianthus caryophyllus* L. *Plant Molecular Biology*, 35(6), 777-789.
- Yang, W. L., and Bernards, M. A. (2006). Wound-induced metabolism in potato (*Solanum tuberosum*) tubers: biosynthesis of aliphatic domain monomers. *Plant Signaling and Behavior*, 1(2), 59-66.
- Yu, X. H., Gou, J. Y., and Liu, C. J. (2009). BAHD superfamily of acyl-CoA dependent acyltransferases in *Populus* and *Arabidopsis*: bioinformatics and gene expression. *Plant Molecular Biology*, 70(4), 421-442.
- Zheng, H., Rowland, O., and Kunst, L. (2005). Disruptions of the *Arabidopsis* enoyl-CoA reductase gene reveal an essential role for very-long-chain fatty acid synthesis in cell expansion during plant morphogenesis. *The Plant Cell*, 17(5), 1467-1481.
- Zhong, W., and Sternberg, P. W. (2006). Genome-wide prediction of *C. elegans* genetic interactions. *Science*.

Appendices

Appendix A Potato homologs of *A. thaliana* candidate genes with possible roles in suberin biosynthesis.

Arabidopsis Gene	Potato candidates Gene ID (PGSC0003)	Potato Candidates Protein ID (PGSC0003)	Potato Candidates Transcript ID (PGSC0003)
ASFT (<i>At5g41040</i>)	DMG400031731	DMP400054926	DMT400081182
	DMG400014152	DMP400024883	DMT400036695
	DMG400011189	DMP400019784	DMT400029079
	DMG400007155	DMP400012693	DMT400018441
	DMG400018700	DMP400032596	DMT400048130
FACT (<i>At5g63560</i>)	DMG400031731	DMP400054926	DMT400081182
	DMG400014152	DMP400024883	DMT400036695
	DMG400011189	DMP400019784	DMT400029079
	DMG400007155	DMP400012693	DMT400018441
	DMG400018700	DMP400032596	DMT400048130
	DMG400018699	DMP400032595	DMT400048126
<i>At1g24430</i>	DMG400007800	DMP400013752	DMT400020175
	DMG400029264	DMP400050944	DMT400075236
	DMG400029262	DMP400050942	DMT400075231
	DMG400007171	DMP400012715	DMT400018478
	DMG400016360	DMP400028581	DMT400042163

Appendix B Expression data used to select potato homologs of *A. thaliana* candidates genes (Woolfson, 2018).

FPKM: Fragments per kilobase of exon model per million reads mapped.

Expression level (FPKM) post wounding							
Arabidopsis Genes	Potato Candidates Protein ID (PGSC0003DMG4)	Day 0	Day 0.5	Day 1	Day 2.0	Day 3	E. value
<i>At1g24430</i>	00007800	0.1	15.8	15.4	27.8	28.8	1.3e-23
	00029264	0.5	3.4	3.1	18.7	21.2	8.1e-30
	00029262	0.2	1.2	1.2	6.0	11.4	1.4e-11
	00007171	0.4	2.8	5.4	6.3	6.9	1.1e-43
	00016360	0.1	0.1	0.2	2.8	5.7	1.6e-51
ASFT (<i>At5g41040</i>) /FACT (<i>At5g63560</i>)	00031731	0.5	761.4	484.7	2038.2	3836.9	1.1e-166/5.6e-145
	00014152	117.4	649.9	491.4	751.4	957.8	1.9e-34/3.7e-54
	00007155	0.3	277.7	228.3	301.1	236.0	5.4e-37/1.1e-29
	00018700	9.7	36.7	63.6	133.3	177.4	2.5e-29/3.1e-23
	00000429	0.01	74.3	64.2	81.2	92.8	2.7e-33/5.3e-30
	00018699	0.3	0.7	9.3	32.7	55.4	1.3e-27/8e-25
	00011189	108.3	231.6	311.9	349.4	292.8	3.3e-53/3.7e-54

DMT400081182 --CCACACTCACAAGTATAACCATTTCTAG--ACTCAAAATATCAGAACATTAACCTGCATT
 DMT400036695 CAACCCACTCTCAACCATATTATCACCCATAACTTAAAGGCCAAAAAGCTCAACAACATT
 DMT400018478 -----

DMT400081182 TTTTCCCCGTCTTTTAGGATTTTAAATTTGAGAAATGGAGAGTGGTAAACACAATGTTGC
 DMT400036695 ATCCTGCTCCTTCTC----TTTTCA---CAAGAAAACAGAGTTGATTGAT-CAACGATGA
 DMT400018478 -----

DMT400081182 AATTGAGCTTATTGTGAAGCAAGGAGTGCCAAGTTTGGTGGCACCAGCAGAGGAAACAGA
 DMT400036695 AG-----ATCGAGGTGAAAAAATCAACGATGGTGCAGCCAGCAGCGGAGACGCCGCA
 DMT400018478 -----ATGGAGTTGATTAAACC--TGTTTCTCCTACTCCTAATCACCTTAAATGT
 * * * * *

DMT400081182 GAAGGGGCAATATTACT-TATCAAATCTTGATCAGAATATAGCCGTGCCGGTTCGAACAA
 DMT400036695 ACTGAGGCTGTGGAACCTAATGTAGATTTGGTGGTGCCTAATTTCCACACGCCCAGTG-
 DMT400018478 TTTGAATACTCTTTTTTGGATCAAATGGCCATACCCTTATATGCTCCCTTAGCTCTATTT
 * * * * *

DMT400081182 TTTACTGTTTTAAATCAGAAGAAAAGGGGAATGAGAATGCTGCTGAAGTGATGAAGGATG
 DMT400036695 TTTATTTCTATAGGCCAACGGGATCCCCAAATTTTTTCGACGGAAAAGTGCTTAAGGAGG
 DMT400018478 TATCCTCCTCCTCATTCAAATTATGAGCAAGCAATCTCAATCAATTCAT-CGAGATTACT
 * * * * *

DMT400081182 CTTTGTCAAAGGTTCTTGTTCATTATTATCCACTAGCAGGGAGATTGACAATTAGCCAGG
 DMT400036695 CACTAAGCAAAGCCCTAGTGCCGTTTTATCCGATGGGTGGGAGGCTGTGCAGAGATGAAG
 DMT400018478 CGTTTTGAAGAAATCTTTCTGAAACTCTTACTCGTTATTACCCT-TTTGCTGGTCGAA
 * * * * *

DMT400081182 AAATGAAGCTTATTGTGGACTGTAGTGAGAGAAGGGGCAGTTTTTGTGAGGCAGAAGCA-
 DMT400036695 ATGGCCGTATTGAGATTGATTGTAAAGGGCAAGGTGTGCTTTTTTGTGGAAGCTGAGTCT-
 DMT400018478 TCAAGGGCGTCTCAATAGAATGCAACGATGAGGGAGCGCCTTTTTTACGAGGCATTTGCTC
 * * * * *

DMT400081182 --AATTGTAACATAGAGGATATTGGTGATAATACTAAGCCTGATCCTGTTACACTTGCCA
 DMT400036695 --GATGGTGTGGTGGATGATTTTGGCGATTTTGCA----CCGACGTTG--GAGCTCCGAC
 DMT400018478 ATAATTATGAGTTCGAGAACGTTCTTAGAAATCACGACTTAACCAAAGATTTCCCTCCCA
 * * * * *

DMT400081182 AACTTGTTTATGATATCCCTGGTGCTAAA---AATATACTAGAAATGCCTCCCCTGGTGG
 DMT400036695 GACTTATTCGGCAGTTGATTACTCACAA---GGAATCGAATCTTATGCTCTCTTAGTGT
 DMT400018478 ATATTGTTGCTGAAGTTGGTCTTTCAGTATTCAATAATTCAACTTTGTATCCCCTGCTTG
 * * * * *

DMT400081182 CTCAGGTGACAAAGTTCAAATGTGGGGGATTTGTGCTTGGTTTGTGCATGAACCATTGCA
 DMT400036695 TGCAGATAACACATTTTTAAATGTGGGGGAGTTTCCCTTGGTGTGGGCATGCAACATCATG
 DMT400018478 TCCAAGTCACACTTTTCAAATGTGGAGGTATGGTTATTTGTATGTGTGCTTTTCACCAAG
 * * * * *

DMT400081182 TGTTTGTGATGGGATCGGAGCGATGGAGTTTGTG**AATTCCTGGGGTGAAA**CTGCTAGAGGTT
 DMT400036695 CAGCAGATGGAGCTTCTGGTCTTCACTTCATCAACACATGGTCAGACATGGCTCGTGGTT
 DMT400018478 TTGCTGACGGGGCCACGTTGTATGGCCTCGCCAACGCCTGGGCAATAGGTAGCTGCAACG
 * * * * *

DMT400081182 **TACCTATCAAAGTCATTCCATTCCCTAGACAGGAGCATACTCAAGCCTAGAAATCCACCAA**

DMT400036695 TGGACATTACTATCCCACCTTTCATTGATCGTACCCTCCTCCGTGCTCGTGATCCACCTC
DMT400018478 AGTTACCTGAATTCGTTGCAGCTGCCAA-----ATTCTTACCACCACCTATCCCATAT
* * * * *

DMT400081182 AGCCTGAATATACTCATAACGAGT-TTGCTGAAATTGAAGATATATCAGACTCTACTAAA
DMT400036695 AGCCTCAGTTCACCCACGTCGAGTACCAGCCACCTCCCCTCTCGAGGCAACAGAAAGAAA
DMT400018478 GTCTCAAACGGACCAATGTTGCAC--TCTCAACTTACCAATTTCTGCCATAACCAAGAAC
* * * * *

DMT400081182 CTATACCAAGAAGAAATGCTGT-----ATAAGACCTTCTGTTTTGACCTTGA---GAA
DMT400036695 ATGCCCGAATGCAGATACTGTTCCCTGAAACGAGTGTGTCCATCTTCAAACCTAACCCGCA
DMT400018478 GTGTTTCAAATTTACCTTT-----GATGCCTCTACTATAGCATCG-----
* * * * *

DMT400081182 GCTTGAACAA---CTAAAAGCAAAAGCCAGAGAAGATGGCAATGTTACCAAAATGCACCTT
DMT400036695 ATCAAATCAATACCCCTCAAAGCTAAGTCCAAAGAAAGATGGAAATACCGTTAACTACAGCT
DMT400018478 -----CTCAGGGCTAAGGCCATGAGCGA-GGATGTACCCGTGCCTACACG-
* * * * *

DMT400081182 CATTGAAGTCCTTTTCAGCTTTCGTCTGGAAAGCGCGAACTCAGGCATTACAAATGAAGC
DMT400036695 CCTATGAGATGTTGGCAGGACATGTGTGGCGCTCCACTTGTATGGCACGAGGACTCACTC
DMT400018478 -GGTTGAAGCTGTATCAGCTCTGATTTGGAAA-----TGTGTCATAACTGCTGGTGC
* * * * *

DMT400081182 CTGATCAAAAGA--CAAACTTCTCTTCGCTGTTGATGGAAGATCAAGATTTGATCCCTC
DMT400036695 AGGATCAAGAAA--CCAAGTTGTACATAGCAACTGATGGGCGTGCTAGGCTCCGACCTTC
DMT400018478 TGGTGTGGTGTCTTCAAATTTGACAACTTTGTAATATGCGAAGGCGATTTGTTCCCTCC
* * * * *

DMT400081182 AATTCACAAGGATATTTTTGGAAACGGAATTGTTTTAACTAATGCACTCTGCACTGCTGC
DMT400036695 TCTCCACCAGGCTATTTTTGGTAATGTGATATTACAGCCACTCGCTGTTGCTGTTGCTGG
DMT400018478 ATTGCCAGATCATTGTGTAGGAAATGTTATTGCAGTTGCCACAGCGTGTAAAGGTGAGAA
* * * * *

DMT400081182 AGAGATAGTCGAAAA---TCCACTTCTGTTGCTGT-TAAGTTGGTTCAAGAAGCTGTT
DMT400036695 TGATCTCCAATCAAA---GCCTATTTGGTACGCAGC-CAGTAAAATCCATGATCAATTG
DMT400018478 CGATGATGGATCTGACTTGGCCACATTGGTCAATTGTATAAGAAAATCGTTGTCACAATT
* * * * *

DMT400081182 AAATTGGTTACAGACAGTTACATCAAATCTGCTATAGACTATTTTGAA---GCAACAAGA
DMT400036695 GCTATAATGGACAACGATTATTTAAGATCAGCTCTTGATTATTTGGAATT-GCAGCCTGA
DMT400018478 GAGTTCCAAATATGTGGACAAACAGAGTCGAGATGAGGCGATTTTCGCCCTTTCCCTATGA
* * * * *

DMT400081182 GCTAGGCCTTCT-----TTAACTGCT--ACTCTTCTTATTACTAC
DMT400036695 CTTGAAGGCTCTAGTCCGCGGTGCACATACATTTAAGTGCCCGAATTTAGGAATAACTAG
DMT400018478 CTTAATGGAGATAA-CTGAAGGGCTAATCCGAGGGGAGATC--GCGTTGCAAGTTAGTAG
* * * * *

DMT400081182 TTGGTCTAGGCTTTCTTTCCACACCACGGATTTCCGGTGGGGAGAGCCTAT-TGTATCAG
DMT400036695 CTGGTCTAGGCTGCCTATCCATGATGCTGATTTCCGGATGGGGTAGGCCAATATTTATGGG
DMT400018478 CTTGTGT-GGCTATAAATCA--TACGTTGATTTTGGTTGGGGCAAACCGTCATGGGTTAG
* * * * *

DMT400081182 GGCCAGTGGCTTTACCAGAGAAGGA--AGTTTCTCTGTTTCTTCTCATGGAAAGAGAG
DMT400036695 ACCTGGTGGTATTGCTTATGAAGGCTTAAGCTTTTATATTGCCAAGTCCCATCAACGATGG

```

DMT400018478   TCCAAATCCAAGGATATCTACGAAT---AATGTTTCGATTGATGGATTCAAAGGATTATGG
                *   *                               *   **   *           *   *   *
DMT400081182   GAGAAGT-GTCAATGTGCTTCTTGG-ATTGCCAGCTTCTGCTATGAAGACATTTGAAGAA
DMT400036695   CAGTCA--ATCAGTTGCCATCTC---ACTGCAAGCAGAACATATGAAACTTTTCGAGAAG
DMT400018478   TGGAAATAGATGTGTTGATATGTTTGAAAGATAAAGCTATTATGTCAAATTTCAACAAGA
                *   *   *   *   *   *   *           *   *   **   *
DMT400081182   CT----TATGGAGATCTAAACAGCCATATTGCAGCTCTAATTTTCCATGAAATTTACTTT
DMT400036695   TTCTTGTATGACATTTGAAAGAAGCGGATTTCTTGTGCTGCTTTGATTGGGATTTACATT
DMT400018478   GATAGAGCTACAGTTGCTATCGTTTGGATCAGTCAACTAA-----
                *           *   *           **
DMT400081182   -ATTTATGTGTAATTGATTGTGTTTTTTACTCTGTGGTGTTGTTATTATTAGTACTTTGT
DMT400036695   GACGGATATGTAAAAGAGACTCCTTTTTTATCTTTT--TTTCATTAGAGGTTGTTCTTT--
DMT400018478   -----
DMT400081182   ATTGTTATTTCTGTTTGGCATCAATTCATGCTCTTTTGCTTGTTTCTAAATGT-TCATTT
DMT400036695   ATTTCTTTTTTTGTTTGCCTGGACATCA-GTTTTATTTCTGATTCTATGATGCATTGATT
DMT400018478   -----
DMT400081182   TTATCTCCA---TCCCATTGAGATCA-----
DMT400036695   ATATACTCAAAGTTATACTGCAAGTGTTGTATGTCTGTGAAGGACCTCAATCTTTTTTCA
DMT400018478   -----
DMT400081182   -----
DMT400036695   CTTCCACTAATGTGGCAAGATGTTAATGCAGAAGCTCCTAGTAGGATTGTAGCAATAGAT
DMT400018478   -----
DMT400081182   -----
DMT400036695   TGGAACCGCGGATGGCTTAGTTGGACTATCTTTTATTTCGCTAATATTCTGAATATCTGC
DMT400018478   -----
DMT400081182   -----
DMT400036695   AAATATAATATTATCACTGTG
DMT400018478   -----

```

Legend

```

-----      selected region for AtASFT homolog
AAATATAATATTATCACTGTG      selected region for AtFACT homolog
-----      selected region for At1g24430 homolog

```

Appendix C. Nucleotide sequence alignment of the selected potato homologs (DNAMAN).

Target selected regions for the RNAi construct design are shown (highlighted in yellow, green, and blue). Dashed represent the gap generated after the alignment, and asterisk indicate conserve regions.

AT5G41040_ASFT MVAENNKNKDVTLASMDNNNNNNIKGTNIHLEVHQKEPALVKPESETRKGLYFLSNLDQN
 AT5G63560_FACT -----MADSFELIVTRKEPVLVSPASETPKGLHYLSNLDQN
 AT1G24430 -----
 DMP400054926 -----MESGKHNVAIELIVKQGVPSLVAPAEETEKQYYLSNLDQN
 DMP400024883 -----MVQPATETPQLRLWNSNVDLV
 DMP400012715 -----MELIKPVSPTPNHLKCFEYSFLDQMAIPLYAP

AT5G41040_ASFT IAVIVR-TIYCFKSEERGNEEAVQVIKKALSQVLVHYYPLAGRLTISPEGKLTVDCTEEG
 AT5G63560_FACT IAIIVK-TFYYFKSNSRSNEESYEVIKKSLSSEVLVHYYPAAGRLTISPEGKIAVDCTGEG
 AT1G24430 -----
 DMP400054926 IAVPVR-TIYCFKSEEKGNENAAEVMKDALSQVLVHYYPLAGRLTISQEMKLIIVDCSGEG
 DMP400024883 VPNFHTPSVYFYRPTGSPNFFDGKVLKEALSALVPPFYPMGGRLCRDEDGRIEIDCKGQG
 DMP400012715 LALFYPPPHSNYEQAISINSSRLLVLKKSLSSETLTRYYPFAGRIKG-----VSIECNDEG

AT5G41040_ASFT VVFVEAEANCKMDEIGDITKPD--PETLGKLVYDVVDAKNILEIPPVTAQVTKFKCGGFV
 AT5G63560_FACT VVVVEAEANCGIEKIKKAISEIDQPETLEKLVYDVPGARNILEIPPVWVQVTFKCGGFV
 AT1G24430 -----MSQILENPNPNEINLKLHPFEFHEVSDVPLITVQLTFFECGGLA
 DMP400054926 AVFVEAEANCNIEDIGDNTKPD--PVTLGKLVYDIPGAKNILEMPPIVACVTKFKCGGFV
 DMP400024883 VLFVEAESDGVVDDFGDFAPTL----ELRRLIIPAVDYSQGIESYALIVLQITHEFKCGGVS
 DMP400012715 APFYEAFAHNYEFENVLRNHDLTkdflpniVAEVGSSVFNSTLYPLLVQVTLFKCGGMV

HxxxD motif

AT5G41040_ASFT LGLCMNHCMFDGIGAMEFVNSWGQVARGPLPTTPPFSDRTILNARNPPKIENLHQEFEEI
 AT5G63560_FACT LGLGMNHNMFDDGIAAMEFLNSWAETARGPLPSVPPFLDRTLLRPRTPPKIEFPHNEFEDL
 AT1G24430 LGTGLSHKLCDAISGLIFVNSWAAFAR-----GQTDEIITPSFDLAKMFPPCDIENL
 DMP400054926 LGLCMNHCMFDGIGAMEFVNSWGETARGPLPKVIFPFLDRSILKPRNPPKPEYTHNEFAEI
 DMP400024883 LGVGMQHHAADGASGLHFINTWSDMARGLDITIPPFIDRTLLRARDPPQPFPHVEYQPP
 DMP400012715 ICMCAFHQVADGATLYGLANAWAIGSCN-----ELPEFVAAAKFLPPPIPYVSNPMLH

AT5G41040_ASFT EDKSNINSLYT-KEPTLYRSFCFDPEKIKKIKLQATENSESLLGNSCTSFEALSFAFVWRA
 AT5G63560_FACT EDISGTGKLYS-DEKLVYKSFVLFGEPEKLERLKI MAETRST-----TFQTLTGFLWRA
 AT1G24430 NMATGITKEN-----IVTRRFVFLRSSVESLRERFSGNKK----IRATRVEVLSVFIWRSR
 DMP400054926 EDISDSTKLY--QEEMLYKTFCFDPEKLEQLKAKAREDN--VTKCTSFEVLSAFVWKA
 DMP400024883 PTLEATEENAPNADTVPETSVSIFKLTRNQINTLKAKSKEDGNTVNYSSYEMLAGHVWRS
 DMP400012715 SQLTNFCHNQE----RVSKLFTFDASTIASLRAKAMSEDVP----VPTRVEAVSALIWKC

AT5G41040_ASFT RTKSLKMLSDQ--KTKLLFAVDGRRAKFEPLQLEKGYFGNGIVLTN--SICEAGELIEKPLS
 AT5G63560_FACT RCQALGLKPDQ--RIKLLFAADGRSRFVELEPKGYSNGGIVFTY--CVTTAGEVTLNPLS
 AT1G24430 FMASTNHDDKTGKIYTLIHPVNLRRQADFDIPDNMFGNIMRFSVTVPMMIINENDEEKAS
 DMP400054926 RTQALQMKPDQ--KTKLLFAVDGRSRFDFSIIPQGYFGNGIVLTN--ALCTAAEIVENPLS
 DMP400024883 TCMARGLTQDQ--ETKLYIATDGRARLRPSLPPGYFGNVIIFTAT--PVAVAGDLQSKPIW
 DMP400012715 VITAGAGAGAS----KLTNFVNMRRRFVPLEDHCVGNVIAVAT--ACKGENDDGSDLAT

AT5G41040_ASFT FAVGLVREAIKMTVDGYMRSALIDYFEVTRARPSLS-----STLLITWRSRIGFHTTD
 AT5G63560_FACT HSVCLVKRAVEMVNDGFMRSALIDYFEVTRARPSLT-----ATLLITSWAKLSFHTKD
 AT1G24430 LVDQMREEIRKIDAVYVKKLQEDNRGHLEFLNKQASGFVNGEIVSFSFTSLCKFPVYEAD
 DMP400054926 VAVKLVQEAVKLVTDYSIKSALIDYFEATRARPSLT-----ATLLITWRSRISFHTTD
 DMP400024883 YAASKIHDQLAIDMNDYLRSAIDYLELQPDALKALVRGAHTFKCPNLGITSWSRLPIDHAD
 DMP400012715 LVNCIRKSLSQLSSKYVDKQSRDEAIFAFPYDLMEITEGLIRGEIALQVSLCGYKSYVD

FGWG motif

```

AT5G41040_ASFT  FGWGEF ILSGPVALPEKEVTLFLSHGEQRRSINVLLGLPATAMDVFEQEQFLQI-----
AT5G63560_FACT  FGWGEF VVSGPVGLPEKEVILFLPCGSDTKSINVLLGLPGSAMKVFQGIMDI-----
AT1G24430        FGWGKELWVASARMSYKNLVAFIDTKEGDG-IEAWINLDQNDMSRFEADEELLRYVSSNP
DMP400054926    FGWGEF IVSGPVALPEKEVSLFLSHGKERRSVNVLLGLPASAMKTFEELMEI-----
DMP400024883    FGWGRF IFMGPGGIAYEGLSFILPSPINDGSQSV AISLQAEHMKLF EKFLYDI-----
DMP400012715    FGWGKF SWVSPNPRISTNNVRLMDSKDYGGIDVLI CLKDKAIMSKFQQEIELQLLSFGSV
                **** *                               . * *

```



```

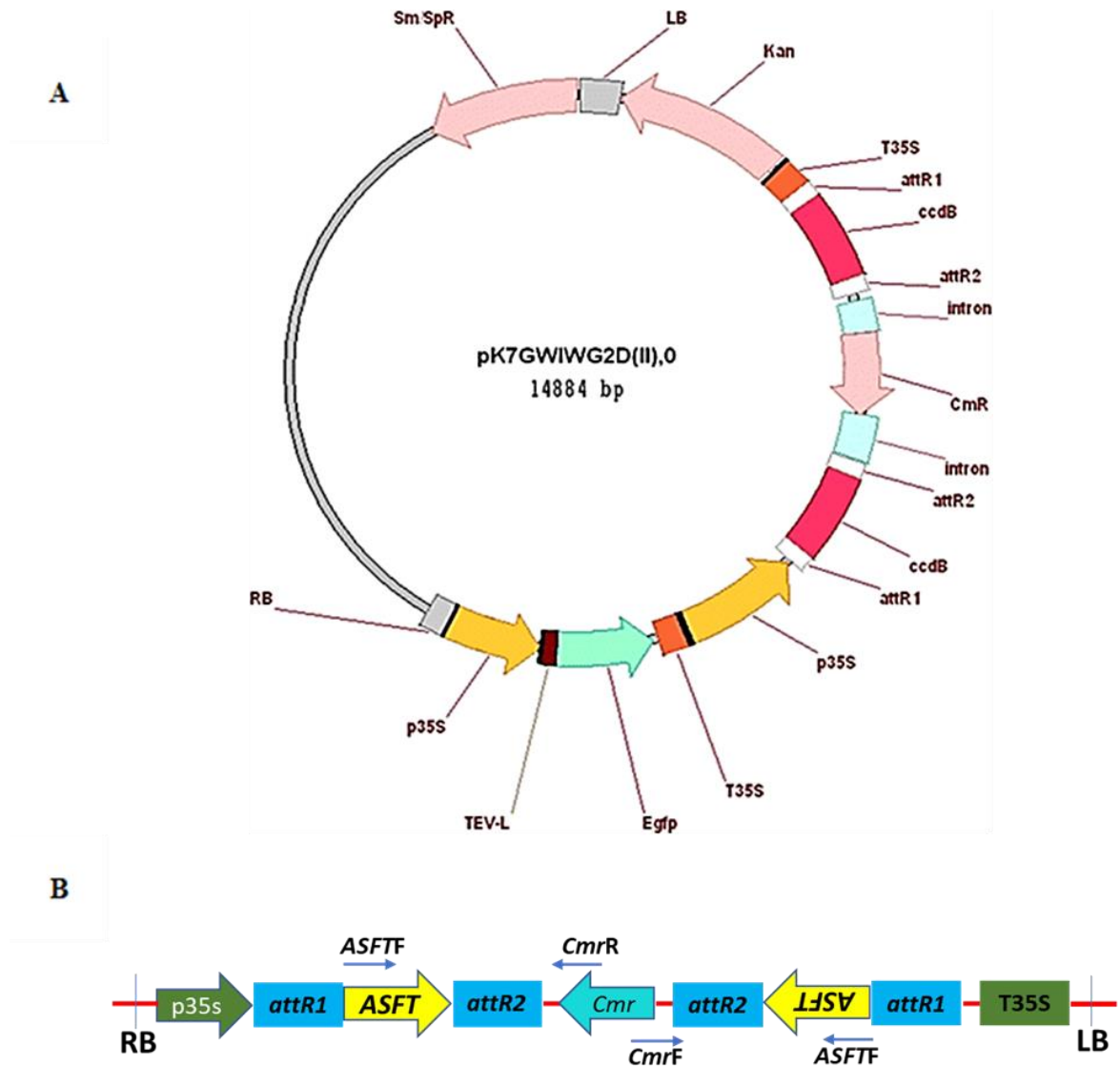
AT5G41040_ASFT  -----
AT5G63560_FACT  -----
AT1G24430        SVMVSVS
DMP400054926    -----
DMP400024883    -----
DMP400012715    N-----

```

Appendix D Amino acid sequence alignment of the Arabidopsis genes and selected potato homologs (DNAMAN). The two conserved motifs (HxxxD and DFGWG) characteristic of BAHD acyltransferase family are shown (highlighted in red). Dashed represent the gap generated after the alignment, asterisk indicate conserve regions, and the period indicate sites with some similarities.

Appendix E List of primers used for PCR amplification and genotype analyses. The underline base pairs represent the *attB1* (in the forward primers) and *attB2* (in the reverse primers) recombinant sequences.

Genes and Vector ID	Primer name	Sequence (5' - 3')	Amplicon size (bp)
PCR amplification primers			
PGSC0003DMG400031731	ASFT-RNAi-F ASFT-RNAi-R	<u>GGGGACAAGTTTGTACAAAAAAGCAG</u> <u>GCTTCAATTCTTGGGGTGAAACTGCT</u> <u>GGGGACCACTTTGTACAAGAAAGCTG</u> <u>GGTCGTAATGCCTGAGTTCGCGCTT</u>	304
PGSC0003DMG400014152	FACT-RNAi-F FACT-RNAi-R	<u>GGGGACAAGTTTGTACAAAAAAGCAG</u> <u>GCTTCAACGAGTGTGTCCATCTTCAA</u> <u>GGGGACCACTTTGTACAAGAAAGCTG</u> <u>GGTCCTTAAATAATCGTTGTCCATT</u>	351
PGSC0003DMG400007171	At1g24430-RNAi-F At1g24430-RNAi-R	<u>GGGGACAAGTTTGTACAAAAAAGCAG</u> <u>GCTTCAACGGACCAATGTTGCACTCT</u> <u>GGGGACCACTTTGTACAAGAAAGCTG</u> <u>GGTCATCCATCATCGTTCTCACCTT</u>	322
Genotype primers			
pK7GWIWG2D(II),0	pK7GWIWG2-Fw pK7GWIWG2-Rv	TCAAGCTGACCTGCAAACAC GGGCGAAGAAGTTGTCCATA	796
PGSC0003DMG400031731	ASFT-gDNA-F ASFT-gDNA-R	AATTCTTGGGGTGAAACTGCT GTAATGCCTGAGTTCGCGCTT	304
PGSC0003DMG400014152	FACT-gDNA-F FACT-gDNA-R	AACGAGTGTGTCCATCTTCAA AAAATAGCCTGGTGGGAGAGA	229
PGSC0003DMG400007171	At1g24430-gDNA-F At1g24430-gDNA-R	AACGGACCAATGTTGCACTCT ATCCATCATCGTTCTCACCTT	322



Appendix F Gateway silencing vector and screening strategy for BAHD1, 2, 3 inserts orientation. A) RNAi destination vector pK7GWIWG2D(II),0 for gene silencing. B) Schematic representation of the screening strategy to check the inserts orientations in the destination vector. The image illustrates the orientation of the potato homolog for ASFT as an example.

Appendix G. Medium composition for *Agrobacterium* infection, callus induction, shoot induction, and root induction. The culture medium used were adjusted to pH 5.8. AIM (Agrobacterium infection medium), CIM (callus induction medium), SIM (shoot induction medium), RIM (root induction medium).

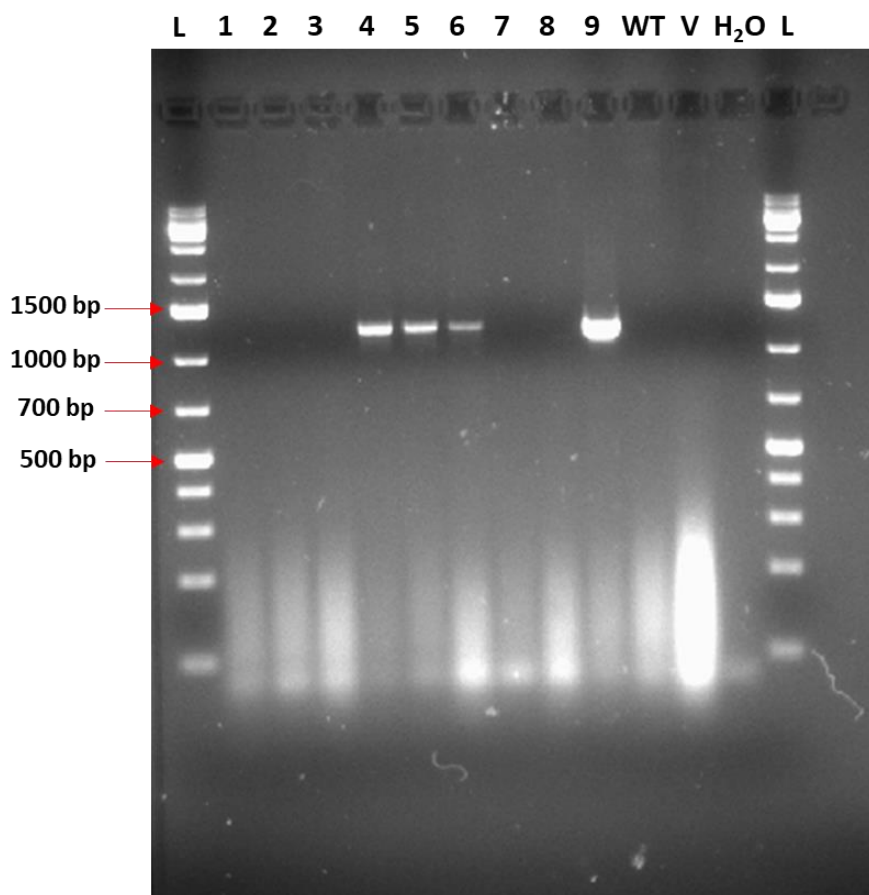
Media components (L)	Type of medium			
	AIM	CIM	SIM	RIM
MS salts (g)	4.4	4.4	4.4	4.4
MS vitamins (1000X) (mL)	1	1	1	1
Sucrose (g)	30	20	20	20
Myoinositol (mg)	0	100	100	100
IAA (mg)	0	1	1	1
Zeatin (mg)	0	2.5	2	0
GA ₃ (mg)	0	0.02	0.02	0
Gelrite (g)	0	2	2	2

Appendix H. Gene information and primer sequences used for gene expression analysis (RT-qPCR). Asterisk (*) indicate the references genes used for data normalization based on Nicot *et al.* (2005).

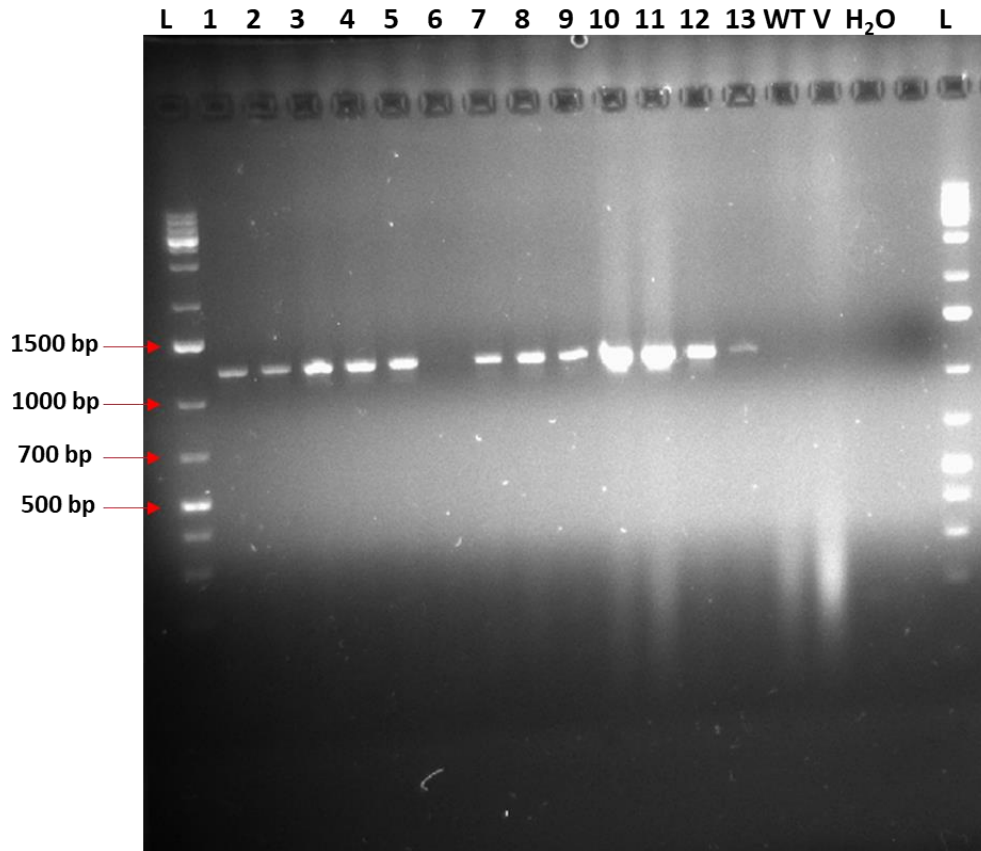
Gene	Potato Candidates Gene ID PGSC0003DMG4	GeneBank Accession No.	Primer Sequence (5'- 3')	Product length (bp)	Efficiency (%)
<i>St430</i>	00007171	XM_006364742.2	F: ACGATGAGGGAGCGCCTTTT R: TGACTTGGACAAGCAGGGGA	165	93.1
<i>StASFT/ FHT</i>	00031731	NM_001288261.1	F: TGTGAAGCAAGGAGTGCCAA R: ACCGGCACGGCTATATTCTG	99	103.7
<i>StFACT</i>	00014152	XM_006341351.2	F: ATGGCTCGTGGTTTGGACAT R: ACTGAGGCTGAGGTGGATCA	82	110.5
<i>StEF1- α*</i>	00023272	AB061263.1	F: TGGTCGTGTTGAGACTGGTG R: AACATTGTCACCGGGGAGTG	133	108.1
<i>StAPRT*</i>	00021527	XM_006361995.2	F: GAACCGGAGCAGGTGAAGAA R: GAAGCAATCCCAGCGATACG	121	104.0

Appendix I. Transgenic plants identification by genotype analysis

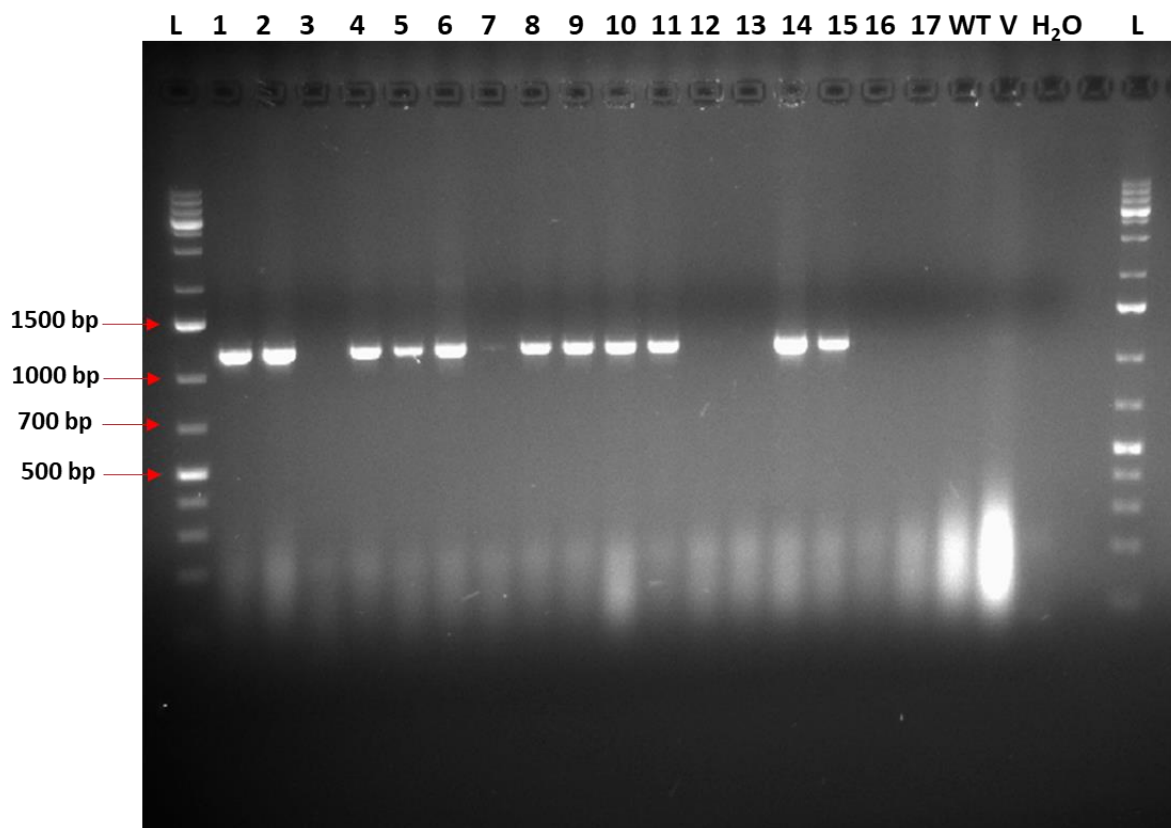
Gene of interest	Tested transgenic lines	Confirmed transgenic lines
<i>StFHT</i>	17	11
<i>StFACT</i>	13	12
<i>St430</i>	9	4
pk7GWIWG2D(II) (empty vector-EV)	26	23



Appendix J. Agarose gel picture of the genotype analysis for the *St430* transgenic lines. To screen and confirm the *St430* construct insertion in the transformed *in-vitro* plants, the insert specific forward primer (At1g24430-gDNA-F) with the empty vector chloramphenicol region reverse primer (pK7GWIWG2-Rv) were used in the PCR reaction. The expected amplicon size was about 1118 bp. bp = base pair; L = ladder; the numbers on top of the wells represent how many transgenics plants were screened.



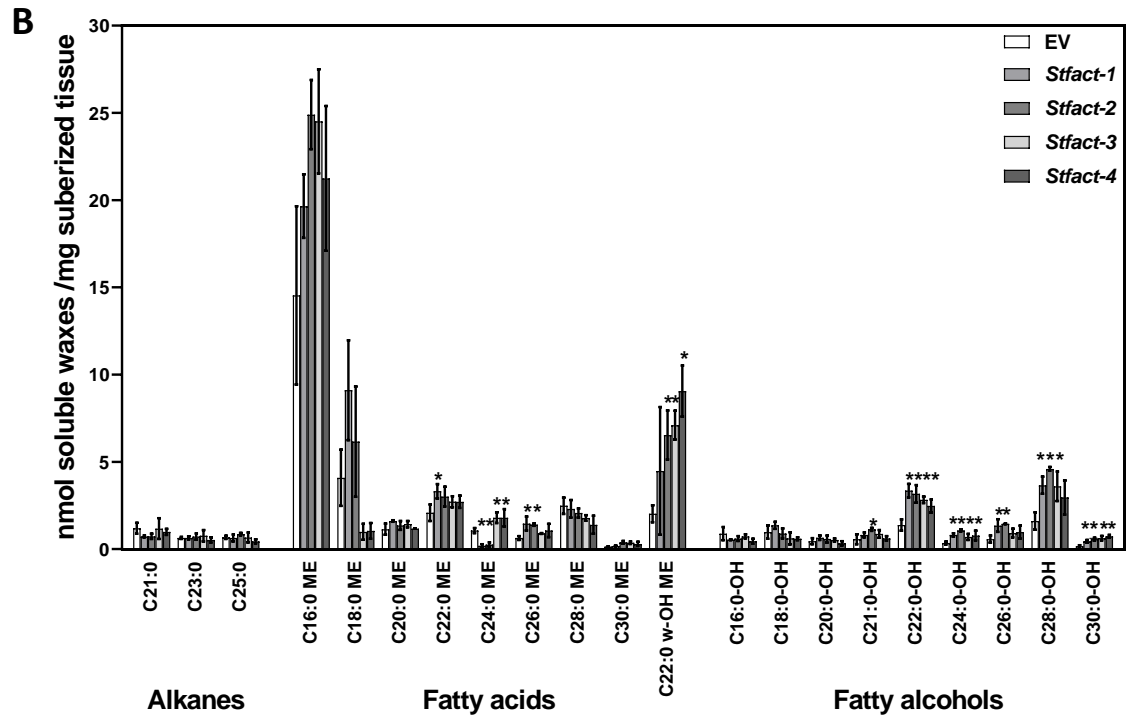
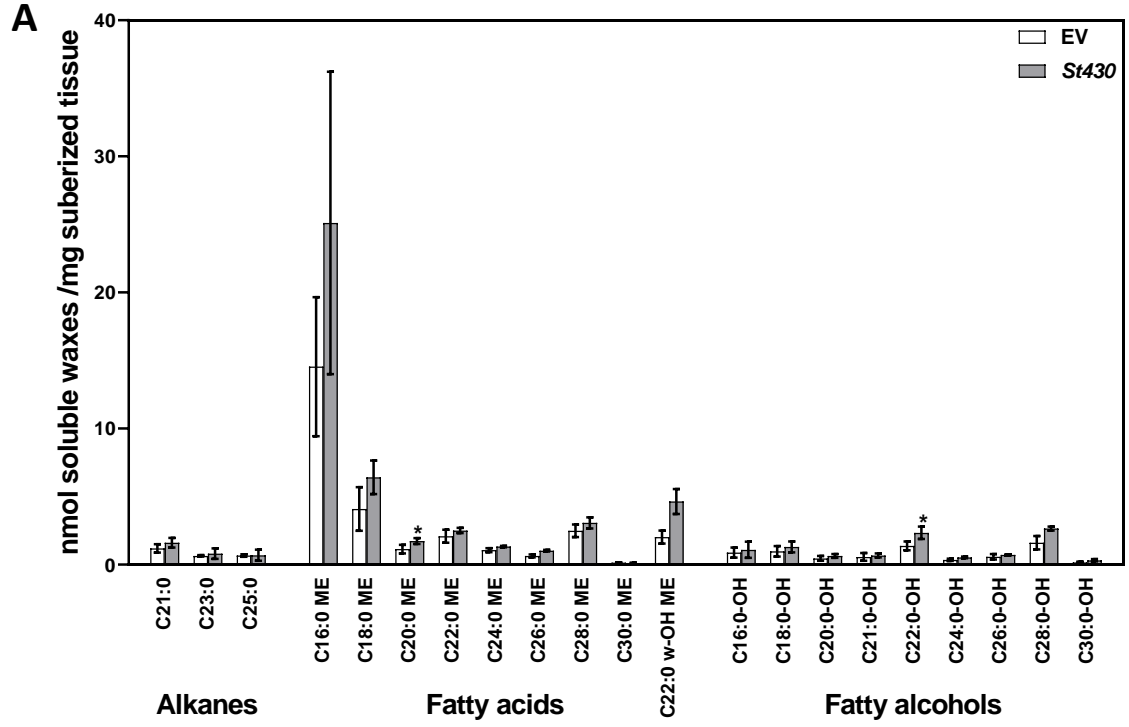
Appendix K. Agarose gel picture of the genotype analysis for the *StFACT* transgenic lines. To screen and confirm the *StFACT* construct insertion in the transformed *in-vitro* plants, the insert specific forward primer (FACT-gDNA-F) with the empty vector chloramphenicol region reverse primer (pK7GWIWG2-Rv) were used in the PCR reaction. The expected amplicon size was about 1147 bp. bp = base pair; L = ladder; the numbers on top of the wells represent how many transgenics plants were screened.

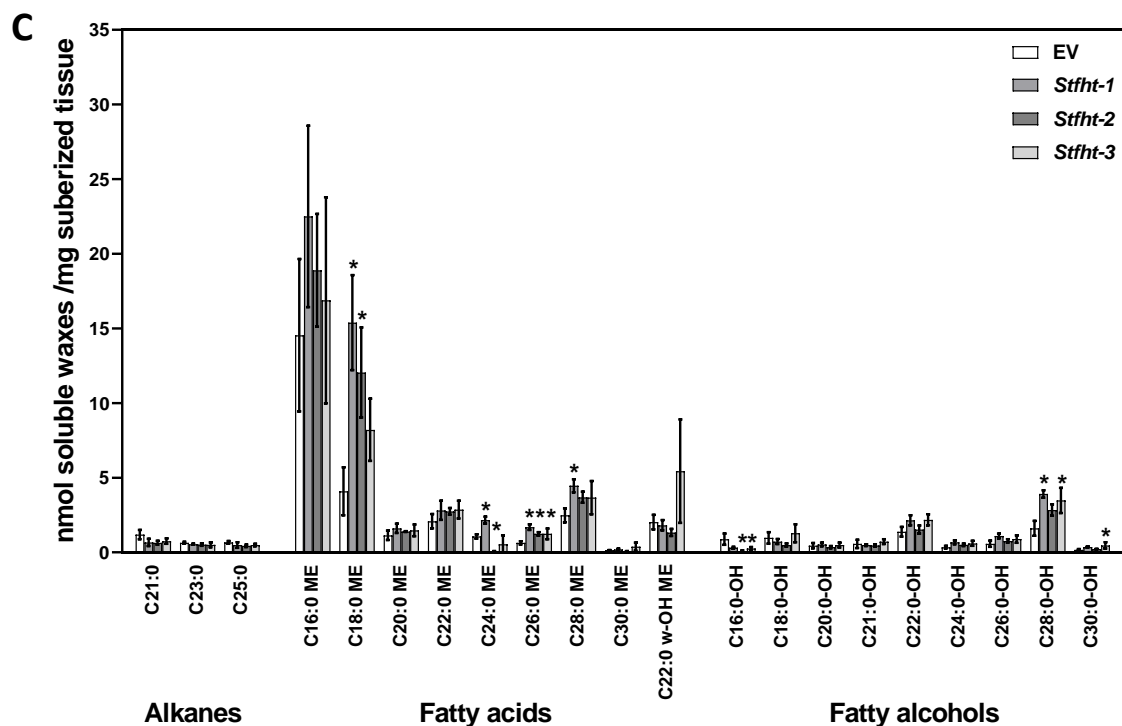


Appendix L. Agarose gel picture of the genotype analysis for the *StFHT* transgenic lines. To screen and confirm the *StFHT* construct insertion in the transformed *in-vitro* plants, the insert specific forward primer (ASFT-gDNA-F) with the empty vector chloramphenicol region reverse primer (pK7GWIWG2-Rv) were used in the PCR reaction. The expected amplicon size was about 1100 bp. bp = base pair; L = ladder; the numbers on top of the wells represent how many transgenics plants were screened.

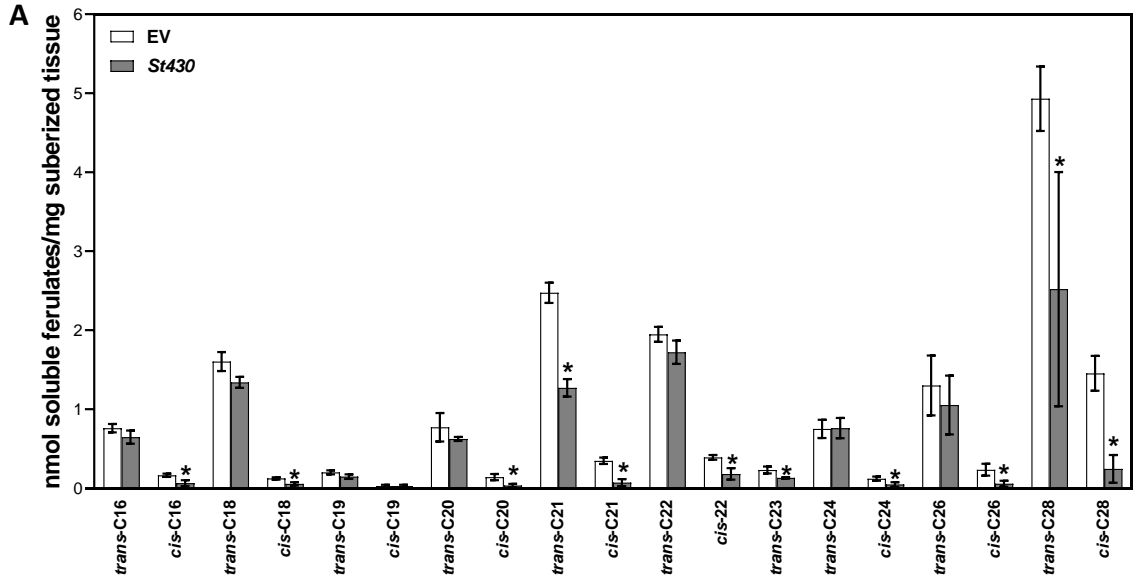
Appendix M. Gene knockdown verification by gene expression analysis

Gene of interest	Number of lines screened by RT-qPCR	Number of confirmed knockdowns
StASFT/FHT	7/11	4
StFACT	9/13	4
St430	3/4	1

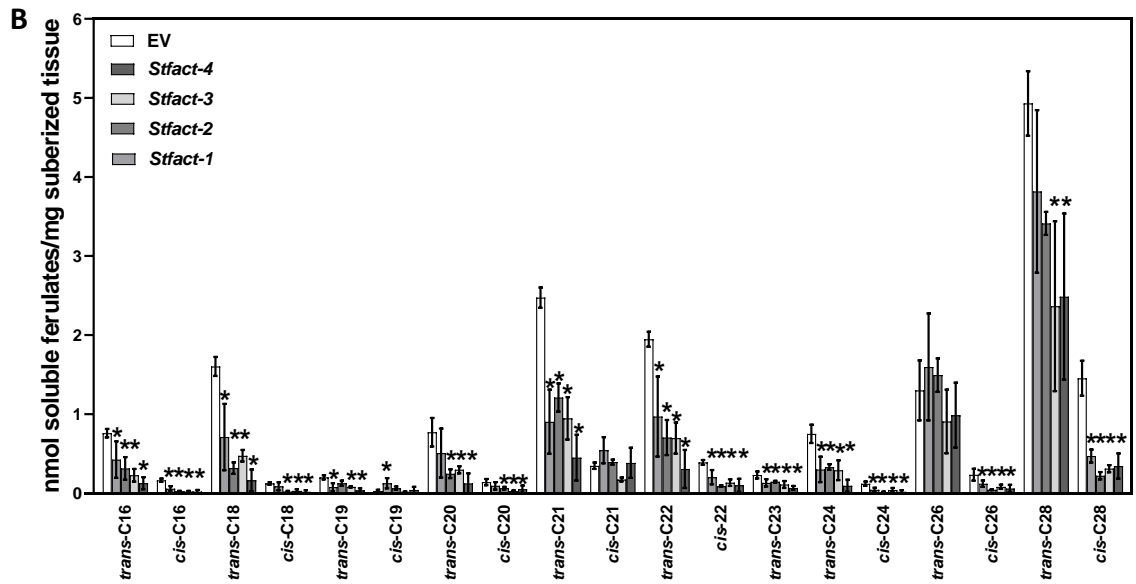




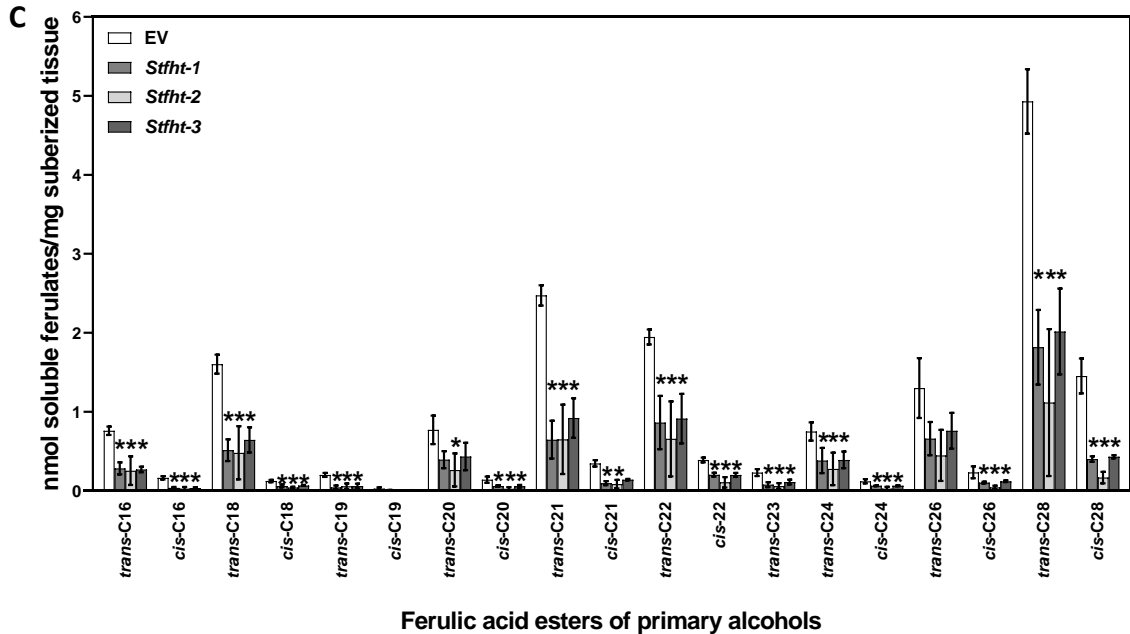
Appendix N. Soluble wax composition of potato knockdown lines. Individual suberin-associated wax compounds of StBAHD RNAi knockdown lines and empty vector were released from wound induced suberized periderm tissues after chloroform: methanol (2:1 v/v) treatment and analyzed by GC-MS/GC-FID. Soluble waxes were extracted from (A) *St430*, (B) *Stfact* (*Stfact-1*, *Stfact-2*, *Stfact-3*, *Stfact-4*), and (C) *Stfht* (*Stfht-1*, *Stfht-2*, *Stfht-3*) transgenic lines, and empty vector (EV) control. Data are presented as the mean \pm SD of three biological replicates ($n = 3$, for each RNAi transgenic lines), and three independent empty vector lines ($n = 3$). Asterisks denote significant differences from empty vector control (one-way ANOVA followed by Dunnett test, $p < 0.05$).



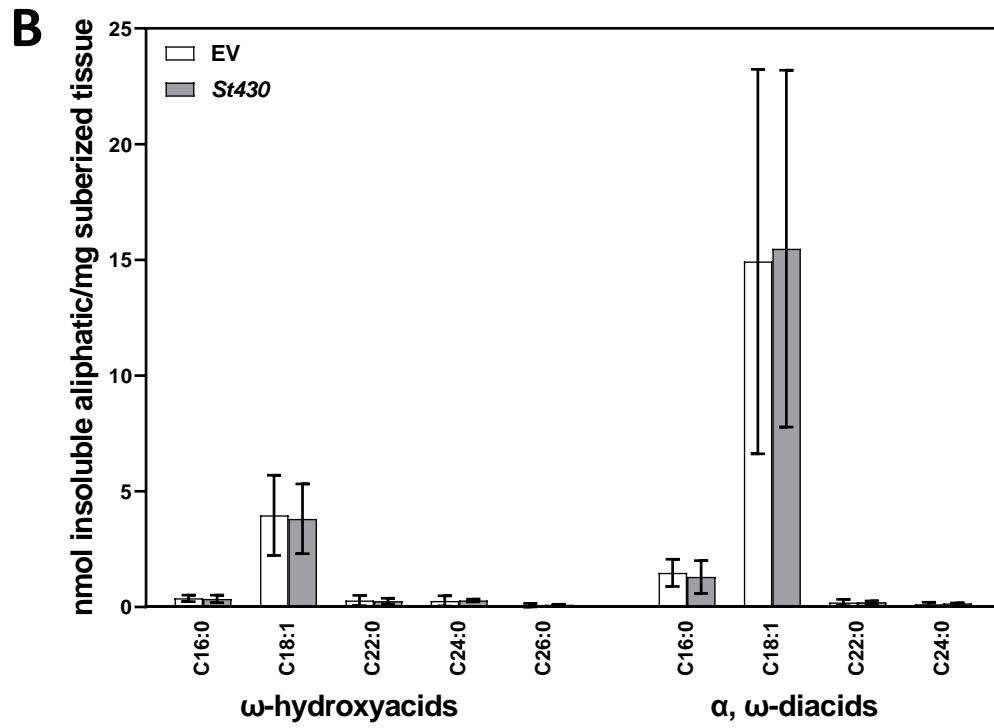
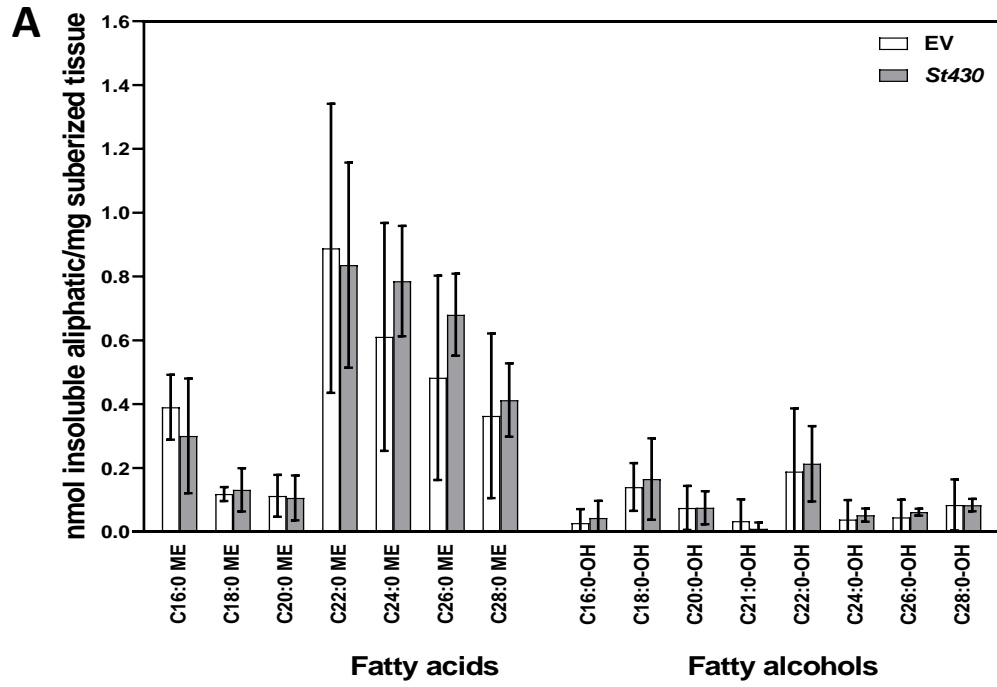
Ferulic acid esters of primary alcohols



Ferulic acid esters of primary alcohols

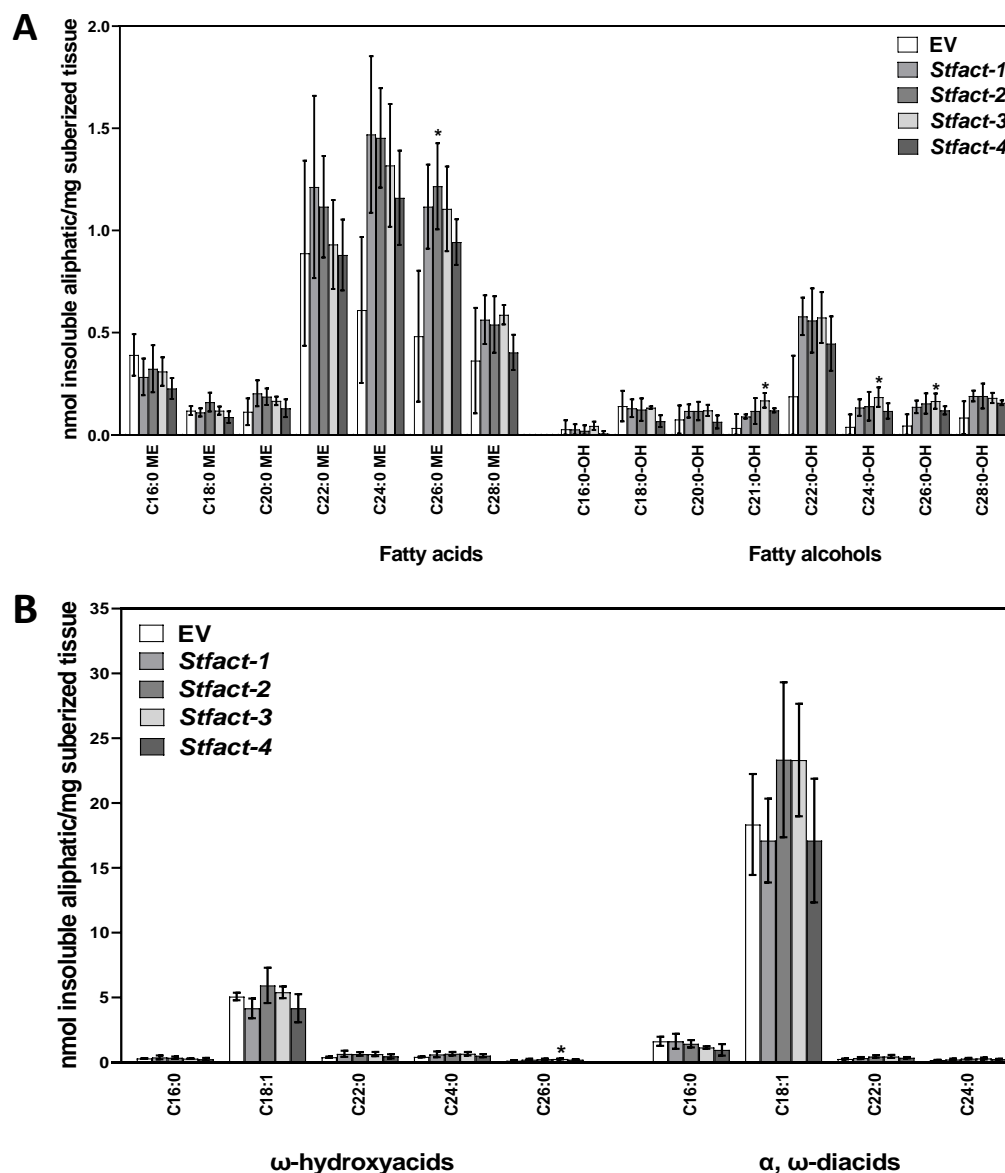


Appendix O. Soluble alkyl ferulates of potato knockdown lines. Individual alkyl ferulates compounds of StBAHD RNAi knockdown lines and empty vector were released from wound induced suberized periderm tissues after chloroform: methanol (2:1 v/v) treatment and analyzed by LC-UV-MS. Soluble alkyl ferulates were extracted from (A) *St430*, (B) *Stfact* (*Stfact-1*, *Stfact-2*, *Stfact-3*, *Stfact-4*), and (C) *Stfht* (*Stfht-1* *Stfht-2*, *Stfht-3*) transgenic lines, and empty vector (EV) control. Data are presented as the mean \pm SD of three biological replicates ($n = 3$, for each RNAi transgenic lines), and three independent empty vector lines ($n = 3$). Asterisks denote significant differences from empty vector control (one-way ANOVA followed by Dunnett test, $p < 0.05$).

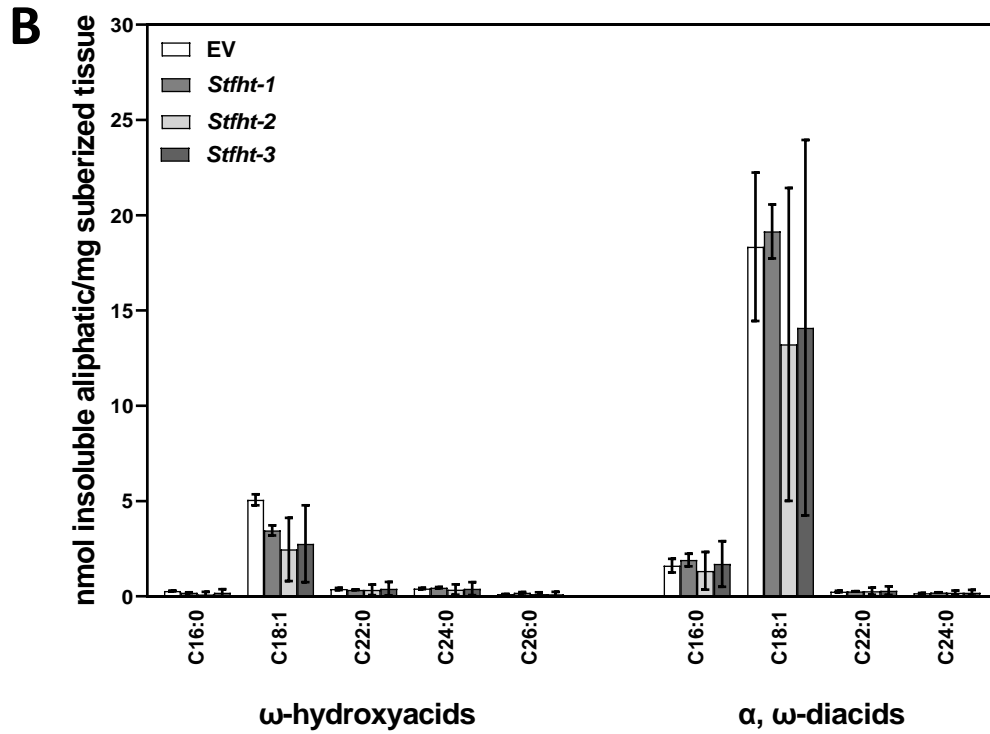
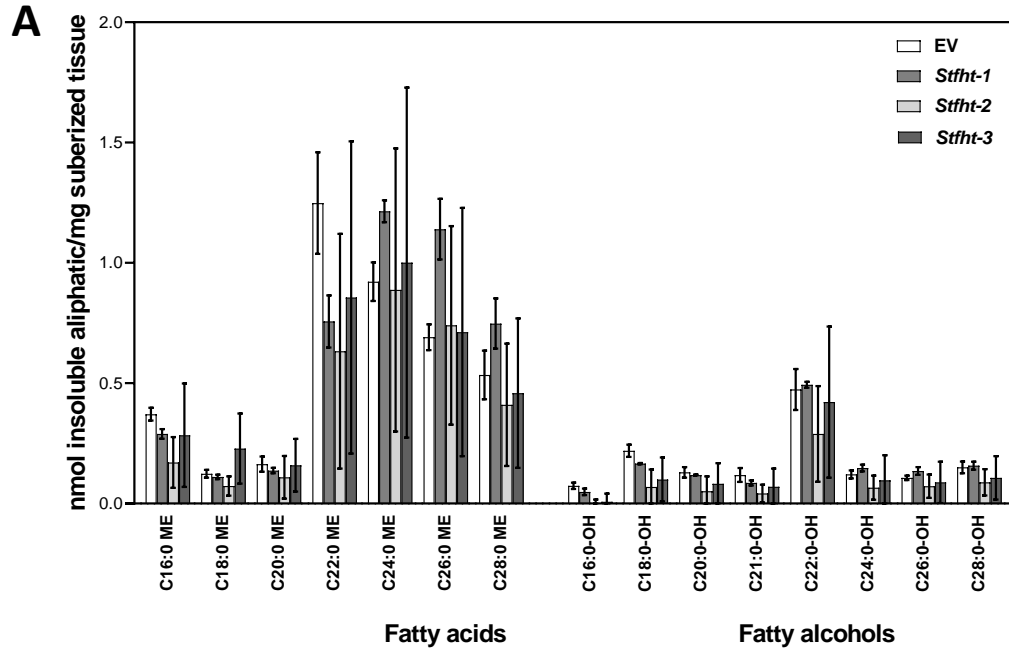


Appendix P. Total aliphatic suberin monomers composition in *St430* transgenic line.

Individual insoluble aliphatic suberin monomers were released after methanolic transesterification of wax-free suberized tissues from the *St430* transgenic line, and empty vector (EV) control. (A) Fatty acids and fatty alcohols amount. (B) ω -hydroxy fatty acids and α,ω -dioic fatty acids amount. Data are presented as the mean \pm SD of three biological replicates ($n = 3$, for the RNAi transgenic lines), and three independent empty vector lines ($n = 3$). Asterisks denote significant differences from empty vector control (one-way ANOVA followed by Dunnett test, $p < 0.05$).



Appendix Q. Total aliphatic suberin monomers composition in *StFACT* transgenic line. Individual insoluble aliphatic suberin monomers were released after methanolic transesterification of wax-free suberized tissues from the *StFACT* transgenic line, and empty vector (EV) control. (A) Fatty acids and fatty alcohols amount. (B) ω -hydroxy fatty acids and α, ω -dioic fatty acids amount. Data are presented as the mean \pm SD of three biological replicates ($n = 3$, for the RNAi transgenic lines), and three independent empty vector lines ($n = 3$). Asterisks denote significant differences from empty vector control (one-way ANOVA followed by Dunnett test, $p < 0.05$).



Appendix R. Total aliphatic suberin monomers composition in *StFHT* transgenic

line. Individual insoluble aliphatic suberin monomers were released after methanolic transesterification of wax-free suberized tissues from the *StFHT* transgenic line, and empty vector (EV) control. (A) Fatty acids and fatty alcohols amount. (B) ω -hydroxy fatty acids and α,ω -dioic fatty acids amount. Data are presented as the mean \pm SD of three biological replicates ($n = 3$, for the RNAi transgenic lines), and three independent empty vector lines ($n = 3$). Asterisks denote significant differences from empty vector control (one-way ANOVA followed by Dunnett test, $p < 0.05$).

Curriculum Vitae

Name: Yudelkis Indira Queralta Castillo

Post-secondary Education and Degrees: Algoma University
Sault Ste. Marie, Ontario, Canada
2012-2017 Honours B.Sc. with specialization in Biology

The University of Western Ontario
London, Ontario, Canada
2018-2022 M.Sc. in Biology

Related Work Experience Teaching Assistant
The University of Western Ontario
2018-2020 (taught three courses)

Research Assistant
Algoma University
2014-2018

Publications:

Yadav, V., Molina, I., Ranathunge, K., **Castillo, I.Q.**, Rothstein, S.J., Reed, J.W., (2014). ABCG transporters are required for suberin and pollen wall extracellular barriers in *Arabidopsis*. *The Plant Cell*, **26**, 3569-3588.

Renard, J., Martínez-Almonacid, I., **Queralta Castillo, I.**, Sonntag, A., Hashim, A., Bissoli, G., ... & Bueso, E. (2021). Apoplastic lipid barriers regulated by conserved homeobox transcription factors extend seed longevity in multiple plant species. *New Phytologist*, **231**(2), 679-694.

Chai, M., **Queralta Castillo, I.**, Sonntag, A., Wang, S., Zhao, Z., Liu, W., ... & Wang, Z. Y. (2021). A seed coat-specific β -ketoacyl-CoA synthase, KCS12, is critical for preserving seed physical dormancy. *Plant Physiology*, **186**(3), 1606-1615.

Conferences:

Castillo, I.Q., Bernards, M.A., Molina, I. (2019). Functional Characterization of *Arabidopsis thaliana* HXXXD-motif Acyltransferases involved in suberin metabolism. Plant Canada: Communicating Innovation in Plant Science, Guelph, Ontario (poster)

Castillo, I.Q., Bernards, M.A., Molina, I. (2018). Functional Characterization of *Arabidopsis thaliana* HXXXD-motif Acyltransferases involved in suberin metabolism. Canadian Society of Plant Biologists Eastern Regional Meeting (CSPB- ERM), London, Ontario (poster)

Molina, I. **Castillo, I.Q.**, (2017). Chemical characterization of the Arabidopsis loss-of-function double mutant *asft x fact*. Plant Apoplastic Diffusion Barriers (PADiBa), Oeiras, Portugal (co-author, poster)